JOURNAL OF THE AERONAUTICAL SCIENCES

VOLUME 6 MAY, 1939 NUMBER 7

On the Rib Stiffness Required for Box Beams

EUGENE E. LUNDQUIST

National Advisory Committee for Aeronautics

ABSTRACT

In the design of stressed-skin wings, it is common practice to assume that the shear webs and ribs are equivalent to rigid supports. As an idealized example of this problem the flat compression flange of a symmetrical box beam is regarded as a plate supported by transverse ribs and subjected to edge compression. A general theory for the stiffness required of the ribs to be equivalent to rigid supports is given. In addition, an approximate theory and a conservative theory for the rib stiffness are also given. The greater part of the paper is devoted to a design problem that shows in detail how to apply each theory.

INTRODUCTION

IN THE design of stressed-skin wings, it is common practice to assume that the shear webs and ribs are equivalent to rigid supports which divide the stiffened-skin covering into small panels and that the bending strength of the wing depends upon the compressive strength of these panels. This assumption is sound provided that the ribs are sufficiently stiff. The purpose of this paper is to discuss the stiffness required of the ribs to divide the compression side of a stressed-skin wing into small panels of length equal to the rib spacing.

As long as it is customary to static test complete wings, any weakness or faulty design is immediately discovered and corrected. The trend toward larger airplanes, the increased cost of static tests, and the possibility that static tests may be discontinued, however, make it especially desirable that the fundamental design assumptions be carefully examined.

Acknowledgment is here made to E. Z. Stowell, Joseph N. Kotanchik, Ivar C. Peterson, John K. Bussey, and, especially, to W. D. Kroll for help in the preparation of this paper.

Presented at the Structures Session, Seventh Annual Meeting, I. Ae. S., January 25, 1939.

ASSUMPTIONS

For purposes of theoretical analysis it is necessary to idealize the problem of the wing. In this paper, the main strength element of the stressed-skin wing is assumed to be a box beam. It is further assumed that the compression flange is flat, that the box beam is symmetrical and subjected to pure bending in the plane of symmetry, that all cross-sections have the same dimensions, that the bending stresses are uniformly distributed over the compression flange, that the ribs are alike, equally spaced and have zero torsional rigidity, and that the material is elastic. With these assumptions, the compression flange may be regarded as a flat plate under edge compression with continuous support along the shear webs and bulkheads. The support received from the ribs depends upon the type of construction used and the stiffness of the ribs.

SYMBOLS

x, y, z = coordinate axes

I_x, I_y = moment of inertia per in. for bending in the x and y directions, respectively

D_x, D_y = flexural rigidity per in. for bending in the x and y directions, respectively

GJ = torsional rigidity of plate per in.

B_i = flexural rigidity EI of the i^{th} rib

a, b = length and width of plate, respectively

μ = 0.3, Poisson's ratio for the material

μ'_x, μ_y = Poisson's ratio for load applied in the x and y directions, respectively

P = total compressive load on plate of width b

w = displacement in z direction

$f(y)$ = a non-dimensional function of y giving the relative values of w in sections parallel to the y axis

E = tension-compression modulus = 10.66×10^6 lb. per sq.in. for 24ST aluminum alloy
$G = E/2(1+\mu) = 0.385E$ = shear modulus
t_s, t_c = thickness of skin and corrugated sheet, respectively
p = pitch of corrugations
d = depth of corrugations measured on center line of sheet
K = ratio of pitch to developed length of a corrugation
$C_1, C_2, \ldots C_i$ = distance of ribs from y axis
L = spacing of ribs
$j = a/L$ = an integer giving the number of rib spaces in the length of the plate
k = an integer with values 0, 1, 2, 3, etc.
q = an integer 1, 2, 3, etc., that does not exceed $(j-1)$
m = an integer 1, 2, 3, etc. In the final equations of the general solution, m is the subscript of R
λ = half wave length of buckle

$$D_x = \frac{(EI)_x}{1-\mu_x\mu_y}, \qquad D_y = \frac{(EI)_y}{1-\mu_x\mu_y} \tag{a}$$

$$\beta = a/b \tag{b}$$

$$l = (2/b)\int_0^b [f(y)]^2\,dy \tag{c}$$

$$g = (2b^3/\pi^4)\int_0^b [\partial^2 f/\partial y^2]^2\,dy \tag{d}$$

$$r = Pb/\pi^2 D_x \tag{e}$$

$$s = gD_y/D_x \tag{f}$$

$$t = \frac{4}{\pi^2}\frac{GJb}{D_x}\int_0^b \left[\frac{\partial f}{\partial y}\right]^2 dy - \frac{2}{\pi^2} b\left(\mu_y + \frac{D_y}{D_x}\mu_x\right)\int_0^b \frac{\partial^2 f}{\partial y^2} f(y)\,dy \tag{g}$$

$$\gamma_i = B_i/bD_x \tag{h}$$

$$R_m = [(lr - t)\beta^2 m^2 - lm^4 - s\beta^4]/2g\beta^3 \tag{j}$$

Critical Compressive Load for a Flat Plate with Transverse Stiffening Ribs

General Solution

The problem considered is that of a flat plate rigidly supported along its four edges and elastically supported at intervals by transverse ribs. The loading is a uniform compression in the x direction. (See Fig. 1.) Timoshenko (reference 1, p. 378) has already given a general solution of this problem by the energy method when the plate rigidities are the same in all directions. In a stressed-skin wing, however, the plate rigidities of the stiffened skin are different in spanwise and chordwise directions. It is therefore necessary to repeat Timoshenko's solution with proper consideration given to the different rigidities in the x and y directions.

The deflection equation used in the energy method is

$$w = f(y)\sum_{m=1}^{m=\infty} a_m \sin\frac{m\pi x}{a} \tag{1}$$

The strain energy V in the plate when buckling occurs is assumed to be given by the following equation, which is similar to Eq. (199), page 307, reference 1, and is obtained in the same manner except that M_x, M_y, and M_{xy} are given by Eqs. (o), page 381, of reference 1.

$$V = \frac{1}{2}\int_0^b\int_0^a \left\{D_x\left[\left(\frac{\partial^2 w}{\partial x^2}\right)^2 + \mu_y\frac{\partial^2 w}{\partial y^2}\frac{\partial^2 w}{\partial x^2}\right] + D_y\left[\left(\frac{\partial^2 w}{\partial y^2}\right)^2 + \mu_x\frac{\partial^2 w}{\partial y^2}\frac{\partial^2 w}{\partial x^2} + 2GJ\left(\frac{\partial^2 w}{\partial x\,\partial y}\right)^2\right\} dx\,dy = \frac{\pi^4}{8}\left(D_x\frac{bl}{a^3}\sum_{m=1}^{m=\infty} m^4 a_m^2 + D_y\frac{ag}{b^3}\sum_{m=1}^{m=\infty} a_m^2 + D_x\frac{t}{ab}\sum_{m=1}^{m=\infty} m^2 a_m^2\right) \tag{2}$$

The strain energy in the ribs when buckling occurs is given by the following equation which is, except for the summation sign, similar to Eq. (c), page 372, of reference 1:

$$V_i = \sum_i \frac{B_i}{2}\int_0^b \left(\frac{\partial^2 w}{\partial y^2}\right)^2 dy = \frac{\pi^4 g}{4b^3}\sum_i B_i\left[\sum_{m=1}^{m=\infty} a_m \sin\frac{m\pi c i}{a}\right]^2 \tag{3}$$

The loss of potential energy T by the forces applied at the ends of the plate is given by the following equation which is similar to Eq. (c), page 327, of reference 1:

$$T = (P/2b)\int_0^b\int_0^a (\partial w/\partial x)^2\,dx\,dy = (P\pi^2 l/8a)\sum_{m=1}^{m=\infty} m^2 a_m^2 \tag{4}$$

The general equation for the calculation of the critical value of P is obtained by equating the total strain energy $(V + V_i)$ to the loss of potential energy T of the load P

$$P = \frac{\pi^2 D_x}{b\beta^2}\left[\frac{l\sum_{m=1}^{m=\infty} m^4 a_m^2 + s\beta^4\sum_{m=1}^{m=\infty} a_m^2 + \frac{4\beta^3}{b}\frac{g}{D_x}\sum_i\frac{B_i}{2}\left(\sum_{m=1}^{m=\infty} a_m \sin\frac{m\pi C_i}{a}\right)^2 + t\beta^2\sum_{m=1}^{m=\infty} m^2 a_m^2}{l\sum_{m=1}^{m=\infty} m^2 a_m^2}\right] \tag{5}$$

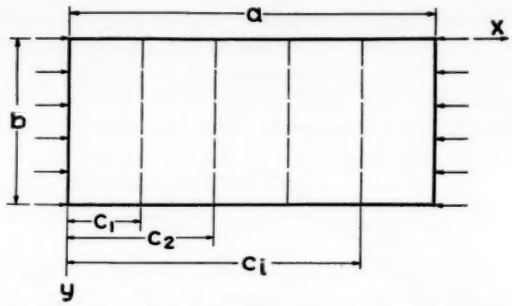

FIG. 1. Flat plate under edge compression stiffened by transverse ribs.

The coefficients a_m must be chosen so as to give minimum P. This condition is obtained by setting the derivative of P with respect to each of the coefficients a_m equal to zero. Thus a system of homogeneous linear equations in $a_1, a_2, a_3, \ldots\ldots$ are obtained. These equations are expressed by the relation

$$a_m R_m - \sum_i \gamma_i \sin \frac{m\pi C_i}{a} \left(a_1 \sin \frac{\pi C_i}{a} + a_2 \sin \frac{2\pi C_i}{a} + a_3 \sin \frac{3\pi C_i}{a} + a_4 \sin \frac{4\pi C_i}{a} + \ldots. \right) = 0 \quad (6)$$

The solution of these equations yield values for a_1, a_2, a_3 ... different from zero only if the determinant formed by the coefficients of $a_1, a_2, a_3, \ldots\ldots$ is equal to zero. A careful study of this determinant revealed that, when the ribs are alike and equally spaced, the determinant can be easily expanded and factored. When each factor in turn is set equal to zero, an equation is obtained relating the critical load with the stiffness of the ribs and the plate for the particular wave pattern described by that factor. If the factors that describe wave patterns with a node at each rib are set equal to zero, the rib stiffness does not enter into the equation obtained. If the factors that describe all other wave patterns are each set equal to zero, it is found that the resulting equations can all be represented by the following relation

$$\gamma = \gamma_i = \frac{2/j}{\sum_{k=0}^{k=\infty} \frac{1}{R_{2jk+q}} + \sum_{k=0}^{k=\infty} \frac{1}{R_{2j(k+1)-q}}} \quad (7)$$

where R_m is defined by an equation given in the list of symbols. Thus m is equal to $(2jk + q)$ or $2j(k + 1) - q$ depending upon which series is being evaluated. In Eq. (7) j is the number of spaces into which the plate is divided by the ribs. The various wave patterns are described by integral values of q where $q = 1, 2, 3$, etc., but q does not exceed $(j - 1)$. Hence there are $(j - 1)$ wave patterns represented by Eq. (7).

Eq. (7) applies to a plate of finite length a, where $a = jL$. In this plate the side and the end edges are assumed to be rigidly supported. The effect on the rib stiffness, the critical load, the wave pattern, etc., of the rigid end supports diminishes as the length of the plate increases. In the limit as a, and hence j, approach infinity Eq. (7) becomes

$$\gamma = \frac{1}{g}\left(\frac{b}{L}\right)^3 \Big/ \left[\sum_{k=0}^{k=\infty} \frac{1}{M_k} + \sum_{k=0}^{k=\infty} \frac{1}{N_k}\right] \quad (8)$$

where

$$M_k = (lr - t)\left(\frac{L}{b}\right)^2 \left(2k + \frac{L}{\lambda}\right)^2 - s\left(\frac{L}{b}\right)^4 - l\left(2k + \frac{L}{\lambda}\right)^4 \quad (9)$$

$$N_k = (lr - t)\left(\frac{L}{b}\right)^2 \left(2k + 2 - \frac{L}{\lambda}\right)^2 - s\left(\frac{L}{b}\right)^4 - l\left(2k + 2 - \frac{L}{\lambda}\right)^4 \quad (10)$$

The different equations represented by Eqs. (7) and (8) cannot be conveniently solved for the critical values of P. As presented, however, these equations are in a convenient form to find the rib stiffness required when the critical value of P is known. In a plate of finite length any one of $(j - 1)$ wave patterns is possible. In the plate of infinite length, any one of an infinite number of wave patterns is possible. For a correct solution, the rib stiffness required for each of the possible wave patterns must be determined for the known value of P. The particular wave pattern that requires the highest rib stiffness is the one which must be used in design. In the design problem given later, it is shown that this wave pattern is closely approximated by a simple calculation. Then the applicable Eq. (7) or (8) is used to refine the calculation, if necessary.

If the ribs have zero stiffness, then the factors of the determinant become R_1, R_2, R_3, etc. For this case, the relation between the critical load and the plate stiffness is obtained by setting R_m equal to zero,

$$R_m = \frac{(rl - t)\beta^2 m^2 - s\beta^4 - lm^4}{2g\beta^3} = 0$$

from which

$$r_{crit.} = \frac{1}{l}\left[s\left(\frac{\beta}{m}\right)^2 + t + l\left(\frac{m}{\beta}\right)^2 \right] \quad (11)$$

But m has integral values 1, 2, 3, etc. The particular value of m that applies in a given problem is the value for which $r_{crit.}$ is smallest. For a long plate, the smallest value of $r_{crit.}$ is obtained by setting the derivative of $r_{crit.}$ with respect to β/m equal to zero. By this procedure it is found that

$$\lambda/b = \beta/m = \sqrt[4]{l/s} \quad (12)$$

and that the minimum value of $r_{crit.}$ when the rib stiffness is zero is given by the equation

$$(r_{crit.})_{min.} = (1/l)(2\sqrt{sl} + t) \quad (13)$$

Approximate Solution

Eqs. (11), (12), and (13) can also be used as an approximation when the half wave length of the buckles

extends over several rib spaces. In such cases D_y must also include the rib stiffness, which is assumed distributed over the space between ribs. Thus D_y is increased by the amount B/L.

The value of using Eqs. (11), (12), and (13) when the rib stiffness is included in D_y will be demonstrated in the design problem given later. This approximation, however, will always give a rib stiffness smaller than the correct value given by the general solution.

Conservative Solution

A simple but conservative solution for the stiffness required of the ribs can be obtained if it is assumed that the longitudinal elements of the plate behave as a series of columns. By this assumption the connection between the longitudinal elements that gives rise to the interaction considered in plate theory is neglected.

Timoshenko (reference 1, p. 106) has shown that, when a column is supported by equally spaced elastic supports of equal rigidity, the stiffness required of the supports to cause buckling to occur with a node at each support is easily calculated by a simple energy relation. A similar relation also applies when a series of columns are supported by equally spaced beams or ribs.

Each column is imagined to consist of a series of rigid links hinged at the ends and at the supporting ribs. By a procedure similar to that used in the general solution given previously, it is found that when the ribs are equally spaced

$$B = \frac{\dfrac{P}{\alpha b L}\displaystyle\int_0^b [f(y)]^2\,dy}{\displaystyle\int_0^b \left[\frac{\partial^2 f}{\partial y^2}\right]^2 dy} \tag{14}$$

where the coefficient α has the values given in Table 1. These coefficients are the same as those given by Timoshenko in Table 4, page 107, reference 1:

TABLE 1

Values of α

j	α	j	α
2	0.500	7	0.263
3	.333	9	.258
4	.293	11	.255
5	.276	∞	.250
6	.268		

In Eq. (14), P is the strength of the panel of width b and length L when considered as a pin-ended column.

DESIGN PROBLEM

The purpose of the design problem is to demonstrate in detail how the preceding theory is applied to a practical design problem.

The bending moment to be carried and the general dimensions of the box are determined by the size of the wing and other considerations of no concern in this paper. For this problem, therefore, the box beam shown in Fig. 2 is assumed. The total load in the compression flange is assumed to be 225,000 lb. As stated in the previous theory, this load is treated as uniformly distributed across the flange. It is desired to determine the rib stiffness required to divide the compression flange into small panels of length equal to the rib spacing. If ribs of this stiffness or a greater stiffness are provided, failure will occur in the panels themselves and the design based upon the compressive strength of the panel is valid.

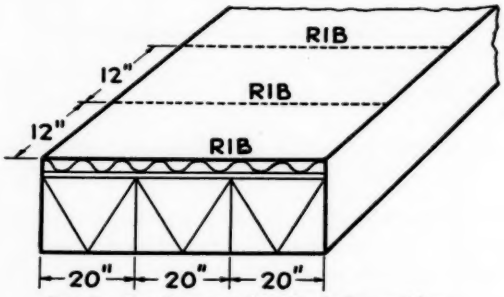

FIG. 2. Box beam used in the design problem.

Compressive Strength of the Panel

The starting point in this calculation is to check the strength of the panel itself. It is assumed that the compression flange consists of corrugated sheet covered with smooth skin, both of which are 24ST aluminum alloy. (See Fig. 3.) Further, it is assumed that only one-third of the smooth skin is effective in carrying compression and that the corrugated sheet is fully effective. On the basis of these assumptions, the area A_x and the moment of inertia I_x is found to be

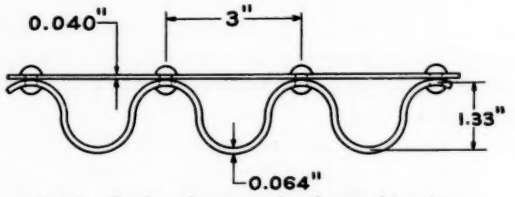

FIG. 3 Section of compression flange of box beam.

$$A_x = 0.1070 \text{ sq.in. per in.} \tag{15}$$

$$I_x = 0.02727 \text{ in.}^4 \text{ per in.} \tag{16}$$

If the rib spacing L is 12 in. as shown in Fig. 2, the slenderness ratio L/ρ for the panel is

$$L/\rho = L\sqrt{A_x/I_x} = 23.77 \tag{17}$$

On the assumption that the column formula given by

Osgood[2] for 24ST applies, the critical compressive stress on the effective material is

$$f_{crit.} = 43{,}700(1 - 0.00752L/\rho) = 35{,}890 \text{ lb. per sq.in.} \quad (18)$$

The total allowable load on the 60-inch-wide compression flange is therefore

$$P = 60A_x f_{crit.} = 230{,}400 \text{ lb.} \quad (19)$$

This allowable flange load is larger than the applied load of 225,000 lb. Therefore the panel itself has adequate strength.

The foregoing calculation on the compressive strength of the panel was made because no test data were available. Where test data are available, such data would invariably be used to check the compressive strength of the panel.

Properties of the Plate

In order to calculate the stiffness required of the ribs it is first necessary to establish μ_x, μ_y, and the three plate rigidities D_x, D_y, and GJ. In the absence of experimental data to the contrary, the most logical values to assume for μ_x and μ_y are

$$\mu_x = \mu_y = 0 \quad (20)$$

These values of μ apply to the fabricated anisotropic plate composed of corrugated sheet covered with smooth sheet and are not to be confused with Poisson's ratio for the material itself.

If $\mu_x = \mu_y = 0$, then Eq. (a) shows that the longitudinal rigidity D_x, for bending in the x direction, is nothing more than τEI_x, where τE is the effective modulus of the effective material loaded as a column. Osgood[2] gives for 24ST material the following equation for τ, when the stress f lies between 19,600 and 41,200 lb. per sq.in.

$$\tau = (f/8{,}925)(1.224 - f/35{,}700)^2 \quad (21)$$

Eq. (21) shows that, in order to evaluate τ, it is necessary to know the compressive stress f on the effective material in the plate. In this problem it is assumed that f is equal to the total allowable load on the panel (230,400 lb.) divided by the total effective area ($60A_x$). In the calculations that follow, the design of the ribs will therefore be consistent with the strength of the panel. Thus

$$f = 230{,}400/60A_x = 35{,}890 \text{ lb. per sq.in.} \quad (22)$$

and by Eq. (21) $\tau = 0.19234$. Thus in all of the calculations that follow

$$D_x = \tau EI_x = 55{,}910 \text{ lb.in.} \quad (23)$$

The most reasonable assumption for the transverse rigidity D_y is that D_y is equal to the sum of the rigidities of the corrugated sheet and the flat cover sheet. It is further assumed that the high compressive stress in the x direction does not alter these rigidities. Thus

$$D_y = \frac{Et_s^3}{12(1-\mu^2)} + \frac{KEt_c^3}{12(1-\mu^2)} = 237.3 \text{ lb.in.} \quad (24)$$

Of the three plate rigidities, GJ is the most difficult to evaluate. The calculation itself is not difficult but the various assumptions that must be made each provide a possible source of error.

First, consider the evaluation of GJ on the assumption that the high compressive stress in the x direction does not alter GJ. The basic equation for GJ is, for this case [see Eq. (208), page 627, reference 3],

$$GJ = 2A^2/p \int \frac{ds}{Gt} \quad (25)$$

where A is the area enclosed between the center lines of the corrugated sheet and the flat cover sheet in a length equal to the pitch p of the corrugation and $\int(ds/Gt)$ is a line integral to be evaluated for the boundary of this area. In this integral the differential length of arc ds and the thickness t should not be confused with the terms designated s and t in the list of symbols. The value of $\int(ds/Gt)$ from the center line of the corrugated sheet to the center line of the flat cover sheet is assumed equal to zero. This assumption is one of the possible sources of error mentioned previously.

Another source of error is the evaluation of $\int(ds/Gt)$ along the flat cover sheet. Because of the high compressive stress in the x direction, there will be a buckling of the flat cover between crests of the corrugation. This buckling may reduce the shearing stiffness Gt for the flat sheet. In this problem it is assumed that Gt for the flat cover sheet is reduced to $\frac{1}{2}Gt$.

The last consideration and the third source of error in the evaluation of GJ is that of the effect of the high compressive stress in the x direction on G itself. In an extensive theoretical and experimental study of the twisting failure of angle columns, Kollbrunner[4] concluded that the reduced shear modulus G_r caused by stress in the x direction is given by the equation

$$G_r = (\tau + \sqrt{\tau})G/2 \quad (26)$$

Kollbrunner, however, evaluated τ by use of the stress-strain curve. When τ is evaluated by use of the column curve as done by Osgood[2] a different function of τ relating G_r and G is required. It will be conservative, however, to use the relation given by Eq. (26) when τ is evaluated as outlined in this paper.

As a result of the foregoing considerations, it is found that

$$GJ = (\tau + \sqrt{\tau})G \times \left(\frac{d}{2} + \frac{t_c}{2} + \frac{t_s}{2}\right)^2 \Big/ \left(\frac{1}{(t_s/2)} + \frac{1}{Kt_c}\right)$$
$$= 1.8350 \times 10^4 \text{ lb.in.} \quad (27)$$

Stiffness Required of Rib for Design Problems

When the rib is attached to the tension flange as well as the compression flange, the tensile force in the tension flange tends to increase the stiffness of the rib. This increase in the rib stiffness is not considered in the following calculation. Consequently, the calculated stiffness required of the rib results in a larger moment of inertia for the rib than would actually be required. However, there is frequently some portion of the wing where a large cut-out is found in the tension flange as, for example, a cut-out for the retraction of the landing gear or some other item within the wing. In such cases the rib that supports the compression flange is not stiffened by attachment to the tension flange. It is for this case that the following calculation of rib stiffness applies.

The general theory given in the first part of this paper applies to a plate or compression flange with any ratio of length to width as designated by the symbol β. The most conservative calculation of the rib stiffness, however, will be that based upon a flange of infinite length.

It will be recalled that, in Eq. (1), the assumed deflection in the transverse direction was designated $f(y)$ but was not specifically defined. This procedure was followed so that the function $f(y)$ could be selected to best fit the problem at hand. If the ribs are considered as simply supported at their ends as in this problem then, when buckling occurs, the wave patterns for the compression flange will be of the type shown in Fig. 4 and

$$f(y) = \sin(\pi y/b) \tag{28}$$

which gives

$$g = l = 1, \quad s = D_y/D_x, \quad t = 2GJ/D_x$$

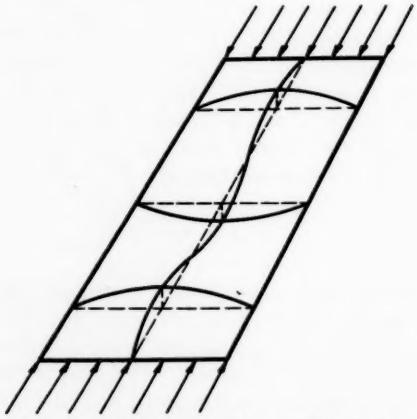

FIG. 4. Wave pattern for calculating the stiffness required of the ribs when the ribs are simply supported at their ends.

Approximate Solution for Plate of Infinite Length

$(a = \infty, b = 60$ in.)

In the approximate solution the stiffness of the rib is assumed continuously distributed between ribs. Therefore B/L is contained in D_y and, from Eq. (13), it is found that s, which includes D_y, is

$$s = (lr - t)^2/4l$$

For this problem, however,

$$l = 1$$
$$r = Pb/\pi^2 D_x = (230{,}400)(60)/\pi^2\,55{,}910 = 25.052$$
$$t = 2GJ/D_x = 2(1.8350)(10)^4/55{,}910 = 0.6564$$

Therefore

$$s = (25.052 - 0.6564)^2/4 = 148.8$$

and by use of Eq. (12)

$$\lambda = b\sqrt[4]{l/s} = 17.18 \text{ in.}$$

As previously mentioned for the approximate solution, the value of s and the rib stiffness B are related by the following equation

$$s = (D_y + B/L)/D_x$$

from which

$$B = L(sD_x - D_y) = 99{,}830{,}000 \text{ lb.in.}^2 \tag{29}$$

General Solution for Plate of Infinite Length

$(a = \infty, b = 60$ in.)

The correct value of the rib stiffness required will now be computed by use of the general solution given in the first part of this paper. In this calculation, the results of the approximate solution are used as a guide.

In the general solution it is necessary to compute the rib stiffness required for a number of possible wave patterns. The wave pattern that requires the highest rib stiffness is the one which applies. Experience has shown that the approximate solution tends to overestimate the half wave length λ. Therefore, the rib stiffness will be computed for assumed values of λ less than the value of 17.18 in. given by the approximate solution.

For the general solution, the rib stiffness is included in the quantity γ, which is given by Eq. (8). In this problem only the first two terms of each series in the denominator of Eq. (8) are considered. Thus the equation for γ is

$$\gamma = \frac{1}{g}\left(\frac{b}{L}\right)^3 \Big/ \left(\frac{1}{M_0} + \frac{1}{M_1} + \frac{1}{N_0} + \frac{1}{N_1}\right) \tag{30}$$

The values of M_0 and M_1, are given by Eq. (9), whereas the values of N_0 and N_1 are given by Eq. (10). In these equations, $k = 0$ or 1, as indicated by the subscript on the quantity being computed. The values of g, l, r, and t required for the evaluation of γ have already been determined in the approximate solution. These values are

$$g = l = 1, r = 25.052, t = 0.6564.$$

For the general solution B/L is not included in D_y. Therefore

$$s = D_y/D_x = 4.244 \times 10^{-3}$$

In Eqs. (9) and (10) the wave length λ always appears in the ratio λ/L, where L is the rib spacing. It is therefore more convenient to assume values for λ/L rather than to assume values for λ itself. In this problem $L = 12$ in. and the value of λ for maximum rib stiffness is not likely to exceed 17.18 in.

Thus the values of λ/L given in Table 2 were assumed and the corresponding values of $1/M_0$, $1/M_1$, $1/N_0$, and $1/N_1$ were computed by use of Eqs. (9) and (10). The values of γ also given in Table 2 correspond to the assumed values of λ/L and were computed by use of Eq. (30).

The values of γ given in Table 2 are plotted against λ/L in Fig. 5. From the curve faired through these points it is found that the maximum value of γ is 40. Therefore

$$\gamma = B/bD_x = 40$$

from which

$$B = 134{,}180{,}000 \text{ lb.in.}^2 \qquad (31)$$

The only error in this value of B is that obtained by neglecting all terms beyond the first two in each of the infinite series contained in Eq. (8). These series are very rapidly convergent, however, as indicated by comparison of the numerical values of the first and second terms of each series. (See Table 2.) Therefore, the value of the rib stiffness $B = 134,180,000$ lb.in.^{2} is a very close approximation to the correct value. The approximate value previously computed is therefore in error by approximately 26 percent.

TABLE 2

Values for Rib

$\frac{\lambda}{L}$	$\frac{1}{M_0}$	$\frac{1}{M_1}$	$\frac{1}{N_0}$	$\frac{1}{N_1}$	γ
1.1	8.101	−0.016	−3.922	−0.012	30.11
1.15	6.021	−0.017	−2.591	−0.012	36.75
1.2	5.118	−0.018	−1.907	−0.011	39.28
1.25	4.653	−0.019	−1.496	−0.011	39.97
1.3	4.400	−0.020	−1.225	−0.010	39.74
1.4	4.210	−0.021	−0.893	−0.009	38.05
1.5	4.234	−0.023	−0.701	−0.009	35.70

General Solution for Plate of Finite Length

($a = 48$ in., $b = 60$ in.)

The general solution for a plate of finite length follows the same procedure as outlined for the plate of infinite length except that the number of wave patterns for which the rib stiffness must be computed is greatly reduced. For this case $\beta = 48/60 = 0.8$ and the quantities g, l, r, t, and s are the same as in the preceding example. For the rib spacing of 12 in., $j = 48/12 = 4$, and the number of wave patterns to be investigated is $(j - 1)$ or 3. Thus the three equations for γ are obtained from Eq. (7) by letting q have the values 1, 2, and 3, respectively. These equations for γ are:

For $q = 1$,

$$\gamma = {}^1/_2 \Big/ \left[\left(\frac{1}{R_1} + \frac{1}{R_9} + \cdots \right) + \left(\frac{1}{R_7} + \frac{1}{R_{15}} \cdots \right) \right] \qquad (32)$$

For $q = 2$,

$$\gamma = {}^1/_2 \Big/ \left[\left(\frac{1}{R_2} + \frac{1}{R_{10}} + \cdots \right) + \frac{1}{R_6} + \frac{1}{R_{14}} + \cdots \right) \Big] \qquad (33)$$

For $q = 3$,

$$\gamma = {}^1/_2 \Big/ \left[\left(\frac{1}{R_3} + \frac{1}{R_{11}} + \cdots \right) + \left(\frac{1}{R_5} + \frac{1}{R_{13}} + \cdots \right) \right] \qquad (34)$$

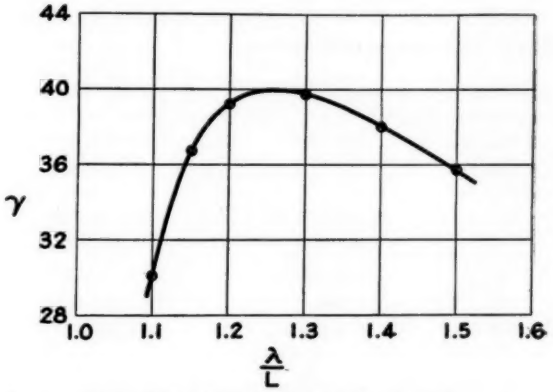

FIG. 5. Theoretical values of γ for the rib when the compression flange has infinite length.

On evaluation of these equations, considering only the first two terms of each infinite series, it is found that the values of γ obtained are as follows:

q	γ
1	7.22
2	24.39
3	39.31

Thus the highest value of γ is obtained for the wave pattern defined by $q = 3$. The value of the rib stiffness B that corresponds to $\gamma = 39.31$ is

$$B = 131{,}850{,}000 \text{ lb.in.}^2 \qquad (35)$$

Comparison of the value of B for the plate of finite length with the value of B for the plate of infinite length shows that the stiffness of the rib is increased less than 2 percent by the latter assumption.

Conservative Solution

The conservative solution for the rib stiffness is obtained by application of Eq. (14). If the ribs are considered as simply supported at their ends as in this problem, then $f(y)$ is given by Eq. (28) and Eq. (14) becomes

$$B = \frac{1}{\alpha\pi^4}\frac{P}{b}\frac{b^4}{L} = \frac{1}{\alpha\pi^4}\frac{Pb^3}{L} \tag{36}$$

For the plate of infinite length $j = \infty$ and $\alpha = 0.250$. Thus

$$B = (1/0.250\pi^4)/(230{,}400)(60)^3/12 = 170{,}300{,}000 \text{ lb.in.}^2$$

For the plate of finite length, $j = 4$ and $\alpha = 0.293$. Thus

$$B = 145{,}307{,}000 \text{ lb.in.}^2$$

Comparison of these values of B with the corresponding values given by the general solution shows these values of B to be in error by about 27 and 10 percent, respectively.

Table 3 is a summary of the rib stiffness B as computed in the various examples.

TABLE 3

Length (in.)	Solution	B (lb.in.^{2})
∞	Approximate	99,830,000
∞	General	134,180,000
∞	Conservative	170,300,000
48	General	131,850,000
48	Conservative	145,307,000

Stiffness Required of Rib Cap Strip for Design Problem

When a truss type of rib is employed, the theory of this paper can be used to calculate the stiffness required of the rib cap strip. In this case attachment of the rib to the tension flange of the box beam does not appreciably stiffen the rib cap strip supporting the compression flange. The procedure for calculating the stiffness required of the cap strip is the same as that already outlined for calculating the stiffness of the rib as a whole.

If the cap strips are assumed hinged at each panel point of the rib truss, when buckling occurs, the wave pattern for the compression flange will be of the type shown in Fig. 6 and again

$$f(y) = \sin(\pi y/b)$$

In this case, b should be regarded as the distance between panel points of the rib truss and the total load P on the panel is reduced by a corresponding amount.

By calculations similar to those made for the rib as a whole the following values of the stiffness B were computed for the rib cap strip:

Solution	B (lb.in.^{2})
Approximate	756,000
General	815,400
Conservative	2,102,000

In each of these calculations $a = \infty$, $b = 20$ in., and $P = 76{,}800$ lb.

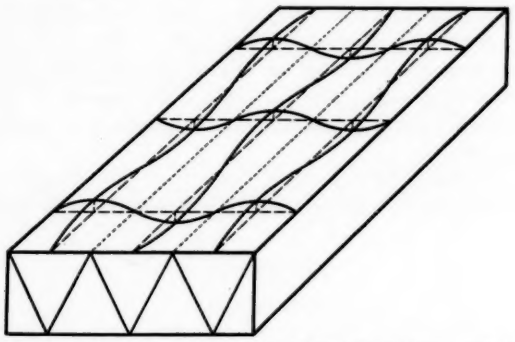

FIG. 6. Wave pattern for calculating the stiffness required of the rib cap strips when the cap strips are simply supported at the rib panel points.

Concluding Discussion

In Fig. 7 are shown the dimensions of a rib and cap strip that have the required stiffness given by the general solution for a plate of infinite length. If the distance between panel points on the rib truss is 20 in., the cap strip shown in Fig. 7 is required. If this cap strip forms the chord member of a rib, the rib would need to be 9.39 in. deep as shown. These dimensions were computed on the assumption that the rib and the cap strip is 24ST aluminum alloy with $E = 10.66 \times 10^6$ lb. per sq.in.

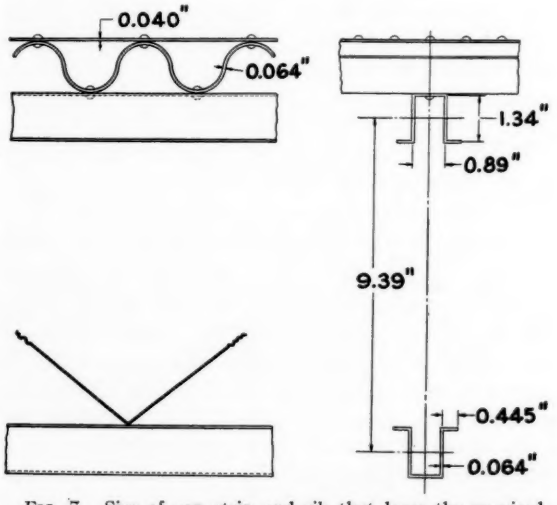

FIG. 7. Size of cap strip and rib that have the required stiffness as given by the general solution for a plate of infinite length.

It is important to notice in Fig. 7 that only a small cap strip is required when $b = 20$ in. By comparison, however, a very large rib is required when $b = 60$ in. If the load per inch of flange P/b does not change as in this case, Eq. (36) shows that the bending stiffness of the rib varies as the fourth power of the width b. It is this fact that accounts for the small cap strip and the large rib in Fig. 7. The fact that the stiffness EI of the rib ($B = EI$) varies as the fourth power of the width b should not be overlooked by designers.

The general solution gives the theoretically correct rib stiffness. The objections to this solution are that it requires a long calculation and a proper knowledge of the plate rigidities.

The approximate solution gives a value for the rib stiffness that is always less than the theoretically correct value. This solution involves almost as long a calculation as the general solution and is usually not justified except as a guide to aid in obtaining the general solution. Only in the cases where the half wave length of the buckle pattern extends over several ribs does it give accurate results.

The conservative solution is by far the simplest and, as its name implies, it always gives a conservative value for the rib stiffness. Its accuracy increases as the spacing of the ribs decreases. In the limit as the spacing of ribs approaches zero it gives the correct rib stiffness.

Without actually testing the conservative solution for many cases, the limits within which this solution applies with good accuracy cannot be defined. It is therefore recommended that, until such time as these limits are defined, designers should apply both the general solution and the conservative solution. If the two solutions are in close agreement, use the conservative solution. If they are in wide disagreement, it is proper to be guided more by the general solution than by the conservative solution.

As the problem discussed in this paper now stands, reliable test data are needed to check the theory and the formulas for evaluating its basic parameters.

References

[1] Timoshenko, S., *Theory of Elastic Stability:* McGraw-Hill (New York), 1936.

[2] Osgood, William R., and Holt, Marshall, *The Column Strength of Two Extruded Aluminum-Alloy H-Sections:* N.A.C.A. Technical Report (to be published).

[3] Timoshenko, S., *Strength of Materials*, Part II; D. Van Nostrand Co., 1930.

[4] Kollbrunner, Curt F., *Das Ausbeulen des auf Druck beanspruchten freistehenden Winkels;* Gebr. Leemann and Company (Zürich & Leipzig), 1935.

Book Reviews

Civil Aeronautics Act Annotated, by CHARLES S. RHYNE; National Law Book Company, Washington, D. C., 1939; 307 pages.

This comprehensive work on the development of civil air transport in the United States is of much wider scope than its title indicates. Mr. Rhyne gives a history of legislation leading up to the present law with explanatory comment and a wealth of references.

In the chapters treating the Civil Aeronautics Act, each section is explained and references given as to its background and purpose. Appendices giving a digest of all Congressional bills relating to civil aeronautics introduced since 1919, as well as full texts of the Civil Aeronautics Act of 1938 and of the Air Commerce Act of 1926 (as amended) are extremely valuable. As many sections of the Civil Aeronautics Act are obscure without reference to the amendments which were made to the Air Commerce Act of 1926, sufficient background is thus given for a complete understanding of the Act. A complete Index makes for easy reference to its sections and purposes.

Great credit is due the author for making this valuable reference book available to operators, pilots, airport officials, private pilots, aeronautical schools, and others engaged in aviation.

The Story of Aircraft, by CHELSEA FRASER; Thomas Y. Crowell Company, New York (Second edition), 1939; 501 pages, $2.50.

There are many popular histories of aviation but they soon grow out of date. Evaluation of events changes with perspective. Flights which made front pages and required chapters in earlier accounts may now only have a third newspaper page value and merit no more than a few lines in a history. The first edition of this book was published in 1933 but the present revised edition is brought up to the DC-4 and the Boeing 314. Accounts of aerial warfare in Spain and China further indicate the thoroughness with which the author deals with the latest developments in the air.

As a history from the earliest days it is not only very complete but is written in a style which is easy to read, in spite of the fact that much essential technical information is included. The numerous illustrations and photographs are wisely selected and excellently done.

In these days when many persons refer to aviation as a new science or a recent art, this book can be recommended as giving a correct idea of the long path leading to the present stage of aeronautical development.

Vibration of Radial Aircraft Engines, Part I*

G. P. BENTLEY

Sperry Gyroscope Company

SUMMARY

A complete theoretical study of gas and inertia vibration forcing functions in 7 and 9 cylinder single row and 14 and 18 cylinder twin row radial aircraft engines with articulated connecting rods is outlined qualitatively in Part I, and the results presented in mathematical terms in chart form.

In Part II† engine vibration in an unrestrained engine mounting arrangement is outlined theoretically and charts provided to permit calculation of free engine vibration in all degrees of freedom. All theoretical work in Parts I and II was verified by full scale tests on two 9 cylinder and two 14 cylinder engines, operating under conditions of negligible restraint, and by full flight vibration surveys on two airplane engine installations of the same freely mounted test engines. Plots are included comparing the test results with the theoretical work both on the ground and in the air.

PART I. THEORETICAL FORCING FUNCTIONS

VIBRATION forcing functions arising from engine unbalances and torque fluctuations are important in the design of engine parts and engine mounting structures. Various aspects of the problem have been treated theoretically by many authors. With the development of electrical vibration measuring methods by C. S. Draper and the author in 1934, it became possible to empirically study the vibration of both engine and airplane, and thereby verify theoretical conclusions.

In 1935, the Massachusetts Institute of Technology and the Bureau of Aeronautics of the United States Navy extended their joint vibration instrument development program of 1934[1] to include a detailed theoretical and empirical investigation of the vibration of single and double row radial aircraft engines. Because of space limitations the detailed research program will not be given in the present paper. Instead, the results and conclusions of the work will be presented with a brief qualitative discussion. Detailed consideration of the theory and analysis methods will be found in the references cited and in forthcoming publications

INERTIA FORCING FUNCTIONS IN RADIAL ENGINES

Alternating "forcing functions" causing vibration of an airplane engine installation originate largely within the engine itself. Forcing functions in internal combustion engines may be due to accelerations of the moving parts, or to gas pressure reactions on the engine frame; if the power plant as a whole is considered, mechanical and aerodynamic unbalances in the airplane propeller must also be considered.

Due to the intimate interconnection between the moving parts of an aircraft engine, it is possible to express the motion of any moving part in terms of a single common variable. For instance, a given position of crank rotation immediately defines the position of all other parts of the mechanism. Since the majority of aircraft engines are of the four-cycle type, the crank angle must change through 720° before an engine cycle is completed, and the basic motions of the engine must be considered as having a corresponding two-revolution

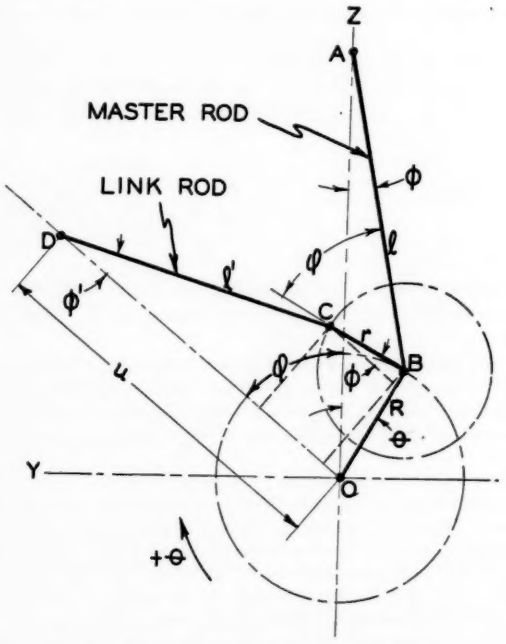

FIG. 1. Articulated Connecting Rod Linkage.

period. Once the positions of each part have been expressed in terms of a single variable, the time derivatives of the positions may be obtained in terms of this variable and its time derivatives. Thus, at each instant in the engine cycle, the displacement, velocity, and acceleration (either angular or linear) of every moving part may be evaluated.

Presented at the Power Plants Session, Seventh Annual Meeting, I. Ae. S., January 26, 1939.

* This paper represents an extended research program in which C. S. Draper and E. S. Taylor of the Massachusetts Institute of Technology collaborated; the test work was carried out at the Naval Aircraft Factory in Philadelphia with the assistance of the personnel of the Aeronautical Engine Laboratory and the Physical Test Laboratory.

† Part II will appear in the June issue of this Journal.

Each moving part in an engine must have a force acting on it equal in magnitude and direction to its time rate of change of momentum. It is only necessary to sum algebraically the time rate of change of momentum of all engine components along and around each axis to obtain the resultant forcing functions acting on the engine frame. The forces and couples resulting due to accelerations of the moving parts only are termed *inertia forces and couples*. The moving parts generating inertia forcing functions are primarily those constituting the piston and connecting rod systems. In the ideal radial engine, where the connecting rods individually center on the crank pin, the alternating forces due to the piston and connecting rod motions can be shown to be balanced by a single counterweight on the crankshaft.

For purposes of strength and simplicity, modern radial engine designs employ "articulated" connecting rod systems as shown in Fig. 1. Motion of the master rod and piston is analogous to that of a single cylinder engine, the piston motion departing slightly from a true simple harmonic motion. Pistons attached to the link rods, however, are subjected to a more distorted motion. Variations of link piston motions from that of the master piston produce harmonic inertia forces on the engine parts of frequencies higher than engine revolution speed, causing vibration which cannot readily be counterbalanced by a single crankshaft counterweight.

If a single piston be considered for the moment, the motion of the unrestrained engine crankcase at any instant must be such that the center of gravity of the moving engine and piston remain fixed in space. The piston mass is a very small portion of the engine mass, however, so the motion of the unrestrained engine in space will be slight, and the piston motion in space will be substantially the same as for a rigidly mounted engine. The force required to accelerate the piston is then very nearly equal to the rate of change of momentum of the piston in a rigidly supported crankcase. This force acts, through the connecting rod, on the crankpin; this inertia force in turn produces a crank torque and a force at the crankshaft bearings. The crank torque so pro-

PLATE I

THEORETICAL FORCING FUNCTIONS ON ENGINE FRAME

SEVEN AND NINE CYLINDER RADIAL ENGINE
(DIRECT DRIVE) *

INERTIA FORCING FUNCTIONS
(APPLICABLE TO ANY SINGLE ROW RADIAL ENGINE)

		TRANSLATIONAL		TORSIONAL				
	X AXIS	Y AXIS	Z AXIS	X AXIS			Y AXIS	Z AXIS
HARMONIC ORDER OF ENGINE REVOLUTIONS		INERTIA FORCE DUE TO RECIPROCATING PARTS	INERTIA FORCE DUE TO RECIPROCATING PARTS	COUPLE DUE TO CRANK TURNING MOMENT OF INERTIA FORCE	COUPLE DUE TO INERTIA COUPLE	COUPLE DUE TO CORRECTING COUPLE		
1	SMALL CYLINDER EXPLOSION FREQUENCY MAY EXIST DUE TO IMPULSIVE GAS FORCE IF OPEN EXHAUST STACKS ARE USED	$\frac{\Delta m_r \omega^2 R}{2} \sin\theta$	$\frac{\Delta m_r \omega^2 R}{2} \cos\theta$	$K\omega^2\frac{S^2}{2}\left[1+\frac{3}{8}(p^2+s^2q^2)\right]\sin\theta$ *	$I_r\omega^2[q]\sin\theta$	$C\omega^2 sq\left[1+\frac{1}{8}(2p^2+s^2q^2)\right]\sin\theta$	LARGE EXHAUST GAS IMPULSE TORQUE OF FIRST ORDER EXISTS IF OPEN STACKS ARE USED - SEE TEXT	
2		$m_r\omega^2 Rhsq\left[1+\frac{3}{8}(p^2+s^2q^2)\right]\sin 2\theta$	$-m_r\omega^2 Rhsq\left[1+\frac{3}{8}p^2\right]\cos 2\theta$	$\frac{K}{32}\omega^2 sq(q^2+6p^2)\sin 2\theta$ *	$-I_r\omega^2\left[\frac{S^2}{2}+\frac{1}{8}q^2\right]\sin 2\theta$ *	$C\omega^2\frac{S^2}{2}q^2\left[1+\frac{3}{4}p^2\right]\sin 2\theta$ *		
3				$-\frac{3}{16}K\omega^2 s^2q^2p^2\sin 3\theta$ *	$I_r\omega^2\left[\frac{3}{8}q^2\right]\sin 3\theta$	NEGLIGIBLE		
4		$-m_r\omega^2\frac{Rh}{2}s^2q^2\sin 4\theta$	$m_r\omega^2 Rhs^2q^2\cos 4\theta$	$\frac{1}{4}K\omega^2 sq^2\left(1+2s+\frac{3}{2}s^2\right)\sin 4\theta$ *	$I_r\omega^2\left[\frac{1}{4}q^2\right]\sin 4\theta$ *	NEGLIGIBLE		

GAS PRESSURE FORCING FUNCTIONS *
(APPLICABLE ONLY TO SEVEN CYLINDER RADIAL ENGINE)

	TORSIONAL X AXIS			
HARMONIC ORDER OF ENGINE REVOLUTIONS	COEFFICIENT $\sin(\frac{n}{2}\theta)$ a'_{n_x} *	COEFFICIENT $\cos(\frac{n}{2}\theta)$ b'_{n_x} *	HARMONIC AMPLITUDE C_{n_x} *	PHASE ANGLE λ_{n_x}
½	-0.003	-0.006	-0.007	67
1	0.014	0.064	-0.056	255
1½	0.014	-0.014	-0.020	135
2	-0.072	-0.024	-0.076	20
2½	-0.041	0.030	-0.051	320
3	0.009	0.003	-0.009	200
3½	-0.517	0.446	-0.674	320
4	-0.002	0.004	-0.004	290
4½	0.064	-0.066	-0.078	130
5	-0.003	-0.021	-0.021	80
5½	-0.014	0.026	-0.038	290
6	0.005	0.023	-0.024	260
6½	0.008	-0.004	-0.009	150
7	0.066	0.126	-0.134	240
10½	0.049	0.000	-0.049	180
14	00.006	-0.020	-0.021	105

COORDINATE SYSTEM

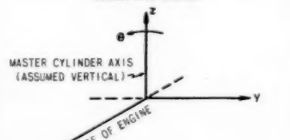

NOTE: IF MASTER CYLINDER IS NOT LOCATED AT TOP OF ENGINE, FORCING FUNCTION VALUES ARE VALID IF THE COORDINATE SYSTEM IS CONSIDERED AS A SYSTEM OF ENGINE AXES, THE Z AXIS LYING ON THE MASTER CYLINDER CENTERLINE

GEARED ENGINES *

ALL GAS PRESSURE TORQUE REACTIONS AND INERTIA TORQUES INDICATED BY STARS MUST BE MULTIPLIED BY $\sqrt{\sigma}$ WHERE

$$\sigma = \frac{\text{PROPELLER SPEED}}{\text{ENGINE SPEED}}$$

OTHER FUNCTIONS REMAIN UNCHANGED. σ IS POSITIVE IF PROPELLER AND CRANKSHAFT ROTATE IN THE SAME DIRECTION

ALL SYMBOLS ARE DEFINED ON PLATE III

MASTER WEIGHT (FOR COUNTERBALANCE PURPOSES) $= (m_r h/z + M_a + \Delta m_r/z)g$

GAS PRESSURE FORCING FUNCTIONS *
(APPLICABLE ONLY TO NINE CYLINDER RADIAL ENGINE)

	TORSIONAL X AXIS			
HARMONIC ORDER OF ENGINE REVOLUTIONS	COEFFICIENT $\sin(\frac{n}{2}\theta)$ a'_{n_x} *	COEFFICIENT $\cos(\frac{n}{2}\theta)$ b'_{n_x} *	HARMONIC AMPLITUDE C_{n_x} *	PHASE ANGLE λ_{n_x}
½	0.006	-0.001	-0.006	170
1	-0.006	0.066	-0.066	275
1½	0.003	-0.002	-0.004	145
2	-0.063	-0.022	-0.067	20
2½	0.020	-0.004	-0.020	170
3	-0.017	0.002	-0.017	350
3½	-0.009	0.034	-0.035	255
4	-0.003	-0.003	-0.004	45
4½	-0.162	0.385	-0.418	290
5	-0.017	0.000	-0.017	0
5½	0.011	-0.062	-0.063	100
6	0.000	-0.013	-0.013	90
6½	-0.011	0.014	-0.018	320
7	0.000	-0.008	-0.008	90
9	0.068	0.044	-0.081	210
13½	0.022	-0.020	-0.030	135
18	-0.009	-0.013	-0.016	55

PLATE II

THEORETICAL CRANKSHAFT FORCING FUNCTIONS

SEVEN AND NINE CYLINDER RADIAL ENGINES
(DIRECT DRIVE OR GEARED) *

INERTIA FORCING FUNCTIONS (APPLICABLE TO ANY SINGLE ROW RADIAL ENGINE)			
HARMONIC ORDER OF ENGINE REVOLUTIONS	COUPLE DUE TO CRANK TURNING MOMENT OF INERTIA FORCE	COUPLE DUE TO INERTIA COUPLE	COUPLE DUE TO CORRECTING COUPLE
1	$-K\omega^2\frac{p^2}{2}\left[1+\frac{3}{8}(p^2+s^2+q^2)\right]\sin\theta$		
2	$-\frac{K}{32}\omega^2 sq(q^2+6p^2)\sin 2\theta$	$I_c\omega^2\left[\frac{3^2}{2}+\frac{5^2}{8}\right]\sin 2\theta$	$-C\omega^2\frac{3^2}{2}\left[1+\frac{3}{2}p^2\right]\sin 2\theta$
3	$\frac{3}{16}K\omega^2 s^2q^2p^2\sin 3\theta$		
4	$-\frac{K}{2}\omega^2 sq\left[1+2s+\frac{3^2}{2}+s^2\right]\sin 4\theta$	$-\frac{1}{4}I_c\omega^2\left[q^2\right]\sin 4\theta$	NEGLIGIBLE

NOTE SEE PLATE III FOR DEFINITION OF SYMBOLS

* THE FORCING FUNCTIONS ACTING ON THE CRANKSHAFT ARE UNCHANGED BY PROPELLER GEARING. THE TORQUE ACTING AT THE PROPELLER IS GREATER THAN THE VALUES GIVEN ABOVE BY THE RATIO OF ENGINE SPEED TO PROPELLER SPEED.

GAS PRESSURE FORCING FUNCTION TORQUE IS GIVEN BY THE RELATION:

$$T_p = G_o\sum G_{nn}\sin\left(n\frac{\theta}{2}+\lambda_{nn}\right)$$

WHERE: G_o = MEAN GAS PRESSURE TORQUE AT GIVEN ENGINE SPEED
$n = 1\ 2\ 3$, ETC

GAS PRESSURE FORCING FUNCTIONS				
	7 CYLINDERS		9 CYLINDERS	
HARMONIC ORDER OF ENGINE REVOLUTIONS	HARMONIC AMPLITUDE G_{nn}	PHASE ANGLE λ_{nn}	HARMONIC AMPLITUDE G_{nn}	PHASE ANGLE λ_{nn}
½	0.007	67	0.006	170
1	0.056	255	0.056	275
1½	0.020	135	0.004	145
2	0.076	20	0.067	20
2½	0.051	320	0.020	170
3	0.009	200	0.017	350
3½	0.674	320	0.035	285
4	0.004	290	0.004	45
4½	0.078	130	0.418	290
5	0.021	80	0.017	0
5½	0.038	290	0.063	100
6	0.023	260	0.013	90
6½	0.009	150	0.018	310
7	0.134	240	0.008	90
9			0.081	210
10½	0.049	180		
13½			0.030	135
14	0.021	105		
18			0.016	55

PLATE III

THEORETICAL FORCING FUNCTIONS ON ENGINE FRAME

FOURTEEN AND EIGHTEEN CYLINDER TWO ROW RADIAL ENGINE
(DIRECT DRIVE) *
MASTER RODS LOCATED 180° APART

INERTIA FORCING FUNCTIONS (APPLICABLE TO ANY DOUBLE ROW RADIAL ENGINE NOTE 3)									
	TRANSLATIONAL			TORSIONAL					
	X AXIS	Y AXIS	Z AXIS	X AXIS			Y AXIS	Z AXIS	
HARMONIC ORDER OF ENGINE REVOLUTIONS				COUPLE DUE TO CRANK TURNING MOMENT OF INERTIA FORCE	COUPLE DUE TO INERTIA COUPLE	COUPLE DUE TO CORRECTING COUPLE	COUPLE DUE TO RECIPROCATING PARTS LARGE 2½ ORDER COUPLE EXISTS IF OPEN STACKS ARE USED - SEE TEXT	COUPLE DUE TO RECIPROCATING PARTS	
1	SMALL CYLINDER EXPLOSION FREQUENCY MAY EXIST DUE TO IMPULSIVE GAS FORCE IF OPEN STACKS ARE USED	ALL FORCES BALANCE OUT BETWEEN TWO BANKS SEE NOTE 1		$K\omega^2\frac{p^2}{2}\left[1+\frac{3}{8}(p^2+s^2+q^2)\right]\sin\theta$ *	$-2I_c\omega^2 q\sin\theta$ *	$2C\omega^2 sq\left[1+\frac{3}{2}(2p^2+s^2+q^2)\right]\sin\theta$ *	$\left[\frac{am_p\omega^2R}{2}\cos\theta\right]D$ SEE NOTE 2	$\left[\frac{am_p\omega^2R}{2}\sin\theta\right]D$ SEE NOTE 2	
2				$\frac{K}{32}\omega^2 sq(q^2+6p^2)\sin 2\theta$ *	$-I_c\omega^2\left[q^2+\frac{3^2}{4}\right]\sin 2\theta$ *	$C\omega^2 s^2q^2\left[1+\frac{3}{2}p^2\right]\sin 2\theta$ *	$\frac{m_p}{2}\omega^2 RhD sq\left[1+\frac{3}{8}(p^2+s^2+q^2)\right]\cos 2\theta$	$-\frac{m_p}{2}\omega^2 RhD sq\left[1+\frac{3}{8}(p^2+s^2+q^2)\right]\sin 2\theta$	
3				$-\frac{3}{16}K\omega^2 s^2q^2p^2\sin 3\theta$ *	$I_c\omega^2\left[\frac{3}{2}q^2\right]\sin 3\theta$ *	NEGLIGIBLE			
4				$\frac{K}{2}\omega^2 sq\left[1+2s+\frac{3^2}{2}+s^2\right]\sin 4\theta$ *	$I_c\omega^2\left[\frac{1}{2}q^2\right]\sin 4\theta$ *	NEGLIGIBLE	$\frac{m_p}{4}\omega^2 RhD s^2q^2\cos 4\theta$	$\frac{m_p}{4}\omega^2 RhD s^2q^2\sin 4\theta$	

COORDINATE SYSTEM

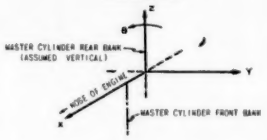

NOTE: IF MASTER CYLINDER, REAR BANK, IS NOT LOCATED AT TOP OF ENGINE, FORCING FUNCTION VALUES ARE VALID IF THE COORDINATE SYSTEM IS CONSIDERED AS A SYSTEM OF ENGINE AXES. THE Z AXIS LYING ON THE CENTERLINE OF THE MASTER CYLINDER, REAR BANK

DEFINITION OF SYMBOLS

h = TOTAL NUMBER OF CYLINDERS IN ENGINE
R = CRANK THROW RADIUS
l = MASTER ROD LENGTH BETWEEN BEARINGS
l' = LINK ROD LENGTH BETWEEN BEARINGS
r = AVERAGE WRIST PIN RADIUS ON MASTER ROD
G_o = MEAN ENGINE TORQUE AT GIVEN ENGINE SPEED
k' = RADIUS OF GYRATION OF LINK ROD ABOUT ITS CENTER OF GRAVITY
θ = ANGLE OF ROTATION OF CRANK FROM MASTER ROD AXIS
b'_c = DISTANCE OF MASTER ROD CENTER OF GRAVITY FROM PISTON BEARING, WITH LINK ROD PINS AND NUTS IN PLACE
ω = ANGULAR VELOCITY OF CRANK
M_c = MASS OF MASTER ROD WITH LINK PIN AND NUTS IN PLACE
I_c = MOMENT OF INERTIA OF THE MASTER ROD, LINK PINS AND NUTS, AND LOWER END OF LINK RODS ABOUT THE COMBINATION CENTER OF GRAVITY, LESS THE MOMENT OF INERTIA OF ONE LINK ROD ABOUT THE SAME POINT.
Δm_p = EXCESS MASS AT PISTON END OF MASTER ROD
D = DISTANCE BETWEEN CENTERLINES OF CYLINDER BANKS
GAS PRESSURE FORCING FUNCTION = $G_o\sum G_{nn}\sin\frac{n}{2}\theta + G_o\sum G_{nn}\cos\frac{n}{2}\theta - G_o\sum G_{nn}\sin(\frac{n}{2}\theta+\lambda_{nn})$ $n=1,2,3,$ etc.
M = MASS OF LINK ROD.
$p = R/l'$ $q = R/l$ $s = r/l'$

$m_p = M(l'-b')/l' +$ PISTON MASS
$M_c = M(h-1)b'/l' + M_c b'_c/l'$
$R = m_p r\omega^2$
$C = M(-k'^2+b'l'-b'^2)\omega^2/l'$

SPECIAL NOTES

NOTE 1: COUNTERBALANCE FOR MASTER WEIGHT = $(m_p b'_c + M_c + \Delta m_p R)g$ IN EACH BANK REMOVES FIRST ORDER UNBALANCE IN EACH BANK, AND ALSO BALANCES COUPLES ABOUT (Y) AND (Z) DUE TO THIS AMOUNT OF UNBALANCE. THE INERTIA FORCE OF REVOLVING PARTS IS ALSO REMOVED BY THE COUNTERBALANCES. FORCES DUE TO EXCESS WEIGHT OF MASTER ROD AT PISTON END BALANCE OUT BETWEEN BANKS, LEAVING COUPLES ABOUT (Y) AND (Z) AXES.

NOTE 2: THE ALGEBRAIC SIGN SHOWN IS CORRECT FOR CYLINDER #1 IN REAR BANK. IF CYLINDER #1 IS IN FRONT BANK, SIGN MUST BE CHANGED

NOTE 3: THE INERTIA FORCING FUNCTIONS ARE APPLICABLE TO ANY DOUBLE ROW RADIAL ENGINE HAVING CRANK THROWS AND MASTER RODS 180° APART AND ARTICULATED CONNECTING RODS. THE GAS PRESSURE FORCING FUNCTIONS APPLY ONLY TO FOURTEEN OR EIGHTEEN CYLINDER DOUBLE ROW RADIAL ENGINES HAVING MASTER RODS AND CRANK THROWS AT 180°

GAS PRESSURE FORCING FUNCTIONS * (APPLICABLE ONLY TO FOURTEEN CYLINDER DOUBLE ROW RADIAL ENGINE - SEE NOTE 3)				
	TORSIONAL X AXIS			
HARMONIC ORDER OF ENGINE REVOLUTIONS	* COEFFICIENT $\sin(n\frac{\theta}{2})$ a_n	* COEFFICIENT $\cos(n\frac{\theta}{2})$ b_n	HARMONIC AMPLITUDE G_{nn} *	PHASE ANGLE λ_{nn}
1	0.014	0.104	-0.066	255
2	-0.072	-0.084	-0.098	20
3	0.009	0.003	-0.009	200
4	-0.002	0.004	-0.005	290
5	-0.003	-0.001	+0.001	80
6	0.005	0.023	-0.024	260
7	0.068	0.116	-0.134	240
14	0.008	-0.020	-0.021	105

GAS PRESSURE FORCING FUNCTIONS * (APPLICABLE ONLY TO EIGHTEEN CYLINDER DOUBLE ROW RADIAL ENGINE - SEE NOTE 3)				
	TORSIONAL X AXIS			
HARMONIC ORDER OF ENGINE REVOLUTIONS	* COEFFICIENT $\sin(n\frac{\theta}{2})$ a_n	* COEFFICIENT $\cos(n\frac{\theta}{2})$ b_n	HARMONIC AMPLITUDE G_{nn} *	PHASE ANGLE λ_{nn}
1	-0.006	0.056	-0.056	275
2	-0.065	-0.087	-0.087	20
3	-0.019	0.007	-0.021	350
4	-0.003	-0.003	-0.004	45
5	-0.017	0.000	-0.017	0
6	0.000	-0.013	-0.013	90
7	0.000	-0.008	-0.008	90
9	0.068	0.044	-0.081	210
18	-0.009	-0.013	-0.016	55

GEARED ENGINES *

ALL GAS PRESSURE TORQUE REACTIONS AND INERTIA TORQUES INDICATED BY STARS MUST BE MULTIPLIED BY σ WHERE:

$\sigma = \frac{\text{PROPELLER SPEED}}{\text{ENGINE SPEED}}$

OTHER FUNCTIONS REMAIN UNCHANGED

σ IS POSITIVE IF PROPELLER AND CRANKSHAFT ROTATE IN THE SAME DIRECTION

PLATE IV

THEORETICAL CRANKSHAFT FORCING FUNCTIONS

FOURTEEN AND EIGHTEEN CYLINDER DOUBLE ROW RADIAL ENGINES
(DIRECT DRIVE OR GEARED) *

MASTER RODS LOCATED AT 180° APART

INERTIA FORCING FUNCTIONS (APPLICABLE TO ANY DOUBLE ROW RADIAL ENGINE)			
HARMONIC ORDER OF ENGINE REVOLUTIONS	COUPLE DUE TO CRANK TURNING MOMENT OF INERTIA FORCE	COUPLE DUE TO INERTIA COUPLE	COUFLE DUE TO CORRECTING COUPLE
1	$-K\omega^2\frac{p^2}{2}\left[1+\frac{3}{8}(p^2+s^2+q^2)\right]\sin\theta$		
2	$-\frac{K}{32}\omega^2 sq(q^2+6p^2)\sin 2\theta$	$I_c\omega^2\left[q^2+\frac{3^2}{4}\right]\sin 2\theta$	$-C\omega^2 s^2q^2\left[1+\frac{3}{2}p^2\right]\sin 2\theta$
3	$\frac{3}{16}K\omega^2 s^2q^2p^2\sin 3\theta$		
4	$-\frac{K}{2}\omega^2 sq\left[1+2s+\frac{3^2}{2}+s^2\right]\sin 4\theta$	$-\frac{1}{2}I_c\omega^2\left[q^2\right]\sin 4\theta$	NEGLIGIBLE

NOTE SEE PLATE III FOR DEFINITION OF SYMBOLS

* THE FORCING FUNCTIONS ACTING ON THE CRANKSHAFT ARE UNCHANGED BY PROPELLER GEARING. THE TORQUE ACTING AT THE PROPELLER IS GREATER THAN THE VALUES GIVEN ABOVE BY THE RATIO OF ENGINE SPEED TO PROPELLER SPEED.

GAS PRESSURE FORCING FUNCTIONS				
	14 CYLINDERS		18 CYLINDERS	
HARMONIC ORDER OF ENGINE REVOLUTIONS	HARMONIC AMPLITUDE G_{nn}	PHASE ANGLE λ_{nn}	HARMONIC AMPLITUDE G_{nn}	PHASE ANGLE λ_{nn}
1	0.056	255	0.056	275
2	0.076	20	0.067	20
3	0.009	200	0.017	350
4	0.004	290	0.004	45
5	0.021	80	0.017	0
6	0.023	260	0.013	90
7	0.134	240	0.008	90
9			0.081	210
14	0.021	105		
18			0.016	55

GAS PRESSURE FORCING FUNCTION TORQUE IS GIVEN BY THE RELATION:

$$T_p = G_o\sum G_{nn}\sin\left(n\frac{\theta}{2}+\lambda_{nn}\right)$$

WHERE: G_o = MEAN GAS PRESSURE TORQUE AT GIVEN ENGINE SPEED
$n = 1\ 2\ 3$, ETC

duced must have an equal and opposite reaction on the crankcase, through the piston-cylinder contact surface. Vibration couples from this source are termed *couples due to crank turning moment of inertia force.*

As the mass of the master connecting rod swings back and forth in the engine cycle, acceleration *couples due to the inertia couple* of the swinging rod react on the engine frame. Angular motions of the link rods also contribute to alternating couples on the crankcase, which may be considered as a correction to the main inertia couple; these are conveniently classed as *couples due to the correcting couple.*

Detailed mathematical discussion of the derivation of these various engine forces and couples is a problem dealing largely with the mathematics of infinite series and is too voluminous for inclusion in this paper. References 2, 3, 4, 5, 6, and 7 show parts of the derivation. Instead, results of the mathematical work have been summarized in Plate I for any conventional single row radial engine. Using the symbols as defined on Plate III, and any consistent system of units, the inertia forcing functions for a radial engine of any odd number of cylinders may be calculated for harmonics of engine speed of order 1, 2, 3, and 4. Higher harmonic orders are of negligible magnitude.

Gas Pressure Torques

Useful crank torque is the sum of a series of explosive efforts from the individual cylinders. Torque reaction on the engine crankcase must, therefore, also be non-uniform and give rise to forcing couples on both crankshaft and engine frame. Calculation of the forcing functions arising from gas torque fluctuations has been described for 7, 9, 14, and 18 cylinder engines in an earlier paper.[8] Harmonic components of gas pressure torque reactions for 7 and 9 cylinders expressed in per cent of mean gas torque are included in Plate I.

The net theoretical forcing functions acting on the radial engine due to both gas pressure reactions and dynamic unbalances may be obtained by addition of the forcing functions from each source.

Crankshaft Torque—Gearing

Not all of the torques acting on the engine frame act on the crankshaft. For convenience in design of single row engine crankshafts, crankshaft forcing functions have been summarized in Plate II.

Propeller torque in a geared engine is greater than the crankshaft torque by the inverse of the gear ratio σ. Since the reaction to propeller torque must be furnished by the engine frame and mount structure, the crankshaft torque reactions on the engine *crankcase* must be multiplied by $1/\sigma$ as indicated in Plate I by the starred functions; the additional torque reaction reaches the engine frame through the reduction gear bearings. In a planetary gear system where propeller and shaft rotate in the same direction σ should be considered positive; for opposite rotations σ is negative.

Additional Effects—Open Exhaust Stacks

In most modern engine installations, some type of exhaust collector system is furnished. The exhaust gases from all cylinders are then forced to leave the engine at one or two points, and any gas impulse reactions will act along the exit axis; such impulses have small effect. With open exhaust stacks, however, the burned gases leave the engine at several points around the engine circumference. The moment arm between the direction of gas flow and the engine center of gravity is sufficiently large that definite forcing torques occur about axes in the cylinder plane, as well as smaller alternating forces along the thrust axis. The net effect of gas jet impulse reactions from all cylinders may be found by addition of component reactions from each cylinder. Individual cylinder reactions may be predicted approximately by gas impulse theory from actual indicator cards and valve opening data. This procedure is shown diagrammatically in Fig. 2 for a single aircraft cylinder; the combined curve for exhaust impulse forcing torques about the engine spanwise axis is plotted in Fig. 3. Harmonic analysis of Fig. 3 shows

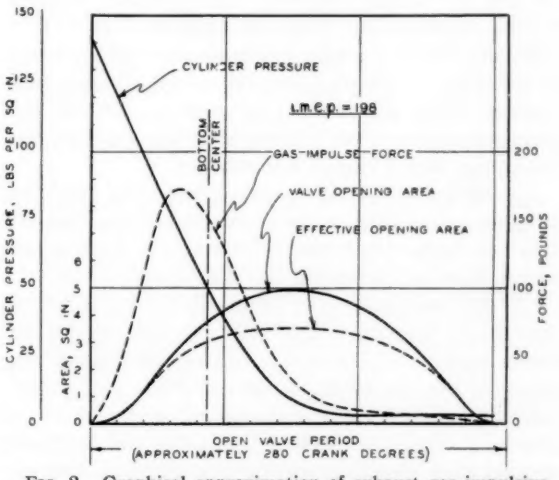

FIG. 2. Graphical approximation of exhaust gas impulsive force. Gas impulsive force = (effective valve opening area) × (cylinder pressure) at each crank position

the principle components to be of engine revolution frequency and $(N \pm 1)$ where N is the cylinder explosion frequency.

Double Row Radial Engines

Single row radial engine theory may be applied directly to the double row engine, by combination of single row forces and torques acting in two parallel planes, with proper phase angle consideration. Modern twin row construction customarily disposes the master rods in the two banks in cylinders diametrically op-

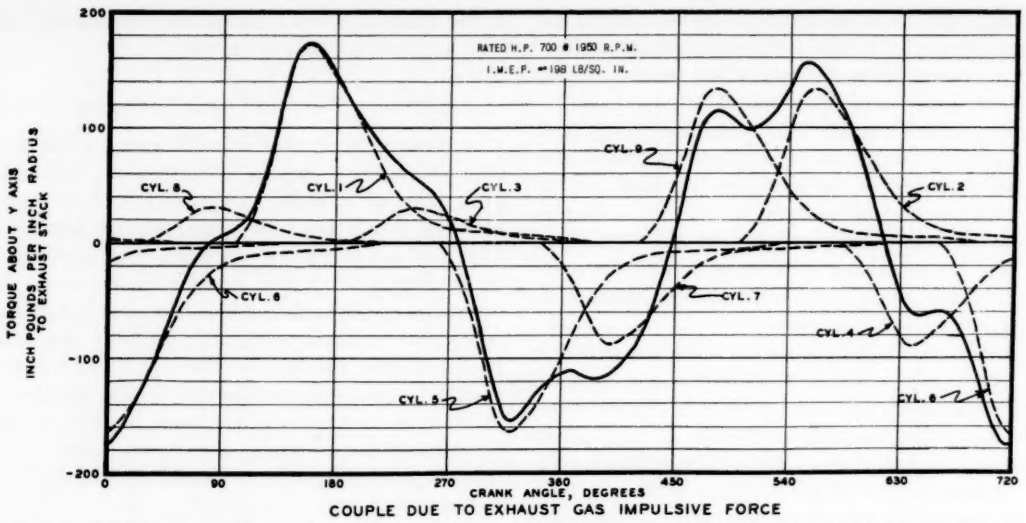

FIG. 3. Graphical summation of exhaust gas torque impulse efforts from each cylinder of a nine cylinder radial engine to determine net exhaust impulse effort.

posed, the master cylinders firing 360 crank degrees apart. Theoretical forcing functions for the two row engine crankcase and engine crankshaft for this particular arrangement are presented in Plates III and IV for 14 and 18 cylinder engines. Gas pressure reaction forcing functions for twin row engines of 14 and 18 cylinders with any master rod disposition may be found in reference 1. Plates I and III permit a comparison between single and double row engines. Double row arrangements have two definite advantages and one disadvantage from a vibration standpoint:

(1) All linear forcing functions from the twin row cylinder banks balance out at any instant, so that the two row engine (with master rods at 180°) has no net forcing functions along the X, Y, or Z axes.

(2) All fractional order harmonic forcing functions due to gas pressure torque reactions balance out between banks. Theoretically, this torque balance also exists in the crankshaft torques of Plate IV; practically, the shaft flexibility will permit torque efforts of fractional orders to reach the propeller and in geared engines even pass through the gear bearings into the crankcase.

(3) Inertia forces from the parallel cylinder planes combine to produce inertia couples about the Y and Z engine axes which did not exist in the single row design.

Torque reaction harmonics appearing in the double row unit are the same percentage of mean engine torque as for the single row engine of equivalent power. Balancing out of the fractional order gas pressure harmonics, however, removes the largest gas component of single row explosion frequency and thereby reduces the *major* twin row gas harmonic component to about 20 percent of that in the single row engine of equivalent power. In addition, the frequency of the major torque component is double that of the single row engine.

Numerical Examples

Comparison of the advantages of single and double row constructions, and of the relative magnitudes of the various forces and couples can best be made by reference to numerical examples. Two typical engines of approximately equal power ratings were selected for study. One was a 9 cylinder single row engine delivering 525 hp. at 1900 r.p.m.; the other was a 14 cylinder twin row radial engine rated at 625 hp. at 2200 r.p.m. Both engines were assumed to operate under fixed pitch propeller loads. This limits the gas torque and torque harmonic components to magnitudes which are proportional to the square of the engine speed.

Calculated vibration forces and torques for the two engines are itemized in Tables 1 and 2. Components of the same frequencies but due to different sources have not been combined so that the relative importance of the expressions in Plates I and III can be observed. If f is the engine revolution speed in revolutions per second, the tables give forces directly in pounds and torques in inch-pounds at any selected engine operating speed.

Several of the components included in the tables are of much smaller magnitude than the reasonable errors in the larger functions. They have been included, however, to show the relative magnitudes even of the forces and torques which may normally be neglected.

Limitations of the Theory

Theoretical prediction of forcing functions in radial engines with articulated connecting rod systems is subject to certain limitations. Aircraft engines rarely operate under ideal conditions, and all engine accessories do not function as perfectly as the theory assumes. Hence, some differences are to be expected when empirical verification of the theory is attempted.

TABLE 1

9 Cylinder Single Row Radial Aircraft Engine Forcing Functions
Rated hp = 525 at 1900 r.p.m.
Fixed Pitch Propeller Load

	Order n	Harmonic Forcing Function Coefficient: Pounds or Inch Pounds Sin $n\theta$	Cos $n\theta$	Source
		Forces		
X Axis	$4\frac{1}{2}$		$.024\ f^2$*	Open exhaust stacks
Y Axis	1	$0.143\ f^2$		Inertia force due to reciprocating parts
	2	$1.53\ f^2$		
	4	$-0.003\ f^2$		
Z Axis	1	$0.143\ f^2$		Inertia force due to reciprocating parts
	2	$-1.53\ f^2$		
	4	$0.003\ f^2$		
		Couples		
X Axis	1	$2.60\ f^2$		Couple due to crank turning moment of inertia forces
	2	$0.06\ f^2$		
	3	$-0.61\ f^2$		
	4	$0.08\ f^2$		
	1	$-10.05\ f^2$		Couple due to inertia couple
	2	$-1.27\ f^2$		
	3	$0.23\ f^2$		
	4	$0.04\ f^2$		
	1	$1.58\ f^2$		Couple due to correcting couple
	2	$0.05\ f^2$		
	1	$-0.21\ f^2$	$+1.00\ f^2$	Gas pressure torque reaction
	2	$-1.43\ f^2$	$-0.53\ f^2$	
	$2\frac{1}{2}$	$0.27\ f^2$	$-1.60\ f^2$	
	$3\frac{1}{2}$	$-0.56\ f^2$	$+0.56\ f^2$	
	$4\frac{1}{2}$	$-3.84\ f^2$	$+7.64\ f^2$	
	$5\frac{1}{2}$	$0.15\ f^2$	$-1.39\ f^2$	
	9	$1.41\ f^2$	$+0.92\ f^2$	
	$13\frac{1}{2}$	$0.46\ f^2$	$+0.42\ f^2$	
Y Axis	1	$0.14\ f^2$*	$-2.16\ f^2$*	Exhaust gas reaction, open stacks
	$3\frac{1}{2}$	$-0.16\ f^2$*	$-0.34\ f^2$*	
	$5\frac{1}{2}$	$0.12\ f^2$*	$-0.04\ f^2$*	
Z Axis	1	$-2.21\ f^2$*	$-0.10\ f^2$*	Exhaust gas reaction, open stacks
	$3\frac{1}{2}$	$0.40\ f^2$*	$-0.22\ f^2$*	
	$5\frac{1}{2}$	$-0.04\ f^2$*	$-0.10\ f^2$*	

* Very Approximate—does not exist with exhaust manifold systems. f is engine speed in revolutions per second to get functions in pounds or in inch-pounds.

TABLE 2

14 Cylinder Double Row Radial Aircraft Engine Forcing Functions
Rated hp. = 625 at 2200 r.p.m.
Fixed Pitch Propeller Load

	Order n	Harmonic Forcing Function Coefficient: Pounds or Inch Pounds Sin $n\theta$	Cos $n\theta$	Source
		Forces		
X Axis	7		$0.006\ f^2$*	Open Exhaust Stack
Y Axis	No Forcing Functions			
Z Axis	No Forcing Functions			
		Couples		
X Axis	1	$1.69\ f^2$		Couple due to crank turning moment of inertia forces
	2	$0.005\ f^2$		
	3	$-0.008\ f^2$		
	4	$0.059\ f^2$		
	1	$-4.27\ f^2$		Couple due to inertia couple
	2	$-0.54\ f^2$		
	3	$0.10\ f^2$		
	4	$0.017\ f^2$		
	1	$0.33\ f$		Couple due to correcting couple
	2	$0.02\ f$		
	1	$0.23\ f^2$	$+0.88\ f^2$	Gas pressure torque reaction
	2	$-1.18\ f^2$	$-0.39\ f^2$	
	7	$1.08\ f^2$	$+1.90\ f^2$	
	14	$0.10\ f^2$	$-0.33\ f^2$	
Y Axis	1		$0.11\ f^2$	Inertia couples
	2		$3.77\ f^2$	
	4		$0.01\ f^2$	
	$2\frac{1}{2}$	$0.64\ f^2$*	$0.36\ f^2$*	Exhaust reaction
	$4\frac{1}{2}$	$-0.07\ f^2$*	$0.17\ f^2$*	
Z Axis	1	$0.11\ f^2$		Inertia couples
	2	$-3.77\ f^2$		
	4	$0.01\ f^2$		
	$2\frac{1}{2}$	$-0.36\ f^2$	$0.62\ f^2$*	Exhaust reaction
	$4\frac{1}{2}$	$0.17\ f^2$	$0.07\ f^2$*	

* Approximate—does not exist with exhaust manifold systems.

The most important single factor neglected in the theoretical attack is the effect of carburetion. Any irregularity in the engine cycle, such as may be due principally to carburetion and unequal distribution of charge to the individual cylinders, or less often by faulty spark plugs or valve operation, will give rise to a half order function that far overshadows the theoretical value. Such sources, due to their transient nature, also contribute slightly to higher order harmonics.

All link pin radii on the master rod have been assumed equal except in gas torque predictions. In practice, there is a slight variation to insure the same top center position and same stroke in all cylinders, but the effect of this variation is negligible.

Important sources of error also include improper engine counterbalance, propeller unbalance, and aerodynamic effects on the propeller. In two blade propellers, variation in the moment of inertia of the engine-propeller combination as the propeller rotates may give rise to apparent forcing effects at twice propeller speed. In propellers, with three or more blades, this does not occur.

REFERENCES

[1] Draper, C. S., and Bentley, G. P., *Measurement of Aircraft Vibration in Flight*, Journal of the Aeronautical Sciences, Vol. 4, No. 4, pages 116–121, February, 1936.

[2] Bentley, G. P., *An Investigation of the Vibration of Freely Suspended Aircraft Engines of the Single and Double Row Design*, Report to Bureau of Aeronautics, June, 1937 (Complete mathematical analysis; not generally available as yet, but to be available through N.A.C.A.).

[3] Tanaka, K., *The Inertia Forces and Couples and Their Balancing of the Star Type Engine*, Report of the Aero. Res. Institute, Tokyo Imperial University, 1925.

[4] Lehr, G., *Analyse Harmonique du Couple du aux Forces d'Inertie dans les Moteurs d'Aviation a Embeillage articule*, Asso. Tech. Maritime et Aeronautique, June, 1926.

[5] Lehr, G., *Note sur un perfectionnement a l'Equilibrage des Moteurs en Etoile*, La Technique Aeronautique, April, 1931, February, 1931.

[6] Ducarme, J., *Notes et abaques sur la Cinematique des Moteurs en Etoile*, Bulletin du Service Technique de l'Aeronautique, October, 1932.

[7] Coppens, A., *Etablissement d'Expressions simples et Completes de la Valeur des Contrepoids a appliquer au coude des Machines a Piston, en particulier des Moteurs d'Aviation*, Congres de Mechanique de Liege, 1930.

[8] Bentley, G. P., and Taylor, E. S., *Gas Pressure Torque of Radial Engines*, Journal of the Aeronautical Sciences, Vol. 6, No. 1, pages 1–6, November, 1938.

A Method of Determining End Fixity

W. L. HOWLAND

California Institute of Technology

ONE of the important factors in the design of a compression member is its end fixity, for, as long as the slenderness ratio of a member is reasonably large, the load-carrying ability of the member is directly proportional to its end fixity. It is unfortunate that the few cases in which the end fixity is definitely known (theoretically) seldom occur in practice. The commonly known theoretical cases are: pin-ended columns where the end-fixity coefficient is 1.0, built-in ends where the end fixity is 4.0, and the case of one fixed end and the other pin ended which has an end fixity of 2.04. These three cases never actually occur in practice, since in pin-ended columns there is always some friction present, and built-in ends are not infinitely rigid. In a few cases of elastically built-in columns, the end fixity can be calculated theoretically, but in general the designer of an airplane does not know the conditions of the ends of his members accurately enough to be able to use these means. Until the present time the designer has had to estimate the end fixity of various panels or columns because he could not take into account the effect of clips, eccentric loading, flexibility of ribs, bulkheads, or edge restraints.

It is the object of this paper to present a method whereby the actual end fixity of a member on an airplane or in a test assembly can be determined experimentally without failing the member. Engesser's modified Euler equation for both long and short columns is

$$P_{cr} = c\pi^2 E_\sigma I/L^2 \tag{1}$$

where P_{cr} = critical load
c = coefficient of end fixity
E_σ = modulus of elasticity at the stress $\sigma = P/A$ (sometimes called tangent-modulus)
I = Moment of Inertia
L = length of member.

In the case of a stiffened panel (such as thin sheet plus stiffeners or corrugation), this equation must be written as follows:

$$P_{cr} = c\pi^2 E_\sigma I_\sigma/L^2 \tag{2}$$

where I_σ corresponds to the Moment of Inertia of the unit at the stress σ. This will be discussed at length later.

Southwell[1] has found by a good approximate theory that the deflection δ, at the center of a strut related to the load P, approximates to a rectangular hyperbola having the axis of P and the horizontal line $P = P_c$ as asymptotes (Fig. 1). Southwell and others have found very good experimental agreement with this result.

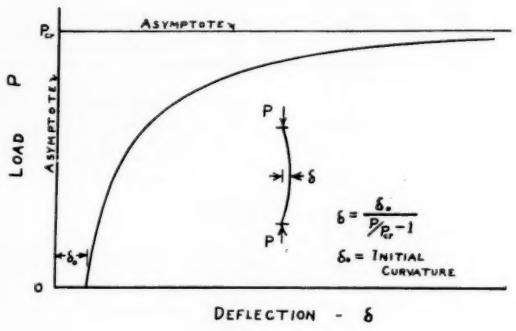

FIG. 1.

It has been proved by Timoshenko[2] that, in the most general case, in which there is initial curvature in the member and eccentricity in the application of the load, theoretically the deflection of a column at its center δ related to the load P still approximates to a rectangular hyperbola. The reason that this is so important, as Southwell pointed out, is that a rectangular hyperbola has the characteristic that, if δ/P is plotted against δ, it will give a straight line, and the inverse of the slope of this line is a measure of the height of the horizontal asymptote, or, in this case, a measure of P_{cr}. A modified form of the Southwell analysis has recently been given by Lundquist[3] and may be used in place of the Southwell method if desired.

In the Southwell and Lundquist methods, it is assumed that the Moment of Inertia of the column remains constant with an increase of load. However, in the case of an airplane panel, this is not true because of buckling of the skin. The analysis must therefore be changed in order to take this effect into account. Southwell gives the equation

$$\delta = \delta_0/[(\alpha^2 L^2/n^2\pi^2) - 1] \tag{3}$$

where $\alpha^2 = P/EI$
δ_0 = initial deflection at center of column
n = number of half waves.

Eq. (3) is valid as long as α^2 is independent of the length (*i.e.*, X). Thus one can write

$$\alpha^2 = PI_f/EI_\sigma I_f \tag{4}$$

Received January 21, 1939.

where I_f = Moment of Inertia at failure. Substituting in Eq. (3),

$$\delta = \frac{\delta_0}{(PI_f/I_o)\dfrac{L^2}{EI_f n^2\pi^2} - 1} \tag{5}$$

but $P_{cr} = \pi^2 EI_f/L^2$ for $n = 1$. Therefore,

$$\delta = \frac{\delta_0}{[(PI_f/I_o)/P_{cr}] - 1} \tag{6}$$

With this equation it can be shown, by a method similar to that used by Southwell, that if $(\delta/P)\cdot I_o/I_f$ is plotted against δ, it will give a straight line, and the inverse of the slope of this line is a measure of P_{cr} (see Fig. 2). Thus, for any combination of initial curvature, eccentricity in application of the load, end fixity, or change in moment of inertia with increase in load, the critical load of a column can be obtained without actually failing the member.

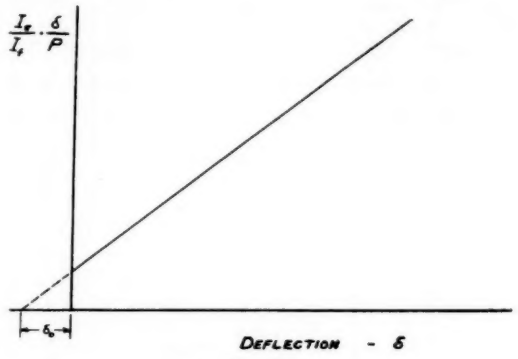

FIG. 2.

In order to be able to secure this information, one must, by some means, measure the deflection δ of the center of the column at various loads, and one must know the load in order to get δ/P. In the case of a panel, the value of I_o/I_f must also be known. Then by plotting the experimental relationship between δ and $(\delta/P)\cdot I_o/I_f$ and drawing a straight line through the points, the critical load which the column is appraching is given by the inverse slope of the straight line. The end-fixity coefficient can then be calculated by the formula

$$c = P_{cr} \text{ (experimental) } L^2/\pi^2 E_o I_f \tag{7}$$

The experimental setup is quite simple: First the load in a panel, say a panel in an airplane, can be calculated from the stress given by one or more extensometers mounted on the stiffener (in the case of a sheet-stiffener combination). Preferably the extensometers should be fastened near the neutral axis of the stiffener. In the case of a tube or rod, the load is obtained easily by averaging the extensometer readings on opposite sides, thus eliminating the deformation due to bending. The readings are then converted into stress, from which one can obtain P by multiplying by the cross-section area. Whenever this method is used, care must be taken in order to be sure that the effect of the bending stresses does not enter in the determination of the end load. In the case of a sheet-stiffener combination, the procedure for determining the load is slightly more complex than for the tube or rod, because of buckling of the sheet, making it necessary to correct the cross-section area A for the change in "effective width." This can be accomplished by using the general equation

$$P = \sigma_{stiff}\,[A_{stiff} + 2W_e t] \tag{8}$$

where P = end load, lbs.
σ_{stiff} = stiffener stress, lbs. per sq.in.
A_{stiff} = stiffener area, sq.in.
W_e = effective width, in.
t = sheet thickness, in.

If Sechler's expression[4] for the "effective width" of a stiffened sheet is used, the equation becomes

$$P = \sigma_{stiff}[A_{stiff} + 0.5bt + 1.81Et^3/\sigma_{stiff}b] \tag{9}$$

where b = stiffener spacing. This equation is valid for stiffener stresses up to approximately 20,000 lbs. per sq.in., and above this value the effective width decreases in a manner described in the above reference.

The deflection of the middle of the stiffener can be obtained by a dial gage which is located at the midpoint and is supported from each end of the stiffener (see Fig. 3), care being taken to insure that the light support frame is free to move so that the change in length of the panel does not affect the deflection readings or the load in the stiffener.

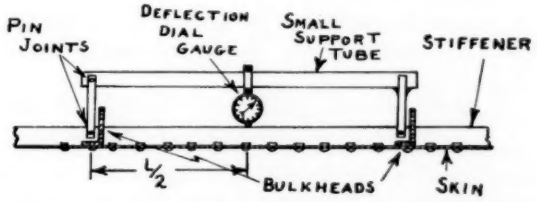

FIG. 3. Sketch of a method for measuring the normal deflection of a panel from the inside of the structure.

When calculating the theoretical critical load for obtaining the end-fixity coefficient, for the case of a sheet-stiffener combination, the value of the moment of inertia or radius of gyration must be corrected for the effect of buckling of the sheet. The author and H. B. Dickinson of the Lockheed Aircraft Corporation have developed a graphical method for solving Sechler's solution of the buckling load of a stiffened panel (see Fig. 4.). These curves are based on a value of E of 10.4×10^6 lbs. per sq.in. and should therefore only be used for aluminum alloys.

The method of using this figure is as follows: First calculate, for the panel in question, the following relations:

$$b/t,\ bt/A_0,\ s/\rho_0,$$

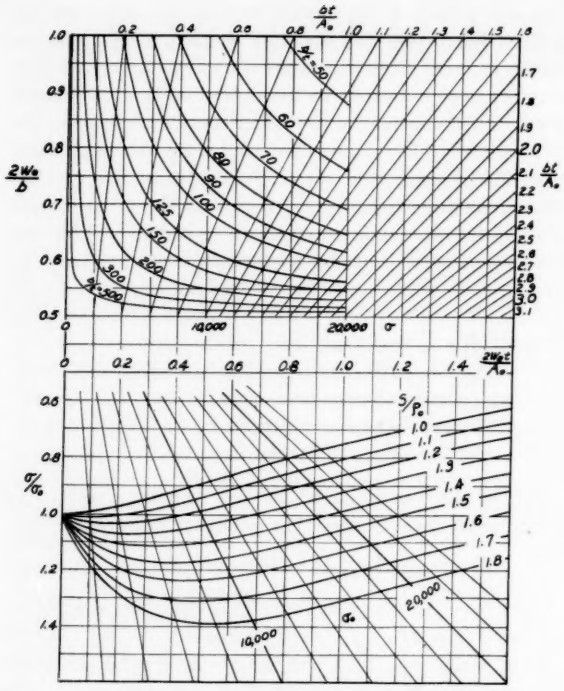

FIG. 4. Curves for obtaining the Euler load of stiffened panels.

where b = stiffener spacing
t = sheet thickness
A_0 = stiffener area
s = distance from the neutral axis of the stiffener alone to the neutral axis of the attached sheet
ρ_0 = radius of gyration of the stiffener alone about an axis parallel to the sheet.

Then calculate the Euler failing stress (for an end fixity of unity) of the stiffener alone from the equation

$$\sigma_0 = \pi^2 E(\rho_0/L)^2 \tag{10}$$

where L is the length of the panel. The critical stress of the stiffener about an axis parallel to the sheet is used because it is assumed that the stiffener cannot fail as an Euler column in the plane of the sheet. Knowing the stress σ_0, enter at the horizontal axis in the center of the figure and proceed from σ_0 vertically upward to the proper curve of b/t, then horizontally to the curve of bt/A_0, vertically downward into the lower quadrant to s/ρ_0 horizontally to σ_0 and finally vertically to a value of σ in the center of the chart, which may be called σ_1. If this value of σ_1 differs materially from σ_0, make a second approximation by proceeding from σ_1 to b/t to bt/A_0 to s/ρ_0 to σ_0 (not σ_1) and returning to σ_2. More than a second approximation is rarely necessary. The final stress σ_2 is that at which the combined column composed of stiffener and effective width will fail as an Euler column with an end fixity of 1.0. In order to obtain the load for computing the end fixity, obtain the effective width of sheet from the ordinate of the upper quadrant in Fig. 5. Move from the final value of σ_2 to b/t and horizontally to $2W_e/b$. This figure should not be used for stiffener stresses greater than 20,000 lbs. per sq.in., because the value of the effective width given by the figure above this limit is incorrect (see reference 2). If an actual panel on an airplane has an end fixity of approximately 2.0, this method will work as long as the critical stiffener stress does not exceed 40,000 lbs. per sq.in.

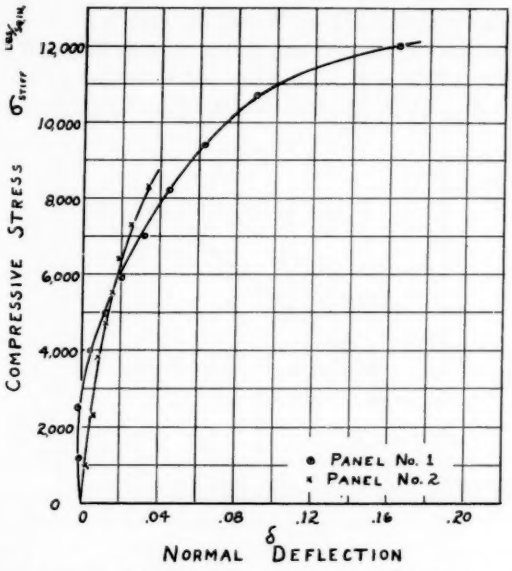

FIG. 5. Experimental curves of compressive stress against normal deflection.

To evaluate the critical stress σ_n to any approximation "n," the general equation which can be used for any value of E or stiffener stress, and which is independent of any particular method of determining effective width, is

$$\frac{\sigma_n}{\sigma_0} = \frac{1 + [1 + (S/\rho_0)^2](2W_e t/A_0)}{[1 + (2W_e t/A_0)]^2} \tag{11}$$

The method of using this equation is to calculate σ_0 as already shown, next to determine the effective width either by Sechler's method or by some other means, and then to calculate σ_1. If the value of σ_1 differs materially from σ_0, a new effective width should be determined based on σ_1 instead of σ_0, until σ_{n+1} is not much different from σ_n. Then σ_{n+1} is the critical stress of the combination sheet and stiffener. Seldom are more than two trials necessary to satisfy the above conditions. The physical meaning of Eq. (11) is that, as the sheet which is attached to the stiffener buckles, the radius of gyration of the combination changes, thus affecting the critical stress.

For the case in which the ratio between I_σ and I_f is needed, in order to obtain the critical load, Eq. (11) can be transformed into the following form:

$$\frac{I_\sigma}{I_0} = \frac{1 + (1 + (S/\rho_0)^2](2W_e t/A_0)}{1 + 2W_e t/A_0} \qquad (12)$$

where I_0 = moment of inertia of stiffener alone,
A_0 = area of stiffener,
W_e = the effective width at the stiffener stress σ.

If I_σ/I_0 is then plotted against the stiffener stress σ, the value of I_f can be obtained from the asymptote which the curve will approach. Knowing I_f, then the ratio of I_σ and I_f can be determined as a function of the stiffener stress from the curve of I_σ/I_0 against σ. Eq. (12) is similar to Eq. (11), in that it is independent of any particular method of determining effective width as a function of the stiffener stress.

As an example, consider a panel in a fuselage for which it is desired to find the end-fixity coefficient. This panel has a bulb-angle stiffener whose area = .075 sq.in., Moment of Inertia I_{xx} = .0045 in.,[4] radius of gyration ρ_{xx} = .245, and s = .2653 in. The skin thickness, t = .025 in., the distance between bulkheads, L = 24 in., and the stringer spacing, b = 7.5 in. From these data

$$b/t = 300,\ bt/A_0 = 2.5,\ s/\rho_0 = 1.082.$$

Taking E as 10.4×10^6, one obtains

$$\sigma_0 = 10{,}700 \text{ lbs. per sq.in.}$$

From the curves in Fig. 4, one finds $\sigma_1/\sigma_0 = .72$, which gives $\sigma_1 = 7700$ for a first approximation. For a second approximation one obtains $\sigma_2/\sigma_0 = .715$ or $\sigma_2 = 7650$. Let σ_{cr} be taken as 7600. Then, finding $2W_e/b$ equal to .532, one obtains $P_{cr} = 7600\ (.075 + .532 \times 7.5 \times .025) = 1328$ lbs. This value would be the Euler load of the panel if it were pin ended. It should not be concluded from this example that σ_{cr} is always smaller than σ_0, since quite frequently this is not the case.

Now consider the experimental results for this same panel which were obtained in a static test of the fuselage. By plotting the observed stress in the stiffener against the deflection at the center of the panel, curves are obtained like those in Fig. 5. If the results are tabulated as in Table 1, P and δ are obtained, the values of δ being taken from Fig. 5 for the corresponding values of σ_{stiff}. In Table 1 the values of W_e/b are obtained from Fig. 6, which corresponds to Fig. 3 of reference 2, for the corresponding values of λ (where $\lambda = \sqrt{E/\sigma_{stiff}} \times (t/b)$). By using Eq. (12) and the values of $2W_e$, it is possible to plot a curve of I_σ/I_0 against the stiffener stress (see Fig. 7). The asymptote value in this case

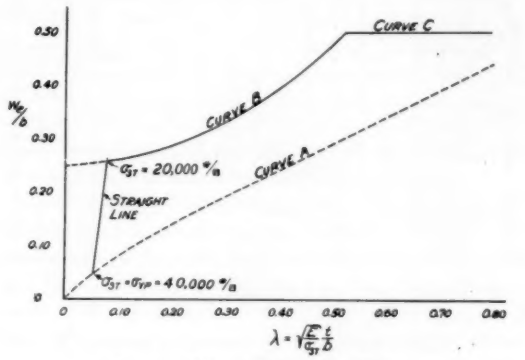

FIG. 6. Values of the ratio W_e/b.

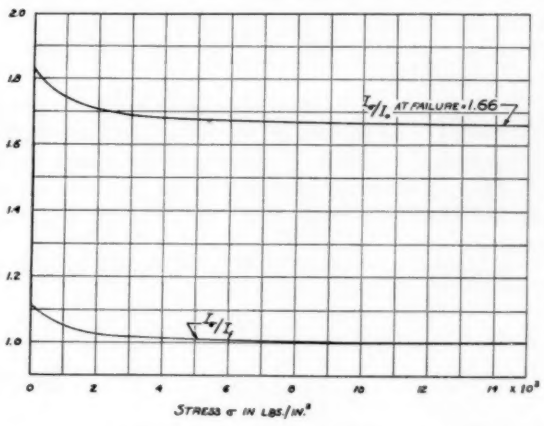

FIG. 7. Values of the ratio I_σ/I_0 and I_σ/I_f as a function of stiffener stress.

TABLE 1

Compressive Stress σ_c	λ	$\frac{W_e}{b}$	$2W_e$	Skin Area $2W_e t$	Total Area Skin Plus Stiffener A_T	Load P	$\frac{2W_e t}{A_0}$	$\frac{I_\sigma}{I_0}$	$\frac{I_\sigma}{I_f}$	Panel No. 1 $\delta \times 10^2$	Panel No. 1 $\frac{I_\sigma}{I_f} \times \frac{\delta}{P} \times 10^6$	Panel No. 2 $\delta \times 10^2$	Panel No. 2 $\frac{I_\sigma}{I_f} \times \frac{\delta}{P} \times 10^6$
0	∞	0.50	7.5	0.1875	0.263	0	2.50	1.84	1.11	0	..	0	..
1000	0.333	0.35	5.25	0.1313	0.206	206	1.75	1.75	1.05	−0.15	−7.65	0.20	10.20
2000	0.236	0.30	4.50	0.1125	0.188	375	1.50	1.70	1.02	−0.15	−4.08	0.40	10.90
3000	0.202	0.287	4.30	0.1075	0.184	550	1.43	1.69	1.02	+0.05	+0.93	0.70	12.98
4000	0.167	0.275	4.12	0.1030	0.178	712	1.37	1.68	1.01	0.50	7.10	1.05	14.90
5000	0.149	0.272	4.08	0.1020	0.177	855	1.36	1.68	1.01	1.20	13.71	1.45	16.57
6000	0.136	0.269	4.04	0.1010	0.176	1056	1.35	1.67	1.01	2.00	19.15	1.90	18.18
7000	0.127	0.267	4.00	0.1000	0.175	1223	1.33	1.67	1.01	3.00	24.80	2.50	20.60
8000	0.118	0.265	3.97	0.0993	0.174	1393	1.32	1.67	1.00	4.20	30.15	3.20	23.00
9000	0.111	0.264	3.96	0.0990	0.174	1565	1.32	1.67	1.00	5.70	36.45	..	..
10000	0.105	0.263	3.94	0.0985	0.174	1735	1.31	1.67	1.00	7.50	43.25	..	..
11000	0.100	0.262	3.93	0.0983	0.173	1905	1.31	1.66	1.00	10.00	52.50	..	..
12000	0.0962	0.261	3.915	0.0979	0.173	2075	1.31	1.66	1.00	16.40	79.10	..	..

is 1.66. Therefore, $I_f = 1.66 \times I_0 = .00747$ in.^{4} Knowing I_f, a curve for I_σ/I_f can be obtained (see Fig. 7). Using Table 1, the values of $(I_\sigma/I_f) \times \delta/P$ can be

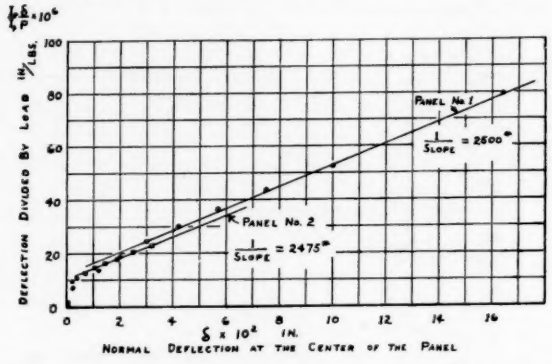

FIG. 8. Experimental results obtained by plotting $\frac{I_\sigma}{I_f} \times \delta/P$ against δ.

plotted against δ, thus obtaining Fig. 8. The inverse of the slope of these two lines gives $P_{exp} = 2500$ lbs. and 2475 lbs., respectively. These values represent the loads at which the panels would fail if loaded to failure. Thus one obtains, as the end-fixity coefficient, $c = P_{exp}/P_{calc} = 2500/1328 = 1.88$ and $2475/1328 = 1.86$, respectively.

These two examples show one case in which the panel was loaded to 83 percent of the failure, and one where it was loaded to about 57 percent of the failure load. (In spite of the close approach to the critical load in the first case, no permanent set was detected upon unloading.)

The above method shows that the failing load of a panel or column can actually be determined quite closely without loading the member to failure. All experimental measurements should be made as accurately as possible, and considerable care must be used in obtaining the load in the member from extensometer readings. It is important to remember, when dealing with end fixity, that the equations and relations developed hold only for members which tend to fail as columns and are not valid for members which fail locally when under compression load. Comparatively few actual members on airplanes can fail completely as Euler columns; however, many may start to fail as Euler columns and then fail locally as the combined bending and direct stresses become large.

In conclusion, the limitations of the method might be mentioned. First, the member must be loaded to about 50 percent of its critical load in order to make the determination reasonably accurate. Second, the deflection divided by length cannot become too large, otherwise the developed relations no longer hold; and third, the member must start to fail as a column, as mentioned above.

REFERENCES

[1] Southwell, R. V., *On the Analysis of Experimental Observation in Problems of Elastic Stability*, Proc. Roy. Soc. A., Vol. 135, pages 601–616, 1932.

[2] Timoshenko, S., *Theory of Elastic Stability*, McGraw-Hill Book Company, Inc., New York, 1936, page 178.

[3] Lundquist, E. E., *Generalized Analysis of Experimental Observations in Problems of Elastic Stability*, N.A.C.A. Technical Note 658, Washington, D. C., 1938.

[4] Sechler, E. E., *Stress Distribution in Stiffened Panels Under Compression*, Journal of the Aeronautical Sciences, Vol. 4, No. 8, pages 320–323, June, 1937.

Book Review

Ordeal, by NEVIL SHUTE; William Morrow and Company, New York, 1939; 280 pages, $2.50.

This thrilling story of air raid consequences around Southampton, England, during an imaginary war deserves the large sale it is enjoying in the United States. It will have added interest in aviation circles when it is known that the author's full name is Neville Shute Norway; that he was Deputy Chief Engineer connected with the development of the Airship R-100, that he has been with the deHavilland Aircraft Company, and that he was one of the organizers and joint managing director of Airspeed Ltd., which has grown to be one of the large English aircraft companies. He is also a Fellow of the Royal Aeronautical Society.

With this background of aviation experience he writes as an expert, even though the book is pure fiction. Obviously he was prompted to write the novel so that he could interest English people in taking air raid precautions well in advance of any hostilities.

He has worked into the story suggestions regarding what preparations for air raids should be made by those living in smaller cities such as Southampton, villages such as Hamble, and in small country houses. The problem of food, and especially a milk supply, is given prominence and this account of the difficulties will probably prompt householders to maintain an adequate supply of canned foods.

The story starts with an air raid by an unnamed enemy, during which several hundred one hundred pound bombs are dropped in the district around Southampton. The results are tragic. Hospitals are overflowing with the wounded, water and gas mains are broken, power lines are down, and all normal life in the area is suspended. An epidemic of cholera adds to the terrifying conditions. Small yachts are used as temporary refuges until even they become dangerous. The young solicitor with his wife and three children, who have moved to their boat, try to land on the Isle of Wight but are threatened with a period of quarantine and, in desperation, try to sail to Plymouth. The sensational episodes that occur in the submarine infested English Channel are as fine a bit of adventure as one could wish to read.

The book deserves high praise for the style of presentation, the objectives sought, and the absorbing interest of the story.

Reduction of Skin-Friction on a Flat Plate through Boundary Layer Control

JOHN R. WESKE

Case School of Applied Science

ALL attempts to reduce the skin-friction of a flat plate must be directed toward reducing the shear stress on the surface of the plate. This can be accomplished either by preventing the boundary layer from becoming turbulent or, in case the boundary layer is already turbulent, by reduction of the velocity gradient or the eddy viscosity at the surface.

The author undertook some tests in which a jet of air was emitted at low speed from a flat plate into the stream of air flowing parallel to the plate. As the jet was deflected downstream, it was reasoned that: (1) a renewal of the boundary layer would take place, which for a while at least, would return to laminar conditions, and (2) a reduction of the velocity gradient normal to the plate would be effected, since the velocity of the jet was chosen smaller than that of the free stream.

It was further assumed that the decreased velocity gradient established in the boundary layer by the jet would continue to exist until the exchange of momentum taking place between the jet and the main body of the fluid would have caused the mixing region to penetrate the jet.

Calculations of the mixing process[1] indicated that in a field of flow extending to infinity in all directions the disintegration of the surface of discontinuity is so rapid that the brief decrease of velocity gradient could not possibly be of practical significance. However, when the mixing process in the proximity of a solid surface is considered, taking into account that the turbulent mixing length near a surface varies directly as the distance from the surface, it follows that in this case the spreading of the mixing zone toward the plate should be very much decreased, theoretically reaching the solid surface at a point infinitely far downstream.

These considerations made experimental investigations appear desirable to determine:

(1) The aerodynamic forces produced by the discharge slot for the emission of the jet.

(2) The effect of the jet of air emitted from the slot upon the drag of the flat plate.

(3) The rate of disintegration of the surface of discontinuity between the jet and the free stream.

The test setup is shown schematically in Fig. 1 and its significant features are explained in the legend. In order to simplify test conditions an attempt was made to approximate two-dimensional flow. The dimensions of the plate alone were $25\frac{1}{2}$ in. long by 12 in. wide. Including the exposed surface of the air chamber containing the slot they were 27 × 12 in.

Three series of tests were made. For the first series the air chamber was mounted rigidly and the plate was placed on the drag balance. For the second series the plate was mounted rigidly and the drag of the air chamber was measured. In the third test both the plate and the air chamber were placed on the balance and their combined drag was determined. Wind tunnel velocities ranged from 40 ft. per sec. to 92 ft. per sec. Further measurements included velocity traverses of the boundary layers at various distances downstream of the slot, with and without emission of air through the slot.

The following notation is used:

v_0, q_0 = Wind-tunnel velocity and velocity pressure, respectively.

v_2, q_2 = Normal velocity through slot and corresponding velocity pressure, respectively.

Δp_s = Pressure difference between a point in the chamber leading to the slot and the outside air.

A = Effective area of discharge slot.

D_0 = Drag at zero emission of air.

D = Drag when emitting air through the discharge slot.

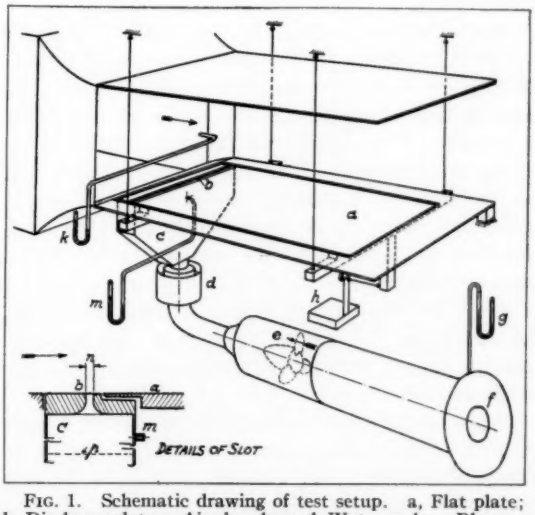

FIG. 1. Schematic drawing of test setup. a, Flat plate; b, Discharge slot; c, Air chamber; d, Water seal; e, Blower; f, Orifice; g, Pressure gage for quantity measurement; h, Hydrostatic drag scale; k, Pressure gage for wind-tunnel velocity; m, Pressure gage and connection for measurement of pressure difference across discharge slot; n, Width of discharge slot, approximately $\frac{1}{8}$ in.; p, Screen for equalization of discharge through slot.

Received January 24, 1939.

The effective area of the discharge slot A was determined from pressure measurements across the slot at zero wind-tunnel speed and at various quantities of discharge, Q, as follows:

$$A = Q/\sqrt{2g\,\Delta p_s/w}$$

where w denotes specific weight of air.

The results are presented in non-dimensional form. The variation of drag produced by the emission of air is represented by the quantity

$$C_D = (D - D_0)/Aq_0$$

Likewise the pressure difference between a point in the air chamber and the outside air is represented by

$$C_p = \Delta p_s/q_0$$

The ratio of energy recovered to energy in the jet as it passes through the slot per unit time is given by the quantity

$$e = (D - D_0)v_0/Av_2\,(\Delta p_s + q_0)$$

or, when substituting non-dimensional quantities

$$e = \frac{-C_D}{(C_p + 1)\,v_2/v_0}$$

which was used previously by F. Rokus and Th. Troller.[2]

Attempts to correlate the test results finally lead to the adoption of the ratio v_2/v_0 as an independent variable defining the conditions of the test. Although this ratio does not take into account variations of Reynolds Number it has been found adequate thus far, since for the range of conditions covered by the tests no appreciable effect of Reynolds Number has been discovered. Therefore, the quantities C_D, C_p, and e are expressed as functions of v_2/v_0 and plotted in Figs. 2 and 3.

The characteristics of the discharge slot are shown on Fig. 2. In addition to the curve of measured values of C_D there is shown the line C_{D_s}, which represents the negative drag of a point source in uniform parallel flow.[3] In calculating this theoretical curve it is assumed that the source flow has the same Bernoulli's constant as the free stream. This assumption does not hold for the actual flow, and this no doubt partly accounts for the fact that the measured drag, which is also negative, does not reach the theoretical drag in magnitude. It was found experimentally that within certain limits the discrepancy between theoretical and measured negative drag of the slot decreases as the width of the slot is decreased.

The total pressure required to discharge a jet of velocity v_2 from a flat plate at right angles into a free stream of velocity v_0 can be approximated by the equation $\Delta p_s = (\rho/2)v_2v_0$ within the range of test conditions. This relation was found to be applicable with fair approximation also to discharges of different shape such as a circular tube normal to, and flush with the flat plate. The tests of the discharge slot show that at $v_2/v_0 = 0.1$ a maximum of 90 percent of the energy of the jet is recovered through the negative drag of the slot.

The reduction of drag of the flat plate produced by emitting air through the slot is presented by the curve C_{D_f} of Fig. 3. In connection with this phase of the work numerous velocity traverses of the boundary layer at various distances downstream of the slot were taken with and without emission of air, and it was hoped that the information thus obtained might permit calculation of the variation of shear stress on the surface of the plate with distance from the slot. This expectation did not materialize because of difficulties in the experimental technique. It was found, however, that a decrease of velocity was registered at a point 0.01 in. from the surface and 12 in. downstream from the slot upon emitting air from the slot.

The integrated effect of reduction of shear stress through emission of air can best be expressed through the width of a hypothetical zone downstream of the slot in which complete elimination of shear stresses would produce the reduction of drag actually meas-

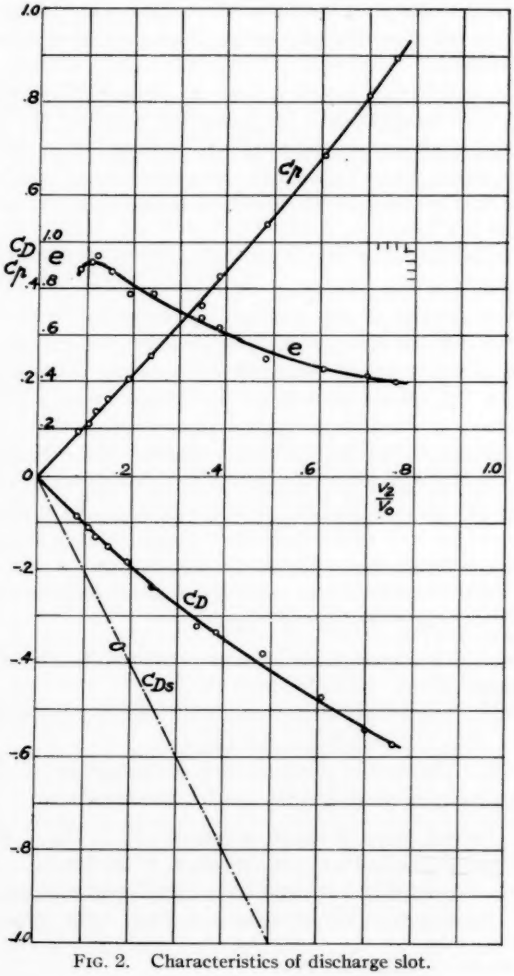

FIG. 2. Characteristics of discharge slot.

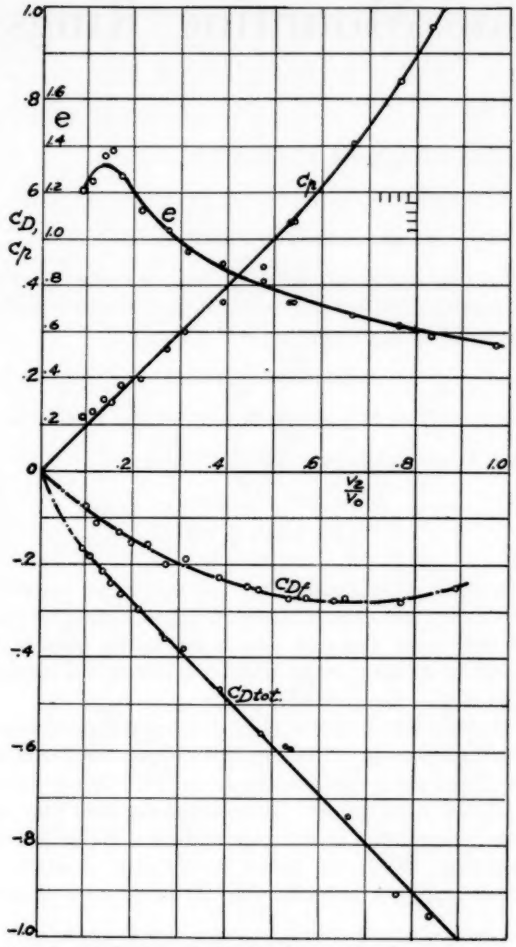

FIG. 3. Reduction of skin-friction of the flat plate and characteristics of flat plate and slot combined.

ured. The equivalent width of the blanketed zone thus calculated is more than 8 in., or 64 times the width of the slot, between $v_2/v_0 = 0.3$ and $v_2/v_0 = 0.9$.

The results further indicate that while there is a slight increase of the width of the blanketed zone with wind-tunnel speed it is not as great as might be expected from the calculations referred to previously.[1] Although the existence of a laminar boundary layer is not impossible on the front part of the plate it appears to be beyond doubt that it has become turbulent before the critical Reynolds Number for a smooth plate was reached because of the roughness of the mouth of the wind-tunnel nozzle and of slight irregularities along the slot and the narrow clearances around the plate. This assumption seems to be confirmed by the character of the velocity patterns of the boundary layer taken at zero discharge.

The characteristics of the plate and slot combined are also shown on Fig. 3. It will be noted that $C_{D_{tot.}}$ is not exactly the sum of C_{D_f} and C_D of Fig. 2 nor do the C_p curves of Figs. 2 and 3 coincide, as would be expected. The reason for this probably lies in the circumstance that in changing the test setup the location of the plate or the width of the slot might have been slightly altered. The discrepancies, however, do not affect the general result of the investigation.

The e curve rises to a maximum of 1.3 at $v_2/v_0 = 0.15$ which means that, disregarding the problem of the intake, for one horsepower spent at the slot in producing the jet, 1.3 horsepower are saved through decrease of skin friction of the flat plate and through negative drag of the slot.

Acknowledgment is made to Dr. Th. Troller, of the Guggenheim Airship Institute, Akron, for valuable suggestions; and to W. B. Champney, assistant, and F. Marble, of the Case School of Applied Science, for assistance in the testing and calculating work.

REFERENCES

[1] Durand, W. F., *Aerodynamic Theory*, Vol. III, pages 167–169; Julius Springer (Berlin), 1935.

[2] Rokus, F., and Troller, Th., *Tests on Ventilated Openings of Aircraft*, Journal of the Aeronautical Sciences, Vol. 3, page 203, 1936.

[3] Prandtl, L., and Tietjens, *Applied Hydro- and Aerodynamics*, page 121, McGraw-Hill (New York), 1934.

Book Reviews

Skies Unknown, by CAPT. J. E. DOYLE; Wright and Brown, Ltd., London, 1938; 248 pages.

Another and somewhat belated story of a war time pilot's experiences with the S. E. squadron of the R.F.C. Espionage, after landing behind the enemy lines, is woven into the story and provides the more interesting part of the plot.

Airman Lost in Africa, by CAREL BIRKBY; Frederick Muller, Ltd., London, 1938; 280 pages, 15s.

Darkest Africa is dark no longer, largely due to the network of airways which criss-cross the continent. This book is an account of the search for a lost Swiss pilot who disappeared while flying up the West Coast from Cape Town. It is a study of the people and villages as well as the story of a flight up the West Coast and back through central Africa. It gives the reader a "close-up of a most interesting and little known region." The interest is heightened by the uncertainties and difficulties encountered in flying a small airplane over long stretches of South Africa with little servicing facilities.

Air Raid Precautions, by COMMANDER R. H. ERRINGTON; Arthur Baker, Ltd., London, 1938; 95 pages, 1s.

This is a very practical handbook for those in Europe who wish to make sure that they have made every possible preparation for an air raid. It gives instructions for carrying out these preparations and leaves blank spaces for notes on what is available, where to go, and the names of those who are to perform specific duties.

Stress Analysis of Engine Mounting Rings

J. G. WILLIS

Fairey Aviation Company, England

ABSTRACT

Notes and equations are given for determining the load distribution and strength of mounting rings for radial engines when fitted with vibration isolating supports.

THE majority of radial engines are mounted on a welded-up tubular structure, consisting of a main mounting ring, supported at four or sometimes three nodes by a simple bracing of tubes to the wing or fuselage structure as the case may be.

When rubber insulators are interposed between the engine mounting bolts and the mounting ring, these usually consist of devices incorporating insulating rubber sleeves having a tangential deflection several times the radial deflection when mounted. The primary object, of course, is to lower the natural frequency of the mounted assembly, so as to preclude resonance with the major harmonics of the engine propeller combination and to reduce the transmissibility to a satisfactory level. A suitable installation of this type greatly effects the load distribution over the ring and the concentrated stresses can be surprisingly high.

For the stress analysis of such an indeterminate structure, standard strain energy methods can be readily applied[1,2,3] as outlined below.

The following notation is used:

δ = vertical deflection of engine relative to ring
k = tangential spring constant of rubber support
m = ratio of tangential to radial deflection of rubber support for unit load
W = total sprung weight of power unit on ring
M_0 = bending moment at any point from external loads
P_0 = axial force at any point from external loads
T_0 = twisting moment at any point from external loads
X_m = bending moment at cut
X_P = axial force at cut
X_V = shear force at cut
X_T = twisting moment at cut
M, P, T, forces in complete ring
$M_m.M_P.M_V.M_T$ denote bending moment at any point due to unit force of subscript applied at the cut; similarly for T_T, T_m, T_V
ds = element of length along neutral axis of ring
B = ratio of flexural to torsional rigidity, EI/GI_P
θ = angle to point considered from vertical
N = load on mounting bolt

Received November 30, 1939.

LOADS ACTING IN PLANE OF RING

For the tangentially disposed type of rubber mounting mentioned above, the vertical reaction which can be developed at any mounting bolt is given by

$$k\delta(m\cos^2\theta + \sin^2\theta) \qquad (1)$$

and, since $W = k\delta\sum_n(m\cos^2\theta + \sin^2\theta)$, the vertical load taken by any mounting bolt r is

$$N_r = \frac{(m\cos^2\theta + \sin^2\theta)_r}{\sum_n(m\cos^2\theta + \sin^2\theta)} \times W \qquad (2)$$

This equation indicates that the maximum variation of N is m, occurring at the vertical and horizontal center lines, and although this is physically obvious it should be borne in mind when considering the natural frequency of the system.

Lundquist and Burke[1] have developed general equations for this type of loading, and the relevant formulas for determining the stresses in the ring are given in simplified form below. It is again assumed that the strain energy due to shearing and axial forces can be neglected. With the forces in the ring positive as shown in Fig. 1 and assuming EI is constant around

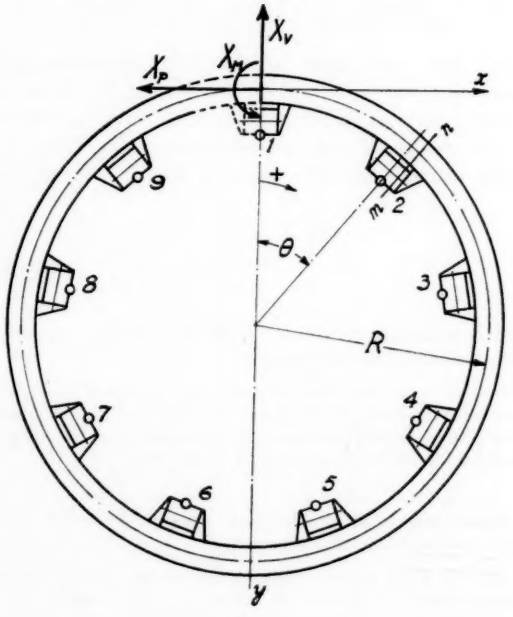

FIG. 1.

the ring the bending moment at any point is expressed as

$$M = M_0 + X_m + yX_P - xX_V \tag{3}$$

and the axial force by

$$P = P_0 + \cos\theta X_P + \sin\theta X_V \tag{4}$$

From Fig. 2 M_0 can be calculated at successive stations 1, 2, etc., by

$$M_2 = M_1 + V_1R(\sin\theta_2 - \sin\theta_1) - H_1R(\cos\theta_1 - \cos\theta_2) + P_2d\sin\theta_2 + P_{H_2}d\cos\theta_2 \tag{5}$$

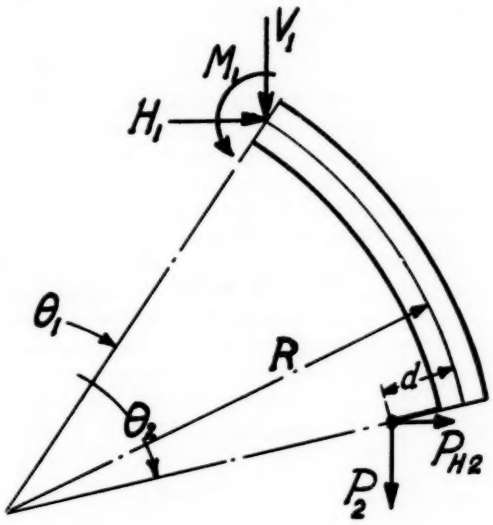

FIG. 2

The values of the unknown forces at the cut are determined from

$$X_m = (D_2 - 1.5\,RD_1)/\pi R^2 \tag{6}$$
$$X_P = (RD_1 - D_2)/\pi R^3 \tag{7}$$
$$X_V = -D_3/\pi R^3 \tag{8}$$

in which

$$D_1 = \int_0^{2\pi} M_0 ds \tag{9}$$

$$D_2 = \int_0^{2\pi} M_0 y ds \tag{10}$$

$$D_3 = \int_0^{2\pi} M_0 x ds \tag{11}$$

For the type of loading usually encountered the integrations are best performed graphically, and if desired, the work can be carried out separately for right and left halves of the ring, and then added. It will also be found convenient to resolve the torque reaction on each rubber mounting into vertical and horizontal components.

Loads Acting Normal to Plane of Ring

The distribution of loads over the mounting bolts for this case can be obtained from

$$N_r = (cy)_r \times \text{Moment}/\sum cy \tag{12}$$

since, by virtue of assumed infinite crankcase stiffness compared to the ring, the deflection at each mounting bolt is proportional to the distance from the neutral plane or center of moments, and in which c is the load for unit deflection, depending upon the stiffness of the ring and the supports. y is the distance from the center of gravity of the mounting bolts to the bolt considered. Particular values for c could be determined approximately for any ring by experiment, but any calculation of these values would involve broad assumptions that would hardly justify the work involved. However, a good approximation can be made by assuming that the stiffness in the axial direction of all mounting points is the same and is constant, which gives the well known formulas

$$N_r = y_r \times \text{Moment}/\sum y^2 \tag{13}$$

about the horizontal axis, and

$$N_r = x_r \times \text{Moment}/\sum x^2 \tag{14}$$

about the vertical axis, assuming these axes can be taken as the center of gravity of the mounting bolts.

It will be noted that Eqs. (13) and (14) will generally give higher loads between the ring supports than would be obtained by Eq. (12).

Neglecting the work due to shearing forces and assuming that the flexural and torsional rigidity is constant around the ring, the internal energy can be written

$$U = \int (M^2/2EI)ds + \int (T^2/2GI_P)ds \tag{15}$$

where

$$M = M_0 + M_mX_m + M_TX_T + M_VX_V \tag{16}$$
$$T = T_0 + T_mX_m + T_TX_T + T_VX_V \tag{17}$$

From Fig. 4 M_0 and T_0 can be calculated at successive stations 1, 2, etc., by

$$M_2 = M_1\cos\alpha + T_1\sin\alpha + V_1R\sin\alpha \tag{18}$$

$$T_2 = -M_1\sin\alpha + T_1\cos\alpha - V_1R(1 - \cos\alpha) - P_2d \tag{19}$$

After taking partial derivatives of Eq. (15) with respect to the three unknowns, substituting Eqs. (16) and (17), equating to zero and simplifying, X_T, X_V, and X_m become

$$X_T = \left(D_6 - D_5R\cdot\frac{1+3B}{1+B}\right)/2\pi BR^2 \tag{20}$$

$$X_V = (RD_5 - D_6)/2\pi BR^3 \tag{21}$$

$$X_m = -D_4/(1+B)\pi R \tag{22}$$

where

$$D_4 = \int_0^{2\pi} M_0\cos\theta\,ds - B\int_0^{2\pi} T_0\sin\theta ds \tag{23}$$

$$D_5 = \int_0^{2\pi} M_0\sin\theta\,ds + B\int_0^{2\pi} T_0\cos\theta ds \tag{24}$$

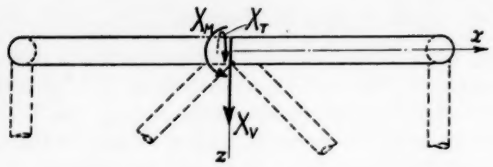

FIG. 3.

$$D_6 = \int_0^{2\pi} M_0 R \sin\theta ds - B\int_0^{2\pi} T_0 R(1-\cos\theta)ds \quad (25)$$

In these equations the forces as shown in Figs. (3) and (4) are considered positive.

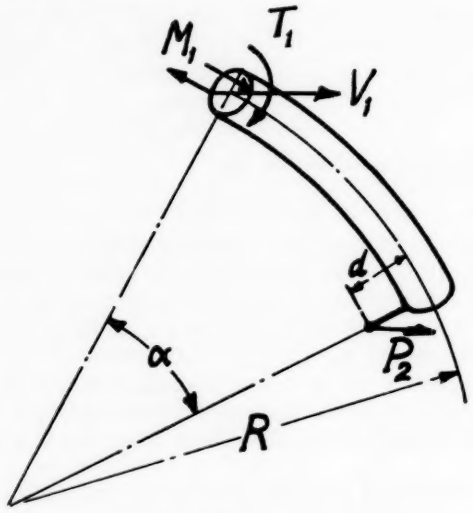

FIG. 4.

Finally the actual bending moment and twisting moment in the complete ring is obtained from

$$M = M_0 + \cos\theta X_m + \sin\theta X_T + R\sin\theta X_V \quad (26)$$

$$T = T_0 - \sin\theta X_m + \cos\theta X_T - R(1-\cos\theta)X_V \quad (27)$$

Applying these equations to a ring similar to Fig. 1 in which the sprung power plant weight (including propeller, cowling, etc.) is about 1700 pounds, for a condition which might be developed with the aircraft encountering a sharp up gust during a banked turn, or similar maneuver, and using a load factor of 6 for gravity forces, with 2 for thrust and torque (see British Requirements), the bending and twisting moments on the ring are as shown in Fig. 5. The maximum direct stress occurs at *mn* and is 77,600 lbs. per sq.in. for a $1^5/_8$ in. diameter .128 in. thick tube, the maximum shear stress is 39,900 lbs. per sq.in.

These are principal stresses based on the simple beam theory. For the ring considered, the radius is about $14^1/_2$ in., and the factor (tR/a^2) is 2.8, so that the effect of the curvature of the ring on the maximum stress can be neglected.[2]

It will be noted that the mounting supporting brackets and the ring supports would contribute to the stiffness of the ring, and that they have not been taken into account.

In conclusion, considering the uncertainty of the load distribution and the high stresses which can occur on a welded-up structure of this type, it would seem highly desirable to have dynamic test data to supplement a rational attempt at design such as outlined.

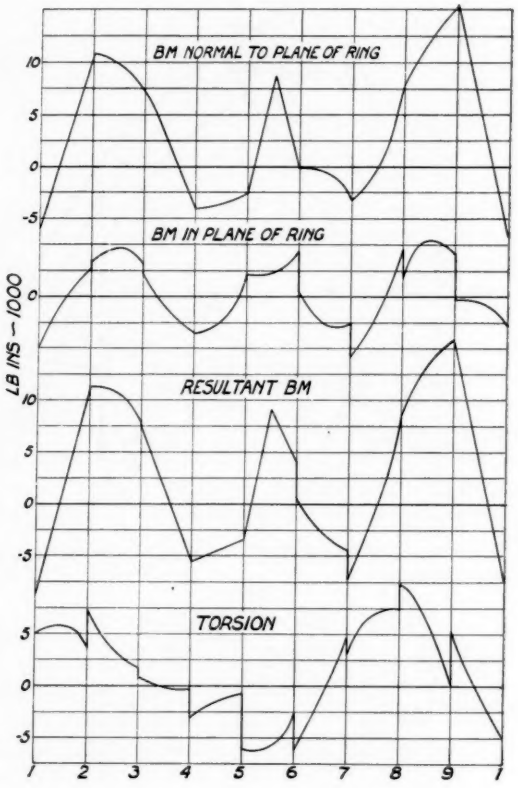

FIG. 5.

REFERENCES

[1] Lundquist, Eugene E., and Burke, Walter F., *General Equations for Stress Analysis of Rings*, N.A.C.A. Technical Report No. 509, 1934.

[2] Timoshenko, S., *Strength of Materials*, Part II, pages 423–473, D. Van Nostrand Co. Inc., 1930.

[3] Pippard, A. J. Sutton, *Strain Energy Methods of Stress Analysis*, pages 41–64, Longmans, Green and Co. Ltd., 1928.

The Use of Isentropic Analysis in Short Term Forecasting

JEROME NAMIAS

Massachusetts Institute of Technology

SINCE the U.S. Weather Bureau, Navy, and Army expanded their programs of obtaining records of temperature, pressure, humidity, and wind in the free atmosphere, meteorologists have attempted to find methods of using these data to best advantage. While maps of atmospheric pressure at various levels have been found especially helpful in weather forecasting, the use of temperatures and humidities on such constant level charts has hardly done more than make atmospheric disturbances seem more complicated in vertical structure than surface weather analyses would indicate. Considering that air moves in the vertical as well as horizontal plane and that vertical displacements lead to adiabatic temperature changes, it is not surprising to find that any chart on which temperatures and humidities are compared level for level is unsatisfactory for tracing the movements of large-scale air currents from day to day.

In order to eliminate the effects of these adiabatic changes Rossby[1] suggested the use of two elements which are invariant with adiabatic processes—specific humidity and potential temperature. Since, in a stable atmosphere air particles tend to flow along surfaces of potential temperature and at the same time retain their specific humidity, Rossby suggested that charts be constructed along surfaces of constant potential temperature, which are identical with isentropic surfaces.

Further support for the use of such isentropic charts is found in the logical assumption that horizontal wind shearing stresses should be chiefly operative along surfaces of potential temperature. While these lateral shearing stresses until recently have been almost completely neglected in the study of atmospheric flow, much evidence is accumulating in support of the hypothesis that these stresses are frequently of an order of magnitude large eough to produce important hydrodynamical effects.

The function of the isentropic chart is thus to serve the two-fold purpose of (1), facilitating the study of the identification and thermodynamic modification of large-scale air currents, and (2), presenting a clear-cut picture of the major patterns of flow of atmospheric currents through the configurations of lines of constant moisture.

Presented at the Meteorology Session, Seventh Annual Meeting, I. Ae. S., January 26, 1939.

Briefly then, isentropic analysis may be defined as a method of determining the structure and flow patterns of the atmosphere, based upon the assumption that over short periods of time individual parcels of dry air are constrained to move within surfaces of constant entropy (constant potential temperature).

One successful application of the treatment of upper air data by this method has been found in the forecasting of summertime precipitation.[2,3] In winter, however, there often arise conditions which, for a reliable analysis, require a greater number as well as a greater frequency of aerological soundings. The main reason for this is that the general circulation over the United States in winter is much more intense than in summer, and the characteristic "flow patterns" observed on the isentropic charts of the winter season are rearely as well-defined by the aerological network as they are in summer. It appears that the eddies of the winter season are much more extensive than those of summer, so that only segments of them may be identified on an isentropic chart only over this country. This increased activity in winter is associated with a southward shift in the prevailing westerly current which, according to Rossby,[4] drives cyclonic vortices on its left (north) and anticyclonic vortices on its right (south). In winter the westerlies are found over the United States, so that this area is alternately to the north or south of the westerlies, and thus becomes a battle ground for both cyclonic and anticyclonic eddies.

In spite of the difficulties brought about by a woefully inadequate network of aerological stations making only one sounding a day, it has been possible to maintain a reasonable continuity of isentropic analyses from day to day, and this fact holds out the hope that many clues for problems of daily weather forecasting may lie, at least partially, in isentropic analysis.

It is the purpose of this report to present a schematic picture of one of the typical synoptic situations in which the isentropic analysis has been found helpful in the daily forecast.

One of the most interesting problems upon which isentropic charts have thrown some light is the cyclone formation associated with diverging flow lines of upper air currents. Scherhag[5] arrived at a number of forecasting rules on the basis of the behavior of upper air winds, or, lacking these data, the pattern of contour lines of certain isobaric surfaces. Scherhag states that in regions where the upper level gradient winds

show marked directional divergence of flow and the lower layers do not show a compensating convergence, there must set in a general pressure fall. Of course, it is possible that isobars may diverge (in which case directional divergence is indicated) while the air stream gradually slows down so that at every point the wind is in balance with the gradient. In that case, the directional divergence is not associated with a real divergence, but is balanced by convergence in the direction of motion. However, Scherhag believes that inertia forces are operating so that the air moves faster than gradient velocity as the isobars spread out, and in this manner real divergence may occur. On this basis he explains certain regions of pressure fall at the surface.

One of the reasons why Rossby has suggested the isentropic chart as a working tool for synoptic metorology is that lateral mixing should take place along isentropic surfaces. It seems logical that lateral shearing stresses acting between currents of different velocity may be responsible for departure from gradient flow, *i.e.*, regions of convergence or divergence. It is entirely possible that marked divergence may be indicated in the flow pattern of the moisture lines of the isentropic chart, yet may not show on a constant level chart. A test for any apparent divergence indicated on the isentropic chart, similar to that applied for the constant level chart, can be applied by making use of the stream function,[6] which affords a picture of the gradient flow in an isentropic surface. If the stream lines cannot be drawn so as to conform with the upper air winds and also with data from airplane or radio meteorograph soundings, the divergence or convergence must be significant.

In order to apply rigorously these tests for divergence, it is necessary to have at hand upper air data from a network of soundings sufficiently dense so that isobars or lines of the stream function are uniquely defined. While the present aerological network is inadequate for this purpose, since the fall of 1938 there have been occasions when the patterns of upper level isobars (at 10,000 feet) and stream function were reasonably well defined by observations. In these cases there has generally been good agreement between the observed winds and the iso-lines. The pattern of the moisture lines on an isentropic chart, however, frequently shows directional divergence better than do either the upper air winds or the isobars at any fixed level. The assumption that the pattern of moisture lines is representative of the instantaneous field of flow (which, strictly speaking, it is not) has led to some interesting empirical results. One of these results offers a clue to the formation of secondary cyclones.

Perhaps the most frequent case of divergence arises with an occluded cyclone whose warm sector is located somewhere south of the primary center. This is the well-known "secondary cyclone" which often forms at the tip of the remaining warm sector.[7] In such cases the flow pattern indicated by the moisture lines of the isentropic chart is like that shown schematically in Fig. 1. The frontal structure at the ground is shown

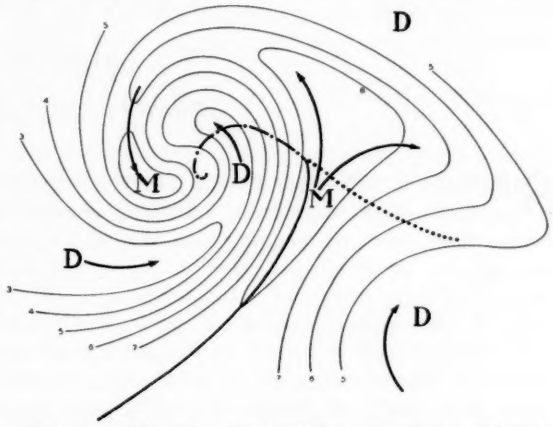

FIG. 1. Schematic flow pattern around an occluded cyclone as shown by the moisture lines in an isentropic surface.

by heavy lines (dotted for the warm front, solid for the cold front, and alternately dashed and dotted for for the occluded front). The light solid lines are lines of constant specific humidity, and the heavy arrows indicate the instantaneous flow of dry (D) and moist (M) currents. In this model two systems are struggling for supremacy: an anticyclonic moist current M to the right, and a cyclonic dry current D to the left. The moist current is normally of tropical maritime air, while the dry flow is of polar origin. The process by means of which both of these systems attempt to dominate the flow pattern of their environment is isentropic mixing. The vast anticyclonic eddy to the right may be considered as the normal type of eddy observed in tropical currents moving northward.[2] The cyclonic whirl of polar air may be considered as an intrusion of polar air which, upon moving southward develops cyclonic vorticity in order to counterbalance the decreasing cyclonic vorticity of the earth's rotation. This dry current spreads some of its momentum to the moist flow on its right and drags it into the cyclonic circulation. Thus, at the junction of the warm sector there is a region where the air is being forced into two divergent paths—one around the anticyclonic eddy to the east, and the other around the cyclonic vortex to the west. If this flow pattern persists through a fairly deep layer of the atmosphere, it creates an area of pressure fall on the weather map below the region of branching currents.

It must be emphasized that this hypothesis postulates the existence of lateral shearing stresses, which, acting along isentropic surfaces, produce components of flow *across* the isobars, although as yet the data is inadequate to verify this.

A specific, though not entirely conclusive, case of this nature is afforded by the charts constructed at the

Massachusetts Institute of Technology on October 26 and 27, 1938. On the surface weather map for the 26th (Fig. 2) an old occlusion lies over the Lake region, running northward and joining up to an old cyclone centered over James Bay. An area of pressure

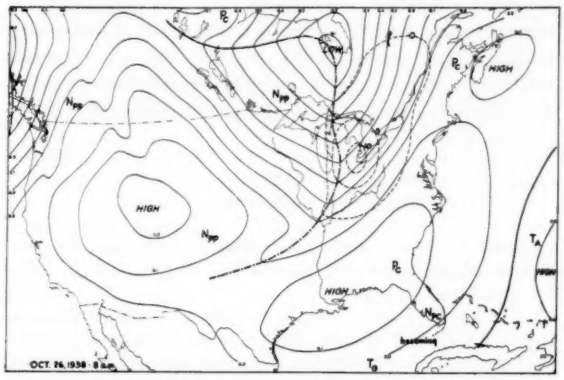

FIG. 2. Fronts, isobars, and isallobars (three hour tendencies) as shown on surface weather map for October, 26, 1938.

fall has set in to the east of this occluded front, and the three hour pressure tendencies, shown by broken isallobars, indicate a concentrated region of pressure fall which is not easily explained on the basis of the surface weather maps. The isentropic chart for the surface characterized by the potential temperature of 300°A. for the 26th (Fig. 3) shows three anticyclonic eddies, the centers of which are marked by large asterisks. The most pronounced one is that whose center is located somewhere over South Carolina, and whose influence extends over the entire area east of the Mississippi River. A cyclonic flow of cold and dry polar air is now invading the northern plains area, and this current has forced a branch of the moist current to take a cyclonic path. The high specific humidity (4.0 gms. per kg.m.) at the 300° isentropic surface over Sault Ste. Marie, Michigan, favors the construction of the cyclonic branch of the moist tongue.

The branching of the moist current appears to be taking place in the region of the maximum 3 hour pressure fall at the ground, and there can be little doubt that this fall is associated with the divergent flow. By the following day a small secondary disturbance has formed and on the morning of the 27th is centered over southern New England.

Some measure of the importance of the divergence may be obtained by the strength of the eddies involved. Thus a weak anticyclonic eddy (characterized by light winds) will generally yield to an invading cyclonic flow pattern, and no secondary disturbance will result. On the other hand, a strong anticyclonic eddy, under

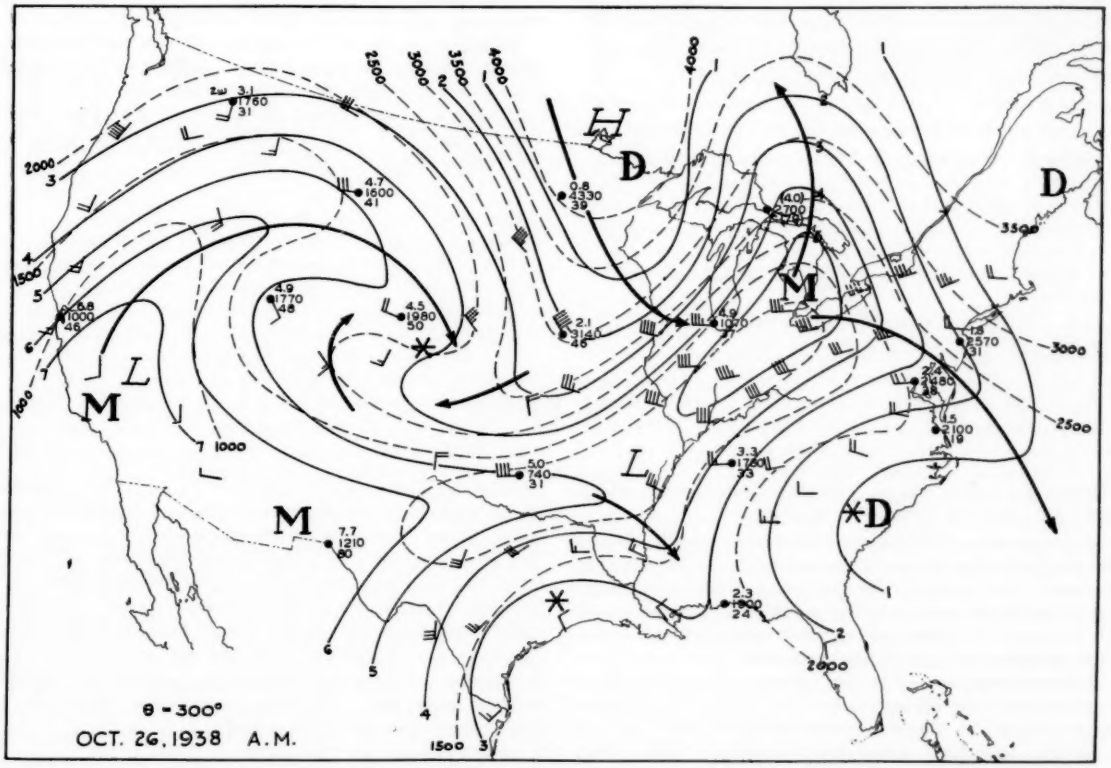

FIG. 3. Isentropic chart for October 26, 1938. Solid lines are lines of specific humidity, while dotted lines are lines of elevation (in meters) of the chosen isentropic surface above sea level. The numbers to the right of the aerological stations are, in the order listed, specific humidity, elevation, and relative humidity at the given isentropic sheet. Winds at the isentropic surface are shown by arrows, the number of half barbs being roughly equivalent to Beaufort numbers of wind force.

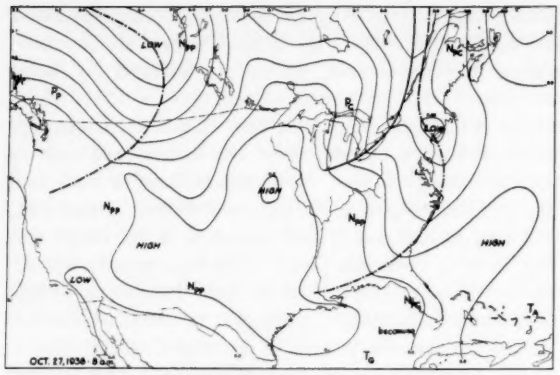

FIG. 4. Fronts and isobars from the surface weather map for October 27, 1938.

similar conditions, will deflect some of the moist flow around it, so that there is produced divergence necessary for the formation of a secondary cyclone.

The results of this preliminary report are summarized as follows:

(1) In order to apply rigorous tests for apparent divergence at a constant level or within an isentropic surface, more upper air soundings are necessary, and they must be made at more frequent intervals.

(2) The isentropic chart has a distinct advantage over Scherhag's method of detecting divergence, inasmuch as the conservative elements, specific humidity, and potential temperature offer the best indices for tracing air particles from day to day, and in this manner the principal flow patterns of the free atmosphere may be defined. Furthermore, if lateral mixing takes place on isentropic rather than level surfaces, it is reasonable to suppose that the main shearing stresses will produce characteristic flow patterns first on isentropic surfaces.

(3) A hypothesis of the formation of secondaries at the tip of warm sectors of old occluded cylcones has been suggested which rests on the foundation of isentropic mixing and which attributes divergence with its associated pressure fall to the shearing stresses operating from two interacting systems—one cyclonically curving polar air, the other anticyclonically curving tropical air.

REFERENCES

[1] Rossby, C.-G., and collaborators, *Isentropic Analysis*, Bulletin of the American Meteorological Society, Vol. 18, pages 201–203, June–July, 1937.

[2] Namias, J., *Technique and Examples of Isentropic Analysis*, Part 1B of *Fluid Mechanics Applied to the Study of Atmospheric Circulations*, Papers in Physical Oceanography and Meteorology, Massachusetts Institute of Technology and Woods Hole Oceanographic Institution, Vol. VII, No. 1, 1938.

[3] Namias, J., *Thunderstorm Forecasting with the Aid of Isentropic Charts*, Bulletin of the American Meteorological Society, Vol. 19, No. 1, 1938.

[4] Rossby, C.-G., *On the Maintenance of the Westerlies South of the Polar Front*, Part 1A of Papers in Physical Oceanography and Meterology, Massachusetts Institute of Technology and Woods Hole Oceanographic Institution, Vol. VII, No. 1, 1938.

[5] Scherhag, R., *Zur Theorie der Hoch-und Tiefdruckgebiete*, Meteorologische Zeitschrift, Bd. 51, Heft 4, 1934.

[6] Montgomery, R. B., *A Suggested Method for Representing Gradient Flow in Isentropic Surfaces*, Bulletin of the American Meteorological Society, Vol. 18, No. 6, pages 210–212, 1937.

[7] Bjerknes, J., and Solberg, H., *Life Cycle of Cyclones and the Polar Front Theory of Atmospheric Circulation*, Geofysiske Publikasjoner, Vol. III, No. 1, 1922.

Book Review

Power and Speed, edited by FREDERICK E. DEAN; Temple Press, Ltd., London, 1938; 250 pages, 8s. 6d.

The importance of the internal combustion engine in changing the social and economic life of the world is perhaps not fully appreciated. This book, by the publishers of several magazines specializing in motoring, aviation, and shipping describes in separate chapters the various uses to which internal combustion engines are put in our present day civilization.

Aviation is represented by five chapters, three of which are written by editors of *The Aeroplane*. These are: "The Aeroplane and its Motor" by Thurstan James, "Air Transport" by F. D. Bradbrooke, and "The Royal Air Force" by C. G. Grey and Mrs. C. M. McAlery. The other two chapters are "Air Routes of the Empire" and "The Aeroplane Height Record." Although written for the general reader they are authoritative and give the essential facts about the development of British aviation. The numerous illustrations are discriminately chosen. The photographs are admirably supplemented by large scale cut-out drawings of outstanding airplane and engine types.

Chapters are devoted to automobiles, busses, trucks, military vehicles, motor boats, and trains. Automobile, motorcycle, and speed boat racing are also described.

Notes on the Proceedings of the 1939 Meeting of the Aircraft Industry with the National Advisory Committee for Aeronautics

The following account of the meeting is slightly condensed from the official release of the National Advisory Committee for Aeronautics.

THE Annual Meeting at Langley Field of representatives of the aircraft industry of the United States with representatives of the N.A.C.A. was held on May 2, 1939. The meeting was for the purpose of affording an opportunity to the engineering representatives of the industry and the universities to inspect the research facilities of the Committee and to receive information on some of the current problems under investigation by the Committee.

About 400 representatives of the aircraft industry and universities attended the meeting. The following equipment was inspected and demonstrated:

The 7 × 10 ft. atmospheric wind tunnel.
The new low-turbulence wind tunnel.
The 20 ft. propeller research tunnel.
The full-scale wind tunnel.
The free-spinning wind tunnel.
The 8 ft., 500 m.p.h. wind tunnel.
The new variable-density free-flight wind tunnel.
The new 19 ft. pressure wind tunnel.
The N.A.C.A. gust tunnel.
The flight-research laboratory.
The N.A.C.A. tank.
The engine research laboratory.

Most of the laboratory facilities were inspected in the morning. In the afternoon, following the dedication exercises, the new 19 ft. pressure wind tunnel and the free-flight wind tunnel were inspected.

The representatives of the industry met in the morning with the members of the Committee for a welcome from Dr. Vannevar Bush, Chairman of the Executive Committee of the National Advisory Committee; from Major General Delos C. Emmons, Commanding General, General Headquarters Air Force, stationed at Langley Field; and from Lieutenant Colonel W. E. Kepner, Acting Commanding Officer of Langley Field.

Dr. Bush presided at the dedication ceremonies. Dr. Edward P. Warner, a member of the National Advisory Committee for Aeronautics, made the dedication address. Colonel John H. Jouett, President of the Aeronautical Chamber of Commerce of America, spoke on behalf of the aircraft industry.

New 19 Foot Pressure Wind Tunnel

The new 19 foot pressure wind tunnel is the N.A.C.A.'s latest step in the development of improved methods for solving aerodynamic problems in the design of large high-speed aircraft.

The tunnel is of steel tubular construction, the tube having a maximum diameter of 60 feet and standing higher than the three-story office building which is constructed adjacent to the tunnel. The test chamber is housed in the 60 foot diameter portion of the tube where the engineers who are operating the tunnel will work under pressures from two or more atmospheres down to a partial vacuum. The jet itself which contains the model is 19 feet in diameter and air can be forced through this jet at speeds in excess of 250 m.p.h.

The operation of this wind tunnel is different from that of any other now existing in that the operators will work inside the pressure chamber. The tunnel is equipped with special air locks and a decompression chamber, and the working section is equipped with air-cooling apparatus and dehumidifiers so as to make working conditions possible. The complete tunnel, including jet, test chamber, and return passages is 271 feet long and 128 feet wide. The propeller, which is 34½ feet in diameter, is driven by an 8000 horsepower electric motor.

In the working chamber a complete balance system for measuring the forces produced on an airplane model is provided. These balances are so designed that they can be operated by one man, the readings being automatically recorded.

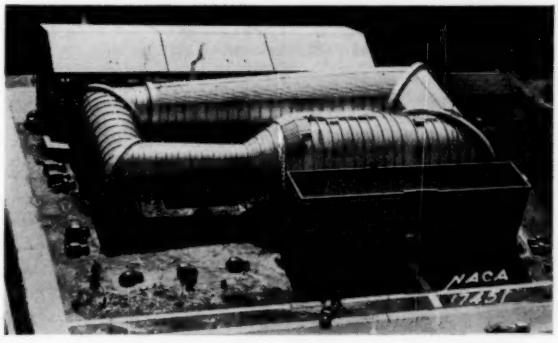

The new 19 ft. pressure wind tunnel.

The 19 foot pressure tunnel, which has taken two years to complete, will be used not only for research on methods of improving large airplanes but will be used to investigate propellers operating at high tip speeds and to investigate the flutter and vibration of wings, propellers, and tail surfaces on high-speed airplanes.

Free-Flight Wind Tunnel

Believing that the investigation of an airplane model in unrestrained flight could most conveniently be conducted in a wind tunnel specially designed for the purpose, the Committee during recent years has developed and operated a small wind tunnel of this type. After thorough investigation of this "model" tunnel, which included correlation of the research in the tunnel with the results of full-scale flight tests, it was concluded that the method offers considerable promise. As a result the construction of a larger free-flight wind tunnel designed to operate under a pressure of several atmospheres in order to achieve more nearly actual flight conditions was undertaken. Construction of the new wind tunnel was started in 1937 and survey flights were begun only a few weeks ago.

An examination of the flow required in the building housing the tunnel led to the adoption of a steel sphere to make possible a uniform return flow. The steel sphere is 60 feet in diameter and can be supplied with air compressed up to two or more atmospheres, as in the 19 foot pressure tunnel. Here likewise a decompression chamber is provided. The tunnel itself, which is mounted on a steel framework inside the sphere, has a test section diameter of 12 feet and is about 30 feet long. The drive consists of a 600 horsepower electric motor turning a 15½ foot diameter

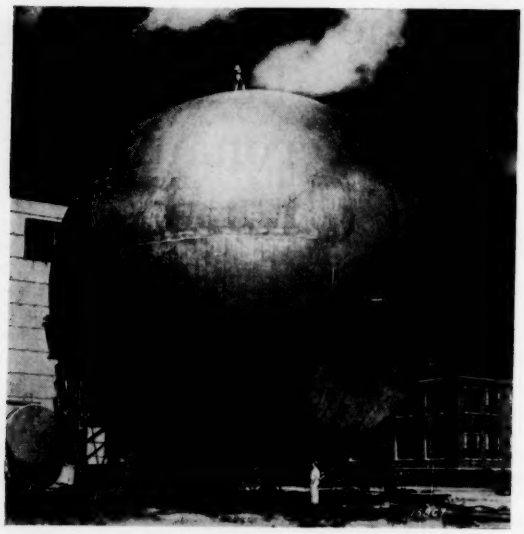

The new free-flight wind tunnel.

propeller. The whole apparatus is mounted on bearings so that the tunnel can be tilted through a wide range of angles to correspond to the angle of glide of the model.

The tunnel is inclined at an angle such that the model will remain stationary in the wind stream. The inclination of the wind stream is continuously variable so that a wide range of control settings can be investigated.

The models used in the tunnel must be specially built to duplicate on a small scale, not only the shape of the full-size airplane, but also the distribution of weight in the wings and fuselage.

Two operators are required to run the tunnel. One of these controls the angle of tilt and the air speed. The second operator is the pilot who actually flies the model during the period of its test flight in the wind tunnel. Riding in the "cockpit," equipped with an observation window just beneath the test chamber, the pilot flies the model by operating switches connected through a fine trailing wire to electromagnets in the model. These operate the control surfaces.

With this tunnel it will be possible not only to give pilots a general "feel" of the flying and handling characteristics of a new airplane before they ever take it up, but it will also be possible to obtain accurate records of the motion of airplanes with various degrees of stability under the action of known amounts of control application. Through such research the new free-flight wind tunnel gives promise of the development of new design standards for stability and control that will result in marked improvement in the safety of future aircraft.

Reduction of Air Friction on Airplane Wings

The Committee took this occasion to announce an outstanding contribution to the design of airplane wings. During the past year a new wind tunnel specially developed by the Committee has revealed previously unknown facts regarding the fundamental aspects of air friction, and these facts not only constitute a marked scientific advance in our understanding of fluid mechanics, but offer promise of large reductions in the drag of airplane wings.

The cause of the transition from laminar to turbulent flow in the boundary layer has long been one of the most baffling mysteries in the field of the aerodynamic research scientist. For many years it has been the dream of research workers in this field to discover methods of delaying transition and so reducing markedly the air friction on wings in flight. This has been achieved in the N.A.C.A. laboratories during the past year.

New wing forms have been developed based on previously untested theories as to the causes of the transition effect, and boundary layers on these forms have been found to remain laminar over almost the entire wing surface. In this way the air friction has been reduced to levels never before expected.

One of these new forms was demonstrated in comparison with one of the best conventional airfoil forms now in use on airplane wings. The conventional form suffers from the drag of the turbulent boundary layer over most of its surface and has about the same amount of drag as the wings on the best modern airplanes. The new shape, however, has the smooth-flowing low-drag laminar boundary layer over almost its entire surface and the demonstration showed that its drag is only a fraction of that of the conventional wing.

Effect of Shock Waves

Investigations regarding the effects of shock waves at various points on a high-speed airplane have been carried out in the 8 ft., 500 m.p.h. wind tunnel. These shock waves around local protuberances have been observed at flight speeds as low as 300 m.p.h.

With the usual blunt-nose N.A.C.A. cowling, for example, an airplane speed of 325 m.p.h. causes local flow speeds at the front curve of the cowling exceeding 710 m.p.h. This design of cowling is a very poor streamline form at 400 m.p.h., though an excellent one at 250. A new design of N.A.C.A. cowling delays the onset of shock waves and thus overcomes the difficulty.

New forms of windshields and propellers developed in these investigations to avoid the onset of shock waves were also discussed. With these new forms it will be possible to achieve top speeds in level flight exceeding 500 m.p.h. without the occurrence of the drag creating compression shock.

Water Flow Lines about the Hull of a Seaplane

Investigations have been carried out in the N.A.C.A. towing tank over a period of years to determine the design factors that will allow seaplane floats of minimum resistance to be designed.

Investigations during the year have been made using a hull fitted with a glass bottom. On the under surface of the glass next to the water, long silk streamers have been placed. Illumination has been provided so that the character of the water flow over the hull can be observed from the beginning of the take-off to the point where the boat rises on the step, assumes a planing angle, and finally leaves the water. Motion pictures illustrated the character of the flow as affected by different design characteristics of the hull.

The streamers showed the details of the water flow near the hull and permitted a close study of the design factors, the correct application of which will lead to minimum resistance hulls. The above method, applied for the first time by the N.A.C.A. offers great promise for further improvements in the take-off and landing characteristics of seaplanes and flying boats.

Use of Hydrofoils for Assisting the Take-Off of Large Seaplanes

Any large reduction in the air drag of conventional flying boat hulls usually results in poor performance on the water as landing and take-off gear.

A possible solution is the fitting of a special landing and take-off gear in the form of hydrofoils which will be retracted in flight and lowered for take-off and landing. The hydrofoils are generally similar to airfoils but run submerged in the water. They develop large lift with small resistance and when suitably arranged beneath a streamline fuselage will lift it out of the water at very low speed and at the same time produce a water resistance of around one-half that of the planing hull that they replace. Thus marked improvement in flying boats should result from the use of an almost perfectly streamlined fuselage for low air resistance and flotation, with retractable hydrofoils for landing and taking off.

Models were demonstrated showing the relative merit of hulls and hydrofoils for take-off purposes. By the use of such a system it appears possible not only to increase the efficiency of the flying boat in the air, but to reduce its resistance in take-off, with marked gains in range and pay load.

New N.A.C.A. Gust Tunnel

A demonstration was given in the N.A.C.A. gust tunnel to illustrate how it is used in measuring on an airplane model the effect of a rising air current to simulate an atmospheric gust acting on a full-size airplane in flight. In this apparatus the airplane model is projected down a track by a catapult. As the end of the track is reached the model is released and glides through a rising current of air delivered from the gust tunnel proper, after which it is caught in a burlap screen. The rising air current can be adjusted to simulate a variety of natural currents encountered in the free air.

Instruments aboard the model record the amount of load placed on the wings when the airplane encounters various typical gusts. Cameras beside the tunnel are used to record the motion of the airplane in response to the gust and determine how much the load may be relieved by the response of the model to the gust effect.

In the past it has been necessary, in the interest of safety, to design new airplanes to withstand the same loads that existing airplanes had already encountered. Different airplanes, however, respond differently to the same gust and thus experience different loads. With the new gust tunnel it is possible to determine more accurately the loads that a new airplane will have to sustain. In one case already tried it was found safe to reduce the loads for which the airplane would otherwise have had to be designed, by a substantial amount.

Study of Recovery from Spins

During recent years the problem of spinning has been extensively investigated in the N.A.C.A. free-spinning wind tunnel and the results correlated with flight experience on a number of airplanes.

As a result of these investigations the Committee has developed a criterion or design standard for airplane tails that will assure satisfactory recovery from spins. By a simple method, described and demonstrated in the free-spinning wind tunnel, a designer can readily check his design of tail surfaces and determine whether or not it will guarantee prompt recovery from a spin. The development of this criterion is another step in improving the safety of military, commercial, and privately owned airplanes.

Increasing the Lift of Wings

A demonstration in the Committee's 7 × 10 foot wind tunnel showed the relative effectiveness of various types of flaps in increasing the lift of airplane wings. A new type of flap recently investigated by the Committee, known as the venetian-blind flap, is of particular interest because it more than doubles the maximum lifting capacity of a plain wing, giving the highest lift yet obtained with any flap device. The demonstration showed the difference between the maximum lift of a normal wing, the lift with a split flap, and the lift with the venetian-blind flap.

Another very promising type, the N.A.C.A. slotted flap, was also discussed.

With the increase in wing loading, it is highly desirable to extend the flap over the entire span of the wing. For use with full-span flaps a new method of lateral control, different from the present aileron, is needed. Various forms of lateral control for this purpose were discussed, including the retracting type and the new "spoiler scoop" type.

Aircraft Icing Problems

The N.A.C.A. has been, for the past few years, conducting investigations on devices and systems for reducing the tendencies toward ice formation on the various parts of aircraft. These investigations are, for the most part, conducted in flight on an airplane especially equipped for the purpose, although some have recently been run in a special, refrigerated wind tunnel.

The airplane used in the icing investigations is provided with a spray apparatus mounted ahead of the part on which the de-icing system is to be investigated. By flying the airplane at sufficient altitude to reach freezing temperatures, icing conditions can be simulated with the spray system all year round, and the investigation is not restricted to the winter months.

The equipment shown dealt with methods for keeping the windshield clear of ice to insure clear vision for the pilot while navigating and landing in bad weather conditions. Three methods have thus far shown promise. The first is a rotating windshield wiper which clears water, snow, and ice off the windshield. The principal difficulty here is that conventional windshield wipers, as used on automobiles, have far too little power to accomplish the desired result. The new design of windshield wiper with much more powerful drive and rotating with sufficient speed so that it does not obscure the pilot's vision is a promising step. An electrically-heated windshield is of further assistance but here again the strength and safety required of airplane windshields and the effectiveness of the ice removal means must be much greater than in automobiles. The system adopted, therefore, is to use two sheets of thick glass with a liquid between and an electrical heating element located in the liquid. In this way the heat is much more effectively transmitted to the outer surface of the windshield and the danger of cracking the glass by excessive local heating is avoided. Another method of providing heat is to pass air that has been heated by the engine exhaust between the two plates of glass. This requires no electrical power and has proved very effective. Continuation of this investigation should provide methods in the near future which will assure the prevention of windshield icing under the conditions encountered in flight.

Safety Fuels to Reduce Fire Hazard

New fuels, called safety fuels, will soon be commercially available and these do not give off inflammable vapors at temperatures lower than 105° F. If these fuels could be used in airplane engines the fire hazard would be reduced owing to the fact that no ordinary temperatures would cause the generation of vapor inside the airplane. The non-evaporative tendency of these fuels, however, makes them unsatisfactory in a carburetor because the carburetor must evaporate the fuel before it is fed into the engine.

During the last year N.A.C.A. investigations have been directed toward the use of safety fuel in engines equipped with a fuel injection system instead of a carburetor. With such a system the fuel is injected under pressure directly into the cylinder when required and the high temperature inside the cylinder is used to evaporate the fuel. These investigations were discussed.

It has been found that safety fuel used in an engine equipped with a fuel-injection system will give as much power output and as low fuel consumption as can be obtained with gasoline.

Institute Notes

Pacific Coast Annual Meeting of the Institute

The Pacific Coast Annual Meeting of the Institute will be held at the California Institute of Technology from June 15 through June 17, 1939. The Program Committee, consisting of Dr. A. L. Klein, Chairman, J. L. Atwood, Hall L. Hibbard, Dr. Clark B. Millikan, Richard M. Mock, Richard W. Palmer, Arthur E. Raymond, and F. R. Shanley have arranged the following tentative program for the technical sessions.

Thursday, June 15, 2:00 p.m.

F. K. Kirsten and F. S. Eastman, University of Washington, "The University of Washington's New 250 m.p.h. Wind Tunnel."

B. C. Haynes, Boeing School of Aeronautics, "Laboratory Experiments in Meteorology" (with motion pictures).

8:00 p.m.

L. B. Rumph and R. S. Schairer, California Institute of Technology, "Some Boundary Layer Experiments in the Wind Tunnel and in Flight."

Jean Wylie, Douglas Aircraft Company, "The Dynamics of the Tricycle Landing Gear."

Friday, June 16, 9:30 a.m.

Fredric Flader, Curtiss Aeroplane Division, Curtiss-Wright Corporation, "Development of Very High Speed Airplanes." (A second paper to be announced.)

2:00 p.m.

Carlton Kemper, National Advisory Committee for Aeronautics, "Aircraft Engine Research at the Langley Field Laboratories of the National Advisory Committee for Aeronautics."

R. F. Gagg, Wright Aeronautical Corporation, "Selection of Aircraft Engines for Specific Services."

8:00 p.m.

Albert Gail, United Air Lines Transport Corporation, "Analysis of Best Rate of Climb and Ceiling as Affected by Ice Accretion."

F. K. Kirsten and F. C. Rosacker, University of Washington, "High Intensity Neon Illumination for Visual Landings in Fog and for Wide Angle Beacons."

Saturday, June 17, a.m.

Paul Hovgard, Curtiss Aeroplane Division, Curtiss-Wright Corporation, "Means for Suppression of Interference Burble."

2:00 p.m.

J. E. Lipp, Douglas Aircraft Company, "Comparison of Various Types of Metal Spars."

E. E. Sechler, California Institute of Technology, "Structural Investigations at the Guggenheim Aeronautical Laboratory of California Institute of Technology."

Branches

The April "Simultaneous Lectures" program consisted of two Annual Meeting papers, "Current Progress in Flight Testing" by N. F. Scudder of the Glenn L. Martin Company, and "Some Problems Pertaining to Pressurized Fuselages" by L. F. Engelhardt of the Curtiss-Wright Corporation.

Polytechnic Institute of Brooklyn. Two meetings of this Student Branch were held in March. At the first, on March 9th, George Ruhe gave a digest of the "Simultaneous Lecture" on "A Terrain Clearance Indicator" by Lloyd Espenschied and R. C. Newhouse. On March 23rd, Robert Kidder talked on "Operating Safety Features of the Modern Transport Airplane." Interesting discussions followed the presentations. About twenty-five students attended each meeting.

Catholic University. On March 2nd, the "Simultaneous Lecture" on "Design Aspects of the Boeing Transatlantic Clipper" by W. D. Beall was presented to this Student Branch. On March 16th, the Espenschied-Newhouse and Lyman-Mosely lectures on Instruments were presented.

Los Angeles. About 110 people attended a meeting of the Los Angeles Branch held on April 11th. The program consisted of a review of the papers presented at the Annual Meeting of the Institute by F. R. Shanley, W. C. Rockefeller, and Clark B. Millikan. The summary prepared by Prof. Alexander Klemin was used as a basis for discussion. This was followed by comments by several members whose papers were reviewed. The meeting was preceded by a dinner.

University of Michigan. Fifty-three students were present at a meeting on March 9th to hear Prof. Pawlowski speak on "The Early Developments of Aeronautics in America." On March 17–18th, the Student Branch visited the Waco Aircraft Company factory at Troy, Ohio, and Wright Field. At a meeting on March 30th, attended by 40 students, Harold K. Owens gave a flight demonstration of a model ornithopter. This was followed by a discussion of the papers at the Annual Meeting of the Institute based on the "Simultaneous Lecture" on that subject by Prof. Alexander Klemin.

San Francisco. At a meeting of this Branch on April 12th, William B. Stout spoke on "The Application of Aeronautical Engineering to Other Industrial Fields." About 60 members attended the meeting which was preceded by a dinner.

Personnel Opportunities

Available

Aeronautical Engineer, A.F. I. Ae. S., familiar with War Department design and contract procedure desires to make new connection with aircraft, engine, or aeronautical accessories manufacturer. Has been continuously employed for 12 years as engineer in connection with production and procurement planning involving the manufacture of products of aeronautical classifications, and concurrently for five years in pedagogical capacity in a leading aeronautical school. Additional experience includes: one year as static test engineer and one year as aerial photographic research engineer. Reply Box No. 86, Institute of the Aeronautical Sciences.

Engineer with 22 years' aeronautical experience in design, research, teaching, production, administrative and corporate promotion; Naval Reserve Officer with considerable active duty experience; wishes to join a going concern where initiative and energy are desired. Reply Box 87, Institute of the Aeronautical Sciences.

Graduate Mechanical and Structural Engineer, with 14 years of aeronautical experience, expert knowledge of commercial aircraft design and requirements for all types of construction, recent experience on two-engine amphibian, and considerable executive ability. Small well-established company in Los Angeles County preferred. Reply Box 88, Institute of the Aeronautical Sciences.

Aeronautical Reviews

These brief reviews of recent articles on aviation subjects are published by the Army Air Corps for the information of its officers, and are printed here each month by permission of the Chief of the Air Corps

Aerodynamics

Hispano Suiza 3000-Kw. Wind Tunnel. In the large wind tunnel constructed at Bois-Colombes actual points of the complete engine-propeller group can be methodically tested under the same technical conditions as on an airplane in flight but with all the advantages of an equipped laboratory. Tunnel is of the Eiffel type with free intake and pressure. Test section consists of a 5-meter-diameter jet at the outlet of the collector and length of 8 meters. A 3000-kw. motor drives a 12-bladed 8-meter-diameter fan at 300 r.p.m. giving a wind speed of 93 meters/sec. or 335 km./hr. This speed can be lowered to 25 meters/sec. and it is possible to obtain a continuous variation of 60 to 90 meters/sec. Description. *Les Ailes*, March 9, 1939, page 8, 3 illus.

Correction Factors for Wind Tunnels of Elliptical Cross Section with Partly Open and Partly Closed Measuring Section. F. Riegels. Wing with rectangular lift distribution was located in a wind tunnel of this type with partly open and partly closed measuring section, and additional flow induced by the tunnel boundary was determined by means of a conforming diagram.

For a jet with elliptical cross section having an axis ratio of $1:\sqrt{2}$, the correction factor was recorded for various conditions of span to tunnel width and different aperture angles (angles formed by the lines connecting terminal points of the fixed portion of tunnel boundary with ellipse center). As in the circular jet, it was found that, for a given aperture angle, correction for the angle of incidence and drag becomes zero, this angle varying with wing span.

Theory is so carried out that it is applicable also to elliptical tunnels with different axis ratio. Application to wings which are suspended above the tunnel center plane also is possible. *Luftfahrtforschung*, January 10, 1939, pages 26–30, 9 illus., 27 equations.

Aircraft Design

The B.M.E.P. Parameter for Airplane Cruising-Power Control. R. E. Johnson and W. G. Lundquist. B.m.e.p. parameter proposed is based upon cruising operation at or near maximum efficiency of the engine-airplane-propeller combination. It is shown how the parameter is related fundamentally to the operating efficiency of the engine as defined by fuel consumption and, therefore, to overall efficiency of the airplane-engine-propeller combination.

Parameter is discussed further as it is related to the engine alone, as it is tempered by considerations of airplane and propeller efficiency, as it is applied to the physical problem of controlling cruising power, and as it is limited by engine and airplane design. *S.A.E. Jour. (Trans.)*, March, 1939, pages 97–103, 13 illus.

Aerodynamic Design. F. G. Miles. Until some really powerful method of controlling boundary layer is discovered, it is considered that research on smoother surfaces is purely of academic value. A more profitable line of attack is to continue the paring process by increasing wing loading and by gradually eliminating all but the wings and control mechanism. Up to a certain limit greater speeds may be attained at high altitudes, which would be quite impossible at lower altitudes on account of very high wing loadings necessary there. Beyond that limit, optimum values of C_L/C_D fall to such a low figure that even high up further increase of speed becomes impossible.

Change of wing section near the tip can give much improved lateral control at stall. Although variable-area wing and flap can give very high lift coefficients, there is difficulty that they may be reached at unpractically high angles of incidence and that presence of the ground in landing will probably prevent full lift from being developed. Fixed-pitch propeller from blades of which boundary layer is removed is considered as a solution to the propeller problem. Means of improving performance, control and stability, landing, and take-off are discussed with illustrations of experimental airplane designs. *Aircraft Engineering*, March, 1939, pages 81–83, 119, 12 illus.

Aeroplane Design for Production. S. D. Davies. Hypothetical design based on an imaginary specification for a high-speed two-engined medium bomber (cruising speed 300 m.p.h. at 15,000 ft. at $^2/_3$ max. power) is examined and possibilities for cooperation between design and production are assessed quantitatively. Tables give performance, characteristics, analysis of weight estimates, departmental estimate of man hours, estimated man hours for fabrication of individual parts and for assembly into major components, and labor reduction and weight increase obtained by simplification of detail design and reduction in number of parts.

Likely possibilities in modifications to improve production qualities of current design without radical alteration of original design are discussed in regard to design of detail parts, design of wings for accessibility in riveting skin covering, and design of installation of controls, power plant, and other ancilliary services. Drawings illustrate: beam utilizing thinnest possible gage (weight 0.481 lb./ft.), beam in which heavy-gage material is advantageous (weight 0.58 lb./ft.), three types of stiffener section, and structures built up with drawn strip stringers (weight, less skin, 69 lb./100 sq.ft.) and extruded stringers (weight, less skin, 83 lb./100 sq.ft.), respectively, indicating greater space possible with latter method. Future requirements, production research, and national view necessary in regard to raw materials are discussed. *Aircraft Engineering*, March, 1939, pages 121–126, 4 illus., 10 tables.

Control Axes. W. E. Gray. Both British and American views of zero yaw about body and wind axes are considered unsound, and necessity for designing for inertia effects is pointed out. Question of axes is reviewed with special reference to lateral control at higher incidences, and attention is drawn to the influence of fuselage inertia on motion caused by the ailerons, "which appears to have escaped notice so far." Plotting of rolling and yawing moments on a body-axis basis in a vector diagram for purpose of assessing merits of a lateral control is considered "just plain nonsense." "N.A.C.A., in changing from body to wind axis, has still not reached a sound basis on which to compare lateral controls." N.A.C.A. Report No. 570 is referred to.

Angle at which the control force must act is shown to depend upon ratio of body-to-wing inertia. Existing and experimental controls are analyzed in light of the inertia aspect. It is suggested that the British Aeronautical Research Committee should test a model for yawing moments while rotating freely under its ailerons. Rate of roll will give some check on balance of rolling moments at the same time. *Flight, Aircraft Engr. Sup.*, March 23, 1929, pages 9–12, 5 illus.

An Elementary Study of the Spin. J. H. Crowe. Rolling and yawing inertia couples; yawing inertia and the spin; propeller moments; autorotation; experiment in wind tunnels; rolling moment due to sideslip; Glauert's criterion of autorotation presented to emphasize points in connection with the shape of the lift curve beyond the stall; different phases of autorotation as shown by the polar diagram; and biplane and monoplane autorotation. Continued. *Aircraft Engineering*, March, 1939, pages 111–114, 8 illus., 6 equations.

Principles of Rotary Aircraft. A. Klemin. Characteristics of the Model K-2 (1932), Model K-4 (1934), Model KD-1 (1935), and specification of a forthcoming Hafner gyro; achievements to date and immediate developments (military utility of the autogiro, safety record, and flight qualities); fundamental problems of the helicopter; the de Bothezat helicopter; Berliner combination airplane and helicopter; Pescara helicopter; Baumhauer's helicogyro; Hellesen-Kahn helicopter; Ascanio helicopter; Asboth helicogyro; Breguet helicopter; Focke helicopter; Platt Cyclogiro; and Vertigiro; further research problems; future for all types and the Dorsey Bill; autogiro, or gyroplane, *versus* helicopter; and airplanes *versus* rotary-wing aircraft. Helicopter problems are discussed in detail but the remainder of the article deals with shorter comments. *Journal Franklin Institute*, March, 1939, pages 354–397, 23 illus.

Some Drag Problems of the Moment. E. F. Relf. Profile drag problems are discussed, especially whether the transition far back from the wing leading edge will occur on suitable sections no matter how far the Reynolds Number is increased, and whether it is possible to encourage a still farther back transition by any alteration of section that is practically possible. It is necessary first to find an airplane capable of attaining the desired high Reynolds Number and having a sufficient spanwise length of wing undisturbed by propeller slipstream or discontinuities such as ailerons, to enable measurements to be made. There is some indication that the second problem may admit of favorable answer in range of Reynolds Number now available. Wing sections likely to lead to far-back transition are discussed. Drag connected with the installation and cooling of the engine is also considered. *Aircraft Engineering*, March, 1939, page 95.

Conditions of Similitude for Flutter Vibrations of Wings. W. Kaufmann. Conditions of similitude which must be fulfilled in order that flutter vibration occurring on large designs can be investigated in model tests. It is shown that under consideration of all acting forces an ideal satisfactory model law is not possible.

By means of wind-tunnel tests it was determined what model conditions for actual conditions of wings with flutter could best be calculated.

Laws of similitude are derived which apply with reasonable accuracy to the field of adjacent flow and beyond this range deviations are inconsiderable. Problem still remains open as to the influence of different surface roughness as well as of greatly deviating degree of turbulence of air flow on the results given. *Luftfahrtforschung*, January 10, 1939, pages 21–25, 5 illus., 16 equations.

Due to Propeller Slipstream Airplanes Could Take Off from a Small Space. S. Pivko. If the Potez 63 had two propellers of 4.18 meter diameter, it would leave the ground as a helicopter with a climb of 1.1 meters/sec. According to calculations, the Morane Saulnier 405 could be flown over a spot at a speed of 0.5 meters/sec. on the condition that diameter of the propeller was increased from 3 to 3.96 meters.

Results of the author's study of the aerodynamics of a wing placed in a jet of air, showed that it is possible to realize the take-off and landing toward the vertical, as well as hovering, with a purely conventional airplane, provided propellers of large dimensions are used, the slipstream acting on a large surface of the wing. Aerodynamic reactions of a lifting wing placed in the slipstream of a propeller turning at a fixed point were found to be very complex functions of wing incidence, of distance and relative elevation of the propeller with respect to the center of wing profile, of ratio of wing chord to propeller diameter, of relative propeller pitch, and of speed of rotation. *Les Ailes*, March 2, 1939, pages 7–8, 2 illus.

Flight Measurements on the Influence of Propeller Slipstream and Landing-Flap Setting on Downwash and Dynamic Pressure at Horizontal Tail Surfaces. E. Eujen. The described method of measurement on an airplane in flight made it possible to investigate flow processes on tail surfaces in particular when circulation over the wing is changed by propeller slipstream effect or by flap setting. By meeting certain suppositions, the selected measuring method yields satisfactory results and therefore may serve to supplement wind-tunnel measurements as well as to determine and eliminate in newly developed airplanes the cause of insufficient stability or great load changes, so far as they are based on influence of horizontal tail surfaces. Description of method and test results. D.V.L. report. *Luftfahrtforschung*, January 10, 1939, pages 38–46.

Formula for the Speed Induced by a Thin Wing Profile at Points Located on the Extended Chord. K. Jaeckel. For some purposes in airplane design the induced speed produced by a wing at a point outside of the profile is sought. In particular the points which are located on the extended chord, or at least not far from it, are of importance. When it is used in the first approximation with the effect which a two-dimensional wing exerts, the expression for induced speed at these points may be given explicitly. *Luftfahrtforschung*, January 10, 1939, page 53, 11 equations.

Influence of Control Masses on Longitudinal Stability with Loose Control Surfaces. R. Schmidt. Longitudinal stability of an airplane is generally measured in model tests only with locked elevator. Stability in flight with free elevator, of much greater importance, is subsequently computed by introducing known values for the automatic aerodynamic setting of the free elevator under effect of air forces. In addition to these aerodynamic influences, moments due to weights of all control parts exert an influence on the elevator of the airplane in flight which affects the automatic setting and consequently the stability. Change of stability can be computed theoretically when course of these control-weight moments is known.

Flight-mechanical relations in the effect of moments due to weight are investigated and stability is calculated for a practical case. Report of the Dornier company. *Luftfahrtforschung*, January 10, 1939, pages 31–37, 10 illus., 9 equations.

Method for Progressive Calculation of Lift Distribution over the Wing Chord. K. Jaeckel. Requirements for an approximate method are devel-

oped. A particular distribution, such as the elliptical chord distribution $l^*(y)$, is used as a basis and actual distribution $l(y)$ is considered in subsequent steps. The Fourier developments of $\frac{l(y)-l^*(y)}{l(y)} = \frac{l^{**}(y)}{l(y)}$ and $\alpha_0(y)$, the angle of incidence distribution, play an important part.

Sufficient conditions are given which guarantee convergence of the method. They are well met for the principal wing forms and are: coefficient totals of the given Fourier developments for $\alpha_0(y)$ and $l^{**}(y)/l(y)$ should absolutely converge. However, the total value should remain below 1 for the chord correction distribution. Method converges like a geometric series, so that in most cases it suffices to discontinue the calculation after the second approximation. *Luftfahrtforschung*, January 10, 1939, pages 47–52, 2 illus., 33 equations.

Sucking away the Boundary Layer. F. G. Miles. Perhaps the idea of sucking over large areas will not be a thing of the near future, if it should ever be proved worthwhile, but very probably it will be used shortly to eliminate unavoidable drag caused by interference such as at the junction of fuselage and wings, or between fuselage and tail unit. Theoretical work done shows that if a means can be found by which boundary layer can be removed in such a way that it never becomes turbulent (or effect of the suction is to produce everywhere an extremely thin laminar layer such as on the leading edge of the wing) then the quantity of air to be removed is an inverse function of Reynolds Number.

Analysis of full-scale flying experiments shows that at top speed the effect of removing boundary layer was to reduce the total drag of the airplane by 8 percent, or a 22 percent decrease in profile drag of the wing. Experiments, results, and equipment are described. In first flight experiments profile drag with and without suction was measured, and in the second change in rate of climb and gliding angle and top speed were measured. *Flight*, January 26, 1939, pages 82b–82d, 7 illus.

Stress Analysis and Structures

Calculation of a Two-Spar Wing with Covering Resistant to Shear. P. Cicola. Determination of forces and deformations on a two-spar structure of the box type subject to a generic distribution of transverse loads. Effects of the flexibility of the ribs are calculated. Discussion and calculations cover: box subject to twisting moments; box subject to bending and twisting moments; determination of stresses produced by transverse generic loads; analysis of deformation; choice of axis of reference; the non-rectangular box, conditions of the connections of the structure; effect of flexibility of ribs; and numerical application to a structure with flexible ribs. *L'Aerotecnica*, January, 1939, pages 1–26, 3 illus., 1 table, 26 equations.

Determination of the Stresses in Shear on Hollow Sections Multifariously Connected and However Unsymmetrical. G. Maraschini. Method for determination of stresses in shear in hollow sections multifariously connected and however unsymmetrical. Method is applied to a monocoque wing structure with several spars, with particular regard to the practical position of the calculation and to the simplification possibilities. Method is extended to the case of stresses higher than the critical. Numerical examples of a rectangular box section are given. *L'Aerotecnica*, January, 1939, pages 33–46, 12 illus., 13 equations.

Increase of Specific Load Carrying in Tension, Compression and Buckling for Welded Steel-Tube Diagonal Members in Airplane Structures by Means of Development in Materials and Structural Design. J. Mueller. New type of aircraft structure described has been developed by improvements in the processing of materials and structural design. Structure has been extensively tested on a number of Focke-Wulf airplanes in series production and has given satisfactory service. Higher tension, compression and buckling loads can be carried than have been possible for the generally known and conventional welded steel-tube diagonal members, and better utilization of material and weight economy is permitted.

Results of tests made in the development of the diagonal members are described including: buckling and strength values for untempered American, German and Swedish chrome-molybdenum steel tubes; buckling resistance and other properties of chrome-moly steel tubes in the condition received; buckling and tensile strength of tempered chrome-moly steel tubes; buckling test results with tempered and then end-welded chrome-moly steel tubes; and buckling test results with tempered chrome-moly steel tube with greatly stiffened ends. Report of the Focke-Wulf Aircraft Company. *Luftfahrtforschung*, January 10, 1939, pages 14–17, 9 illus., 5 tables.

Toward the Lobster-Claw Wing. New type of wing now being tested by DeHavilland consists of a shell, three shear webs and occasional fore and aft diaphragms. Stress-carrying parts of skin and webs are of impregnated wood supported by a new form of expanded or aerated vulcanite. Thin skin is able to carry ultimate stresses approximating to those of the material used. Although vertical longitudinal members are described as shear webs, they come very close to the normal spar when one takes into account the effect of the thick skin and the supporting pieces of flanges or "improved" wood. "While this useful work is going on at Hatfield, elsewhere airfoil surfaces or planes of die-molded 'improved' wood are actually being made." Photograph only. *Aeroplane*, March 8, 1939, page 29B, 1 illus.

Arc Welding in Aircraft. R. H. Upson. Arc-welded concentrated steel construction with screwed on skin under proper normal pressure has qualities which should make it more economical and generally more satisfactory than prevailing aircraft forms. Method of stiffening the surface to withstand pressure forces is accomplished by maintaining and utilizing a pressure difference of small magnitude acting normal to the skin and always in the same direction. Controlling air vents are put at points where pressure is just sufficient to insure the desired result. Wing volume being small and screwed seams relatively tight, only small intake openings are needed. Pressures both inside and outside the wing are automatically generated in proper proportion by effect of airspeed itself and by wing angle of attack. Construction of present wings and of proposed arc-welded stainless-steel wing is illustrated in drawings.

Appendix which deals with mathematical analysis of this type of stressed skin for airplane wings is not included in the article, but frame analysis and cost are covered. Principle of structure of the ZMC-2 airship is applied to an aircraft wing. *Welding Jour.*, March, 1939, pages 143–146, 4 illus.

Use of Plastics in Aircraft. E. P. King. DeHavilland Albatross tailplane showing use of Bakelite, and an experimental wing fabricated in plastics are illustrated, in the latter of which there are no ribs, only shear members and an occasional bulkhead between top and bottom surfaces. Each surface is really a sandwich formed of expanded vulcanite between veneers of impregnated birchwood. Buckling stress of veneers so supported is found to approach 60 per cent of ultimate strength of material used.

First fully-molded hollow Bakelite propeller blade in cord material has been successfully produced by DeHavilland, a sectioned blade for the Rolls Royce engine being illustrated. Production and results of tests of these blades are described.

Properties and possibilities of cellulose acetate, styrene acrylic and vinyl polymerization products, development and application to aircraft of thermosetting resinoid materials of the phenol and urea types, and results of tests on the suitability of the latter for aircraft are discussed. Strength-weight ratios for various types of materials and choice of filler are considered. *Aircraft Engineering*, March, 1939, pages 96–100, 15 illus., 4 tables.

Aircraft

Faster and Faster and Faster. France is to make an attempt to raise the word's absolute speed record of 440 m.p.h. held by Italy and the 100 km. record of 394 m.p.h. held by Germany. Airplane will be a Caudron designed by M. Riffard and a modification of the Caudron C-712. It will be powered by an 800 hp. Renault engine of 19 liters capacity, and will be ready in April. The Nuffield-Heston-Napier airplane, rumored to have been designed for a speed of 530 m.p.h. should be ready this summer. "Roscoe Turner is said to be building a 500 m.p.h. airplane. Fast two-motor fighters with speeds of more than 400 m.p.h. are flying in the U.S.A. already." Dr. Heinkel and General Udet have stated that the Heinkel He. 112U can exceed 430 m.p.h. and Professor Messerschmidt is also very much in the running. Brief reference. *Aeroplane*, March 1, 1939, page 257.

The Test Methods at Villacoublay Are an Advantage in America. Having started by regarding the inspection apparatus of the French Air mission with concern, the Curtiss-Wright engineers are said to have been so much interested by the results obtained that they have requested permission to use, on their own account, the French test methods which undoubtedly will become common in the United States. There is no doubt that the American engineers will derive a certain benefit—which will lead to an improvement of their products—by the application of French test, methods. *Les Ailes*, March 2, 1939, page 7.

A Yank at Grantham. First North American Harvard "Basic" trainer delivered to the Royal Air Force is described in detail and instructions received from America are quoted. Main differences from the American prototype lie in provision of a retractable undercarriage and fitting of a 530-hp. Pratt and Whitney Wasp engine. Fixed leading-edge slots on the Harvard, which were not to be found in earlier U.S. Army Air Corps B.T.9s, are discussed. "Flying characteristics of the type were never vicious and it speaks well for the machine that while, even now, it stalls on the clock without over-much warning, pilots look forward to their next flight." *Flight*, January 26, 1939, pages 84–85, 2 illus.

Czechoslovakia

The 1939 Praga Lightweights. Latest version of the Praga E.114 and its Praga D flat-four 70-hp. engine. Cruising speed 118 m.p.h. Description and reference to the Praga E.210 twin-engined airplane with a maximum speed of 143 m.p.h. *Flight*, March 16, 1939, page 277, 2 illus.

France

Aircraft in Test. Brief references only to the following military aircraft in test: First issue—High-speed three seater, designed by the S.N.C.A. and starting its tests, is a twin-engined airplane of high fineness, with tricycle landing gear and a speed around 600 km. /hr. Of two Curtiss P.36 pursuits the propeller blade of one, incorrectly adapted, warmed up the engine. The other damaged a tail wheel in landing which appeared to have been locked. Another P.36 pursuit with its fuel tanks filled went into a flat spin during acrobatics. LeO-45 bomber (two Gnôme Rhône 14-N.20/21 of 2060 hp.) finished its tests brilliantly. Dewoitine D-520 pursuit (Hispano-Suiza 12-YCRS 860 hp. engine) in tests exceeded 530 km. /hr. With a Hispano-Suiza 1000 hp. engine it should attain 550 km. /hr. and, with 1200 hp., 700 km. /hr.

Second issue—Dewoitine D-520 single-seater pursuit (Hispano-Suiza 12Vers 860 hp. engine). Potez 63-11 (two Gnôme-Rhône Mars engines) and Potez 63-12 (two Pratt-Whitney Twin-Wasp engines) differing from production models by improvement of an observation turret in the fuselage nose. Latecoere 570 bomber (two Hispano-Suiza 14-AA engines). The Sud-Est 100 600-km. /hr. prototype pursuit and attack airplane (two Gnôme-Rhône 14-No-engines, and retractable three-wheel landing gear) has a steel-tube fuselage and wings of wood, but production model will be of duralumin. Commercial and light airplanes also mentioned. *Les Ailes*, February 23 and March 2, 1939, pages 9, and 9.

Caudron "Cyclone" Fighter Airplane. A. Frachet. Cyclone is a low-wing monoplane of mixed wood, duralumin and magnesium construction which weighs 1750 kg. It is armed with four machine guns. With a Renault 450-hp. engine, the fighter has a speed of 485 km. /hr. at 4000 meters to which it climbs in 6 min. 45 sec. Range is 900 km. at 320 km. /hr. Two Hispano-Suiza cannons can be mounted in the wings. Long description of design, construction, armament, characteristics, performances and comparison with other French airplanes. *Les Ailes*, February 23, 1939, page 9, 2 illus., 1 table.

Chamoy Two-seater Trainer. Prototype two-seater trainer low-wing monoplane, designed by F. Chamoy, has retractable landing gear and a 5-cylinder 60/70 hp. radial engine. Speed with landing gear retracted 180 km. /hr. and range at this speed 1260 km. Few details of airplane and engine (also constructed by Chamoy), characteristics and performance. *L'Aérophile*, January, 1939, pages 8–9, 3 illus., 1 table.

French Naval Aviation. Principal patrol planes are 16½-ton Bréguet-Bizertes with top speed of 150 m.p.h. and 1550 miles cruising radius, built in 1933. Navy has 550 service airplanes and 200 officer-pilots and Army has 2000 airplanes and 3000 officers. Newest naval aircraft are the Bréguet 730's (weight 25 tons, top speed 185 m.p.h., much longer cruising range). Aircraft carriers are equipped with 2-ton Dewoitine 273's making 250 m.p.h. and some new folding-wing Nieuports. Few details of types of aircraft. *U.S. Naval Inst. Proc.*, March, 1939, page 417.

Germany

The Arado AR-95 Three-Place Biplane. The AR-95 military airplane can be transformed into a catapultable seaplane. It has a B.M.W. 132 Dc. 880-hp. engine and armament varying according to the plane's mission. Description of construction, armament as a bomber and as an observation airplane, characteristics, and performance. Maximum speed as a land plane 328 m.p.h. at 3000 meters. Time to climb to 6000 meters 12.9 min. Range 1600 km. (as a seaplane 2400 km.). *Rivista Aeronautica*, December, 1938, pages 583–586, 3 illus., 1 table.

Development of Dornier Construction. Development in the design of Dornier aircraft is traced from the first type down to the Do-26. Table gives number and horsepower of engines, wing area, span, weight and maximum velocity. *L'Aerotecnica*, January, 1939, pages 46–55, 9 illus., 1 table.

Great Britain

Another Lifting Fuselage. Fuselage of the low-wing three-engined airplane (three Aero Engine Sprite flat-twin engines), built by F. Helmy, has been designed to take a supplementary roof of airfoil section which is ad-

justable to provide different characteristics in different circumstances. In the ordinary way, lifting section lies flush with the fuselage and is part of it, but if higher lift during approach and landing or at any other time is required, leading edge is raised while trailing edge is carried on runners allowing fore-and-aft movement. In order that airflow over tail surfaces shall not be affected, section is designed with ample flow of air beneath it. Incidence of fuselage-lifting section is such that it cannot be stalled. Inventor claims it will consequently act as a form of "sky-hook" when the somewhat diminutive cantilever low wing has stalled. Diagonally wound ply strips in the fuselage are used to take stresses normally taken by wire bracing or girders. N.P.L. has commented favorably on the device from aerodynamic standpoints but staff consider it mechanically impracticable. Description. *Flight*, March 16, 1939, page 274. Photographs only. *Flight*, March 23, 1939, page 300, 3 illus. *Aeroplane*, March 22, 1939, page 382, 2 illus.

Modernity in a Trainer. Advanced features for the Parnall 382 "ab initio" trainer includes high-lift devices and facilities for inspection. Tapering in plan form and thickness, the cantilever wing is built in three sections, the outer carrying Handley Page automatic slots, and flaps are fitted along 80 per cent of the trailing edge. By use of slots and flaps airplane can be flown at 43 m.p.h. with engine on. Gipsy Six Series II engine. Top speed 155 m.p.h. Long detailed description. *Flight*, March 23, 1939, pages 284–286, 8 illus. *Aeroplane*, March 22, 1939, pages 373–374, 6 illus.

The New Big Empire Boats. New Short G-Class 32-ton flying boats built for Imperial Airways' Atlantic service. Four 1380-hp. Bristol Hercules engines. Cruising speed 180 m.p.h. at 5000 ft. on a total of 34000 hp. Duration of 17½ hours at this cruising speed or 3200 miles in still air. Payload with crew of five for this range, 3750 lb. of mail. Tankage 3600 gal. Top speed 205 m.p.h. Wing loading 33.3 lb./sq.ft. Characteristics and estimated performance. *Aeroplane*, March 22, 1939, page 375.

A New Tailless Design. New tailless airplane is being built for Handley Page Ltd. in one of the smallest airplane plants. Specifications for a two-motored tailless monoplane are quoted as they were set forth in British patent No. 497,969 granted January 2 to Handley Page and G. V. Lachmann. A streamlined central nacelle is attached to a rectangular midwing center section which carries two inline engines driving pusher propellers. Swept-back outer portions of wings carry rudders at their tips.

Two auxiliary airfoils are mounted in front of, and slightly above, the leading-edge of the rectangular center section. They are free to float and arranged to maintain longitudinal trim for the whole airplane whatever the incidence of the main wing. They are not elevators but are there to counteract large changes of longitudinal trim inherent in tailless designs. Disadvantages of some tailless airplanes in regard to longitudinal stability are pointed out, and other auxiliary airfoils patented are referred to. *Aeroplane*, March 15, 1939, pages 341–342, 5 illus.

. . . . . and Bristol Fashion. History of the Bristol Aeroplane Company and descriptions of its past and present aircraft. *Flight*, March 2, 1939, pages 212–218, 33 illus.

British Aeroplanes for Cags, Clubs and Owner-Pilots. Photographs or drawings, characteristics and performances are given for 27 British light airplanes, six forthcoming attractions, 11 foreign attractions on the British market, and three gyroplanes. These aircraft are recommended for C.A.G.'s., clubs, and owner-pilots. *Aeroplane*, March 8, 1939, pages 313–320, 320A, 47 illus.

The Hawker Henley. Hawker Henley light bomber (Rolls Royce Merlin 1030-hp. engine), which is officially to be used to tow targets, climbs to a height of 10,000 ft. in 8.5 min. Radiator installation is of special interest. "It is probably the most efficient layout which has yet been put into production. So far as can be found out the thrust provided by the escaping cooling air offsets the drag caused both by the shape of the radiator cowling and by the increase of skin friction." Performance observed during a flight in the Henley is discussed. Cutaway drawing shows construction and location of equipment and other drawings of structural details, and characteristics and performances are given. *Aeroplane*, March 1, 1939, pages 275–277, 258–260, 22 illus.

The Sunderland I. Sunderland I long-range high-performance flying boat described (four Bristol Pegasus XXII engines each giving 1010 hp. for take-off) is intended for long-distance reconnaissance, patrol and bombing operations and is already extensively used by R.A.F. squadrons. Apart from a heavy bomb load, accommodated in the hull, there are two Nash and Thompson power-driven gun turrets (bow and stern) and two midship gun mountings. In a special fireproof compartment in the leading edge of the starboard wing is a little A.B.C. 2-cylinder 4-stroke engine for driving accessories for refueling and bilging purposes, in addition to a dynamotor for accumulator charging. Nose turret is retractable rearwardly to permit mooring operations.

Maximum speed 210 m.p.h. at 6250 ft. Maximum cruising speed 178 m.p.h. at 5750 ft. Rate of climb 1200 ft./min. Overload range 2500 sea miles. Long description with characteristics, armament and performance. Two-page cutaway drawing showing location of equipment and photographs of cockpit. *Flight*, January 27, 1938, pages 75–80, 6 illus., 1 table.

ITALY

Cant Z 1012. Cant Z 1012 low-wing commercial touring and transport airplane carrying a pilot and three passengers. Either three Alfa-Romeo 110 4-cylinder inline 120-hp. or three Alfa Romeo 115 6-cylinder inline 185-hp. engines are used. Description, weights, characteristics, and performances are given for the airplane with both types of engine. *L'Aerotecnica*, January, 1939, pages 111–113, 2 illus., 2 tables.

The Fiat CR.42 Pursuit Biplane and Macchi C.200. Fiat CR.42 two-seater biplane is derived from the CR.32. Fiat A-74 two-row 840-hp. radial engine. Maximum speed 450 km./hr. at 4000 meters. Climb to 6000 meters in 8 min. 2 sec.

Macchi C.200 single-seater pursuit is powered by a 840-hp. engine. Maximum speed 505 km./hr. at 4800 meters. Climb to 6000 meters with 430-kg. load in 6 min. 30 sec. Characteristics and performances of both aircraft. *L'Aérophile*, January, 1939, page 6, 2 illus., 2 tables.

Saiman LB-2 Touring Airplane. Two-place airplane, produced by Societá Industrie Meccaniche Aeronautiche Navali, has tricycle landing gear and an Alfa Romeo 110 4-cylinder inline engine driving a pusher propeller. Maximum speed 215 km./hr. Characteristics and performance only. *L'Aerotecnica*, January, 1939, page 109, 1 illus., 1 table.

U.S.A.

Private and Commercial Aircraft Manufactured under Approved Type Certificates. Descriptive technical digest of 62 American private and commercial aircraft and data on variations of several types. Specifications, performance, engine, construction, standard equipment, instruments, shipping data, photograph, and drawing for each are included.

Second article gives similar data for 17 basic types of American commercial and private aircraft which had not received C.A.A. Approved Type Certificates at the time the magazine went to press. *Aero Digest*, March, 1939, pages 60–100 and 102–112 (alternate pages), 158 illus.

Aircraft Accessories

Aircraft Accessories. Air Associates rotary windshield cleaner, Norma-Hoffmann bearings, Torrington's Bantam bearings, Aircraft Accessories four-way directional control valve for hydraulic controls, Fleetwings valve mechanism for hydraulically-operated mechanisms for landing gear, flaps, tail wheels, and Cuno Auto-Klean filter for pressure side of hydraulic pumps. Brief reviews of these American Accessories made available in the past year. *Aero Digest*, March, 1939, pages 191, 195, 4 illus.

A Glass De-Icing by Electric Heating. Rideau and Ducret. Constructed in Triplex glass with a network of very fine wires submerged in the thickness of the glass, the safety window described offers a very low thermal resistance which renders it particularly interesting for aircraft. Tests of the Rideau-Ducret process of electrically heating glass windows of the pilot's cockpit carried out by Air France in 1938 have shown it possible to render the ice pasty on melting and easily carried away by means of a normal windscreen wiper brush. Exterior and interior icing, means of protection, thermal processes, heating the glass and experiments are described. *Les Ailes*, March 9, 1939, page 7, 1 illus.

Alighting Gear

Aircraft Accessories. American landing-gear equipment made available in the past year is reviewed, including Aircraft-Associates, Universal-Alloy, and Aeronautical Trading tail wheels, Goodrich brake, Shinn Devices 8-in. wheel and brake, Federal skiis and ski dolly, and Cleveland Pneumatic tail-wheel steering knuckle. *Aero Digest*, March, 1939, pages 188, 191, 6 illus.

New Tailwheel Tire. New type of tailwheel tire (6 × 2.00) put out by the Rose Tire Company is said not to slip on the wheel and to reduce wear and tear. Tire has gum-filled center and is ribbed along the inner circle to fit more snugly to the hub.

A second brief reference mentions a new full-swivel wheel put out by the Universal Alloy Products Company, for attachment to tailskids of light aircraft. Wheel has been tested for aircraft up to 130 lb. static tail load. *Western Flying*, January, 1939, page 32.

Tucking in the Tail Wheel. New Dowty retractable tail wheel. Jack effecting retraction and extension of the unit also operates a locking plunger to hold the wheel in extended positions. Plunger, situated at the upper end of the unit is attached to a sleeve sliding on the outside of the main shock-absorber member. Shock absorber which may be of the spring or oleo-pneumatic type is equipped with a self-centering device to ensure satisfactory retraction within the space provided in the fuselage. Description. *Flight*, March 2, 1939, page 231, 3 illus.

Aircraft Flight Testing

Flight Research in Aerodynamics. R. P. Alston. Part played by flight testing in some of the more topical branches of aerodynamic research and experimental methods used. Measurement of profile drag, take-off and landing, handling behavior in normal flight and stalling are discussed in great detail. Methods of the Royal Aircraft Establishment are referred to. *Aircraft Engineering*, March, 1939, pages 85–86, 6 illus.

Testing Stability and Control of Aeroplanes. A. G. von Baumhauer. Dutch requirements for certificate of airworthiness for civil aircraft. Stability and controllability requirements are discussed and methods of testing and some results are described in detail, including: static conditions; quick control movement from and back to position of balance; going in and coming out of turn; a few values of bank; throttling or opening one or more engines; stalling; and miscellaneous tests. Appendix gives test procedure, and questions and remarks which help the test pilot in applying these requirements by giving more or less sharply defined questions. Summary of results of British tests for control and stability at the stall are included. *Royal Aeronautical Soc., Preprint for Meeting*, March 2, 1939, 27 pages, 10 illus., 3 tables. Abstract of paper and discussion following it. *Aeroplane*, March 15, 1939, pages 344–345.

Aircraft Manufacture

American Methods of Aircraft Production. T. P. Wright. Paper previously abstracted from preprint, and discussion following. *Jour. Royal Aeronautical Soc.*, March, 1939, pages 131–223, 127 illus.

Refueling In Air

Fuelling in the Air. C. G. Grey. Mr. Grey's introduction to "Flight Re-Fuelling" which is a description of a method developed by Sir Alan Cobham and his fellow workers, and is contributed by the staff of Flight Refuelling, Ltd. In the latter article it is explained to just what extent tanking up for fuelling or refuelling in the air can extend the range or payload of airplanes. Discussion covers: assisted take-off in general; refuelling in flight; historical review of development; principles and process of refuelling; the tanker airplane; and effects of high wing loadings on performance. *Aeroplane*, March 1, 1939, pages 270–273, 4 illus.

Air Transportation

The Air Lines of Europe. J. P. Van Zandt. Principle findings of the 1924 report on European airlines, made for the War Department, are quoted and compared point by point with the 1938 survey of European airlines. *Western Flying*, January, 1939, pages 14–16, 46, 3 illus.

Foreign Aircraft Carriers. H. J. C. Harper. Development of aircraft carriers of the United States, Japan, France, Germany, Italy, Russia, and Sweden, including a few details of the older carriers and of the Lexington, Saratoga, Ranger, Yorktown, Enterprise, Wasp, Akagi, Kaga, Ryuzyo, Soryu, Hiryo Koryu, Bearn, Graf Zeppelin, Miraglia, Gotland, and Krasnia Moryak. Number of airplanes carried and armament are given. *Flight*, March 16, 1939, pages 263–265, 3 illus.

Airports and Equipment

For "Big Stuff." Aerojacks heavy-duty aircraft jacks, are made with capacities of 3 and 5 tons, and are of hydraulic type, oil being stored in the tripod legs for transfer by hand pump to the central lifting cylinder. Locking members are used as a safety measure. Photograph only. *Flight*, March 23, 1939, page 304, 1 illus.

Greater Heston. British Air Ministry's plans for improvements and additions to Heston airport include 2000-yd. runs. Details. *Flight*, March 23, 1939, page 292, 1 illus.

QBI—and Why. G. F. Yuill. British control-zone regulations for conditions of poor visibility, known as QBI, air traffic control problems, and the control officer's responsibilities. *Flight*, March 16, 1939, pages 270c–270e, 4 illus.

QBI Contact. New Chance light-strip system for leading the blind-approach pilot visually on the ground. Down the longest runway is laid a concrete strip some 2 ft. wide and at intervals of 50 ft. for 1400 yd. a Chance light is recessed into the ground. At every quarter distance there is a cross-strip with lights placed at 30 ft. intervals. Different color filters on each row of lights identify the cross strips. Few details. *Flight*, January 26, 1939, page 89, 1 illus.

Balloons

Two Balloons Struck by Lightning. Two balloons of the R.A.F. Balloon Barrage were struck by lightning and destroyed by fire during a thunderstorm over North London on February 26. At Stanmore there was only one flash of lightning and immediately after it one of the six balloons in the air was seen to be in flames and fell on the roof of a balloon-storage shed. The other burning balloon at Chigwell drifted while burning and came down beyond the flying field. Brief reference.

A second reference states that a British balloon marked BDE-LZ-A3 landed at Varde, Jutland, on February 27th with its cable trailing. Its barograph showed that the balloon had reached a level of 46,000 ft. *Aeroplane*, March 15, 1939, page 340.

Propellers

Factors Controlling Airscrew Design. H. L. Milner. Short and independent method of establishing relationship between variables by use of the theory of dimensions according to which an equation expressing a physical law must be dimensionally homologous. Method is for convenience of airplane designers who do not wish to go into details of airfoil and propeller theory but have occasion to make preliminary estimates in which some understanding of the properties of the propeller is desirable. Formulas are derived for torque, thrust and efficiency, and effect on these quantities of varying the diameter, pitch and blade width is explained. Particulars of a two-bladed propeller giving maximum performance at speed v is considered as an example of the use of the curves. Estimation of static thrust is outlined. The variable-pitch propeller is taken up and formulas are derived for twisting moment and effect of changing pitch angle. *Aircraft Engineering*, March, 1939, pages 87–91, 9 illus., 21 equations.

The Rotol Airscrew. Hydraulic actuating mechanism of the Rotol three-bladed propeller, under production at Gloucester, is located in the hub and blades are controlled by a combined pump and governor unit situated on the engine. Forward section of hub driving center is of reduced diameter and on this neck a stationary piston is fixed. Around the piston is fitted a free cylinder sealed at both ends and free to slide under oil pressure introduced by pump unit on one or other side of piston.

To prevent magnesium-alloy blades from fretting against steel sockets, at upper end of the socket, a wedge-shaped section ring of Tufanol is fitted into the socket mouth and secured by a locking ring. Spring loaded governor of the governor-pump unit controls opening and closing of a number of ports by means of a sliding plunger, loading of spring being predetermined by remote control from cockpit. Long description of propeller and methods of manufacture. *Flight*, March 23, 1939, pages 296–299, 10 illus. *Aeroplane*, March 22, 1939, pages 369–372, 10 illus.

Aircraft Accessories. American propellers made available in the past year are reviewed briefly including Hamilton Standard's Hydromatic quick-feathering propeller, Curtiss electric propeller and special fast-feathering unit, Engineering and Research 8-ft.-diameter adjustable-pitch propelle with wood and plastic blades, Freedman-Burnham adjustable-pitch propellers for light aircraft, and Lycoming electrically-welded hollow-steel propeller. *Aero Digest*, March, 1939, pages 195–196, 3 illus.

Aircraft Instruments

Acceleration Measurements by Means of Differentiation of the Speed. J. Goerner. With the limits which are set by the sensitivity of accelerometers as a basis, an investigation was made to determine whether acceleration measurement by graphic or electrical differentiation of speed offers advantages as compared with direct measurement. Electrical differentiation of the speed with the help of a condenser is treated extensively, and the results compared with those given by the mechanical accelerometer. D.V.L. report. *Luftfahrtforschung*, January 10, 1939, pages 54–58, 10 illus., 10 equations.

Aircraft Accessories. American aircraft instruments made available in the past year are reviewed briefly, including Kollsman, Pioneer, Lewis Engineering, United States Gauge, Mile-O-Meter, S. F. Bowser, Friez, and General Electric products. Directory of accessory manufacturers also given. *Aero Digest*, March, 1939, pages 180, 183, 184, 11 illus.

A Square Deal for the Navigator. F. Chichester. Ideal cockpit for the navigator of long-distance aircraft, especially trans-oceanic aircraft, and the equipment with which it should be fitted. Duplication of some equipment is suggested so that the navigator will not have to make constant trips to other parts of the airplane.

Recommendations for the navigator's compartment include: a vertical periscopic sight for drift observation; a window with view ahead within 10° and to within 10° of the vertical; rotable and retractable celestial observation dome; use of the loop aerial for the navigator himself, for taking of bearings for position fixing; method for taking sextant observations accurately, chart table; container for navigator's books and tables; and names of books which should be carried. Drawing of navigator's cockpit indicating position of equipment included. *Flight*, March 2, 1939, pages 201–202, 1 illus.

Assisting the Blind Approach. Cobb-Slater variometer, a sensitive rate-of-climb indicator for airplanes, consists of a vertical block of transparent material with two finely tapered holes bored vertically. Each tube contains a small spherical piston, one colored green to indicate ascent and the other red to indicate descent, the rates being shown on a scale between the tubes. Small lever at the base of the instrument controls a damper for use in bumpy conditions. Tubes are connected to a reservoir of air contained in two vacuum flasks. Description. *Flight*, March 23, 1939, page 292a.

A New Met. Instrument. Fox cloud-base predictor, produced by Negretti and Zambra, relies on the characteristic behavior of rising air currents which usually condense into cloud. It will indicate cloud-base height up to 7000 ft., will forecast possible clouding over of a clear sky and will also indicate presence of an inversion with the bumpy flying conditions which it implies. Predictor consists of a wet and dry-bulb hygrometer and rotatable drum chart arranged to be read off against the former. Brief note. *Flight*, March 16, 1939, page 267.

Miscellaneous Equipment

Device Measures Pilot's Ability to See at Night. Ferree-Rand light sense tester developed by Drs. C. E. Ferree and G. Rand, measures a person's ability to look from fields of vision, such as the instrument board in the cockpit, to points outside the window. Brief reference. *Science News Letter*, March 25, 1939, page 185.

Security More Secure. Oddie cowling fastener consists of a two-blade spring of closed-U shape into which the fastener stud is locked by means of slots cut on either side. Stud has only two positions and a glance at a series of fasteners on a cowling will show at once whether all are properly home. Another Oddie safety device, a locknut, has six tongues which bite into the threads of the bolt. Brief description. *Flight*, March 23, 1939, page 303, 4 illus.

Toward Fire-proof Aeroplanes. New Semape fire-proof bullet-proof gasoline tanks described are being made in France and Italy and are being fitted to all military aircraft, motor torpedo boats and Army tanks. The tank is covered with a layer of stuff which looks like Sorbo rubber, then with a vulcanized rubber envelope, and finally with doped canvas. Gas chambers in the aerated material of the first layer are separated from one another so that neither vapor nor liquid can leak out.

If a bullet makes a hole in the covering of the tank, the tension of the covering closes the hole and stops any leakage. If, at exit of the bullet, metal is splayed and prevents the covering from closing by tension, the gasoline in the tank, working out into the covering dissolves the material and makes a sticky mass of the nature of rubber solution, which seals up the hole. Tank has proved to be practically bullet-proof against all ammunition up to 12 mm. Favorable results in drop tests, and the attachment of tank to airplane are also referred to. *Aeroplane*, March 15, 1939, page 342.

Aircraft Accessories. American electric equipment for aircraft, available in the past year, is reviewed briefly including the Cannon firewall disconnect plug and Eclipse 1500-watt generators for either 12- or 24- volt d.c. operation. *Aero Digest*, March, 1939, page 192, 2 illus.

Resilient Bushes. Oscillith bush is reinforced by a helical spring molded within the rubber casing and in perfect adherence. Spring is of course compressible and when bush is subjected to axial pressure the rubber between successive turns is displaced radially. This deformation produces internally and externally a helical formation which decreases and increases the free diameters. When pressure is relieved the spring assists the rubber to return to its free shape. Long description. *Automobile Engineer*, March, 1939, pages 93–94, 7 illus.

Parachutes

Parachuting from the Ground Up. N. P. Ewart. In the parachute-training system advocated, the pilot begins his training from the ground up in more senses than one. He stands over a grating under which a large propeller generates a strong vertical current of air. When motor is started up he releases his parachute and is blown to a height of over 200 ft., then passing out of the slipstream, and descending to earth. He will learn to control his parachute during this short descent and how to land gently. By regulating rotor speed, instructor can start the pilot's training with low jumps. Use is suggested for demonstrating operation of parachute to pilots and results of careless parachute packing, for testing models of new types of parachutes, and for making special strength tests of parachutes. One such device has been installed at Leningrad and proved its practicability. *Aeroplane*, March 22, 1939, page 378.

Testing Apparatus

A Method of Dimensional Gaging with Photoelectric Cells. C. Tuttle and W. Bornemann. Photoelectric photometry applied to gaging. In one arrangement, article to be measured diaphragms the beam to one cell and another beam falls on a second cell which merely monitors the light source. Arrangement for gaging width of an article is illustrated. In the second optical arrangement both beams become measuring beams and both cells measuring cells, a setup to measure pitch of a gear wheel or a toothed rack being illustrated. Discussion covers: details of both methods; optical magnification in a photoelectric gage and accuracy attainable; generalized experiment which the authors have attempted to determine performance characteristics of an automatic gage assembled from various sources of commercial equipment; and data from which it is possible to determine whether a photoelectric recording or controlling gage is suitable for a specific problem. *Instruments*, February, 1939, pages 67–70, 5 illus., 2 tables.

The Month's New Instruments. New devices for measurement, inspection, testing, metering, and automatic control. Short descriptions. *Instruments*, February, 1939, pages 54–65, 42 illus.

Navy to X-ray Vital Parts of Fleet. New Westinghouse portable unit will be used for inspecting vital members of aircraft and ships of the U.S. Navy before leaving the airports or ways. Unit is capable of detecting all-important defects in metals up to 3 in. thick. Brief reference. *Metals & Alloys*, February, 1939, page MA-125.

Materials

Automotive Materials—New Developments. New synthetic-resin plastic, based on vinyl acetate resins, is described by J. M. de Bell of Monsanto Chemical Company as more than doubling the "toughness" of safety glass, and as eliminating cementing and edge sealing.

Hydrodegreasing safety solvent for degreasing and de-oiling aluminum skin construction of air craft is said to have good wetting out and solvent action upon heavy grease and carbon exhaust smut, as well as "automatic emulsifying" properties when associated with a substantial amount of water. Particles in the new Acheson graphite lubricant are so fine that it can be suspended in such liquids as carbon tetrachloride and kerosene. Fales transparent protective metal coating is said to withstand action of sunlight, moisture and climatic changes. New Polydur "high-speed" synthetic enamels are said to set out of dust in a few minutes. Chemical actions involved in the production of plastics are described by G. M. Kline. *Automotive Industries*, March 18, 1939, pages 367–368, 380, 1 illus.

Metals

The Manufacture of Tubes for Aircraft. W. Hackett. Workshop processes from the raw material to the finished product, the range of tubes pro-

duced by Accles and Pollock, Ltd., and their application to aircraft. Piercing and rolling; pushbench; drawing; tools; straightening process; special instrument for measuring ovality of tubes; electric-resistance heat treatment; limitations on steel specifications; summary analysis of manganese-molybdenum and chrome-molybdenum steels; special technique for small tubes; high-pressure tubes; and manipulation of tubing (bending, tapering, bulging, flattening, heat treating, blueing furnaces, machining and grinding). *Aircraft Engineering*, March, 1939, pages 132–137, 15 illus., 4 tables.

Flexible Tubing Made of Knitted Wire. Flexible tubing is now being made by a patented wire knitting process by E. H. Tichener and Company. Through variations in wire gage, mesh size and diameter of tube, a product can be had that is very flexible or one that is rigid enough to hold its shape when bent or formed. Knitted wire can be plated, rust proofed, enameled or coated, and can be covered with rubber or silk. Few details. *Iron Age*, March 9, 1939, page 82A.

Corrosion and Protective Coatings

Engineering Uses of Heavy Nickel Electrodeposits and Other Plating Advances. F. P. Peters. Excellent specific gravity and mechanical property values obtained by W. A. Wesley indicate that the nickel deposited by his process can hardly be of a porous nature, and can compare favorably as to hardness, strength, and ductility with other materials.

Developments described by Wesley in regard to control of properties of deposits, comparison with other forms of metal, electroforming (manufacture or reproduction of articles by electrodeposition), building up or surfacing, and pore-free nickel deposits, and comparison of his opinions with those expressed by A. W. Hothersall, R. A. F. Hammond, C. F. Bonilla, and others. *Metals & Alloys*, February, 1939, pages 42–47, 5 illus.

An Investigation of the Fretting Corrosion of Closely Fitting Surfaces. G. A. Tomlinson, P. L. Thorpe, and H. J. Gough. Mutual corrosion at contact surfaces of closely-fitting machine components subject to vibration, studied at the National Physical Laboratory on behalf of the British Aeronautical Research Committee.

Stainless steel proved most susceptible in any combination. Dissimilar pairs suffered less than samples of the same substance. Combinations including brass produced the minimum amount of fretting corrosion but effect was present.

Slip between surfaces is an essential concomitant of fretting corrosion, and relative displacement need be only one or two millionths of an inch. Amount of corrosion is not greatly influenced by intensity of pressure. So long as vibratory slip and surface contact are both present, fretting corrosion will occur.

Effects were noted in tests upon chemically cleaned dry surfaces. While lubricants reduced the rate of corrosion, none effectively prevented it, not even special lubricants. Process is considered one of molecular attrition rather than mechanical abrasion. Experiments on a Haigh alternating-stress machine are discussed. Apparatus for investigation of spherical and plane surfaces in contact and for slip measurement, and experimental results are described and illustrated. Long editorial comment also. Institution Mechanical Engineers paper. *Engineering*, March 10, 1939, pages 293–295 and 281–282, 5 illus. First half of paper, discussion following, editorial in first issue, last half in second. *Engineer*, March 10 and 17, 1939, pages 325–326, 323–324, 315, and 354–356, 8 illus.

Iron and Steel

Chromium-Molybdenum Steels. A. Pomp and M. Hempel. Comparative tests of 21 steels, some containing nickel and some nickel-free were made at the instigation of the German Air Ministry. Mechanical properties are given for chrome-moly steels containing a little under 3 percent chromium which were especially promising in both ranges of tensile strength.

Commercial specimens of six chrome-molysteels (five aircraft steels) were tested later to determine degree of depth hardening after heat treatment under various conditions of specimens of different sizes. Field of utility for type 1460 seems to be in giving high tensile strength in medium or relatively small sections, while the 3.0: 0.6-percent chrome-moly and the 2.5: 0.3: 0.2-percent chrome-moly-vanadium steels offered best alternatives to nickel-chrome-moly steel for material to be treated in large masses. Abstract from *Mitt. K.W. Inst. Eisenforschung*, 1937, 19, 221, and 1938, 20, 103. *Metallurgist Sup., Engineer*, February 24, 1939, pages 13–15, 6 tables.

The Effect of Arsenic on Steel. E. Houdremont, H. Bennek, and H. Neumeister. Mechanical properties of mild and medium carbon steel, nickel-chromium, chromium-molybdenum, chromium-molybdenum creep-resisting, and carbon tool steel with various percentages of arsenic. No marked effect of arsenic either in improving or lessening corrosion resistance was found. Tests described were made to determine conditions under which arseniuretted hydrogen would be formed during pickling, and the effect of arsenic on a larger scale. Long abstract from "*Archiv fuer das Eisenhuettenwesen*," 1938–39, 12, 81 and comparison with results obtained by previous authors. *Metallurgist Sup., Engineer*, February 24, 1939, pages 3–7.

Fatigue in Theory and Practice. H. H. Bleakney. Alloying alone does not render carbon steel less sensitive to the presence of notches when subjected to alternating stress. Discussion covers: variation of endurance with strength, question of the best steel for operation under corrosion-fatigue conditions, and the seriousness of the problem of decarburization where steel is used without surface conditioning. Review of results found by previous authors. *Iron Age*, March 23, 1939, pages 29–32, 100, 1 illus.

What About Grain Size? C. L. Shapiro. First issue—Final austenitic grain size of any steel is influenced by prior structure or initial grain size, by mechanical deformation (hot and cold work) which remains or is conferred upon it during austenitizing, by rate of heating to austenitic condition, by time and temperature of heating, by method of deoxidization, and by type of inhibitors resulting from the deoxidization process. These factors may either intensify or minimize one another's effects and either refine or increase austenitic grain size, depending on whether they act in a like or opposite manner. Each of these factors are discussed in detail.

Second issue—Effect of grain size on case depth and characteristics; function of grain size upon rate of transformation; and effect of grain size upon hardenability (hardness and penetration), tensile properties, creep, impact properties, temper brittleness, brittleness at subzero temperature, aging, decarburization, machinability, piping, deep drawing characteristics, and magnetic properties. Table shows effect of grain size upon some of the physical, chemical, and structural properties and characteristics of steel. Concluded. *Iron Age*, March 30 and April 6, 1939, pages 23–26 and 33–37, 8 illus., 4 tables.

Recent Researches in Steel Metallurgy. W. H. Hatfield. Determination of nature and degree of heterogeneity in steel, as affected by process employed and composition and conditions of casting of material; experiment to determine if any stress would produce a permanent strain even at normal temperatures; effect of maintaining of a heat-resisting steel (0.21 percent carbon, 12.32 percent nickel, 21.09 percent chromium) under a load of 280 lb./sq.in. for 10,000 hours at 900°C.; effect upon mechanical properties of steels, of prolonged exposures to high temperatures; influence of added elements; and experiments with rustless-steel compositions. Abstract of Royal Institution paper. *Engineering*, March 24, 1939, page 346.

Non-Ferrous Alloys

Light Alloys for Aircraft. H. Sutton. Fatigue properties under reversed bending stresses are reduced somewhat in magnesium-rich alloys by previous straining of the material longitudinally under tension. Duralumin is relatively insensitive to stress corrosion effect if correctly heat treated, that is, depreciation in mechanical properties such as breaking load and elongation is not much affected by static stresses applied simultaneously with salt spray. As in the case with other alloys, including aluminum-rich alloys, corrosion resistance of magnesium alloys is greatest in the cast condition.

Improvements to duralumin and a new high-strength wrought aluminum alloy of recent origin (4 to 6 percent zinc, 2 to 4 percent magnesium, 1.5 to 3 percent copper, 1 percent nickel) are described. Latter is supplied in the form of extrusions, which after double heat treatment have strength properties of 60,000 to 74,000 lb./sq.in. tensile proof stress, and 74,000 to 85,000 lb./sq.in. ultimate tensile strength. Magnesium castings and sheets, a cerium-cobalt-magnesium alloy for parts subjected to high temperature such as pistons, aluminum-coated sheets for aircraft structures, and heat treatment of wrought aluminum alloys are also discussed. Midland Metallurgical Societies paper. *Iron Age*, March 30, 1939, pages 28–31, 92.

Modern Aluminum Alloys. J. R. Hanforth. Specification, chemical composition, and physical properties of aluminum alloys used for British aircraft and aero-engine purposes including: sheets and strips; castings (not heat treated, precipitation hardened at 150–175°C., solution treated, and solution treated and artificially aged); and wrought alloys produced as extrusions and forgings. Most recent alloy, and the light alloy with the highest tensile strength yet made available for aircraft production, is that covered by specification D.T.D.363 (RR77 magnesium-zinc type). Bearings are manufactured by Wellworthy Piston Rings, Ltd., from an aluminum-alloy (5.5–7 percent tin, 1.5–1.8 percent nickel, 0.6–0.9 percent copper, and 0.7–1 percent magnesium) which was developed in experimental work at Rolls Royce. This is referred to as one of the most interesting developments in alloy technique. A German bearing metal is mentioned. *Aircraft Engineering*, March, 1939, pages 101–106, 11 illus., 4 tables.

Defects in Non-Ferrous Ingots. G. L. Bailey. Non-metallic inclusions, recommendations regarding melting and casting, and abnormal methods of casting achieving desirable results to maximum extent (Durville process, Erichsen mold, and Roth method of casting aluminum ingots). Concluded. *Metal Industry*, March 3, 1939, pages 269–271, 2 illus.

The Extrusion of Some Aluminum Alloys. C. E. Pearson. Extrusion test results with aluminum alloys containing 1.5, 2.5, and 5.0 percent copper, with a commercial grade of aluminum, with an alloy which, while relatively easy to extrude possessed good mechanical properties, containing 1.25 percent copper and 10 percent zinc, and with an alloy which showed hot shortness, containing 5 percent zinc.

Alloys were compared by determining, at several temperatures, pressure necessary to cause extrusion at a predetermined rate through a standard die by the inverted method. Extrusion at higher rates and effect of temperature of extrusion on flow in alloys during extrusion also investigated. Mechanical properties of the extruded alloys. *Metal Industry*, March 10, 1939, pages 295–298, 8 illus., 5 tables.

Research Points from Papers (British Institute of Metals). "Creep Curves of Lead and Its Dilute Alloys," J. N. Greenwood. "Effect of Chromium on Annealing Characteristics of Copper," W. O. Alexander. "Elastic Properties of Some Antifriction Alloys," J. W. Cuthbertson. "Vapour Pressure of Zinc in Brasses," R. Hargreaves. "Intercrystalline Corrosion of Some Wrought Aluminum Alloys," J. D. Grogan and R. J. Pleasance. "Embrittlement of Tin at Elevated Temperatures," C. E. Homer and H. Plummer. "Theory of Origin of Rolling Textures in Face-Centered Cubic Metals," M. R. Pickus and C. H. Mathewson. "An X-Ray Investigation of Cobalt-Aluminum Alloys," A. J. Bradley and G. C. Seager. Short abstracts. *Metal Industry*, March 10, 1939, pages 303–306. Short abstracts of first three papers listed above and discussion. *Engineer*, March 17, 1939, pages 352–353. *Engineering*, March 17, 1939, pages 304–305.

Magnesium Alloys: Applications and Future Developments. E. Lay. Mechanical properties of cast and wrought magnesium alloys most widely used in Germany today are given together with those of the strongest aluminum alloys and grey cast iron. Luschenowsky method of refining magnesium which results in marked improvement in properties is described.

High-percentage magnesium-aluminum wrought alloys are more prone to stress corrosion which can be mitigated by heat treatment. Trouble can be overcome by cladding with superficial layers of corrosion-resisting magnesium-manganese sheet. To increase corrosion resistance, magnesium alloys are treated with a nitric acid alkalibichromate pickle. Best protection against electrolytic influences is the use of layers of varnishes. Additions of other metals to increase strength are also considered. Abstract from *Metallwirtschaft*, December 2, 1938. *Metallurgist Sup., Engineer*, February 24, 1939, pages 8–11, 3 illus., 3 tables.

A New Light Magnesium Alloy. German alloy, Magnewin, consisting mainly of magnesium, is alloyed with aluminum, zinc and magnesium in different proportions and becomes endowed with different physical and mechanical properties, giving ductile alloys suitable for pressing, welding, or forging and other alloys particularly suitable for die casting. Specific gravity between 1.76 and 1.86, according to composition. Tensile breaking strength of ductile class between 34,000 and 50,000 lb./sq.in. Compressive strength about 30 percent higher. Very brief abstract from "Engineering Progress," Berlin. *Metal Industry*, March 3, 1939, page 271.

Strain Marking in Aluminum Alloys. Effect of previous cold working on precipitation processes even at an advanced stage. Precipitation occurred first along the slip planes of specimens which had been quenched in cold water (without any subsequent working), but if quenching was in boiling water or in oil no slip bands were produced, indicating absence of internal strain, and uniform precipitation took place throughout the grains. Photomicrographs of peraluman and Avional Z, and table of percentage composition of alloys which showed strain markings. Review of literature. *Metallurgist Sup., Engineer*, February 24, 1939, pages 2–3, 2 illus., 1 table.

The Institute of Metals (British). Vapor pressure of zinc in brasses, intercrystalline corrosion of aluminum alloys, embrittlement of tin at elevated temperatures, X-ray investigation of cobalt-aluminum alloys, effect of work on mechanical properties of non-ferrous metals. Short abstracts of papers on these subjects and discussion. *Engineering*, March 24, 1939, pages 331–334. *Engineer*, March 24, 1939, pages 385–386.

Testing of Metals

Spectrography in the Non-Ferrous Metal Industry F. Twyman. Principles of procedure generally accepted; homologous line pairs; means of

producing radiation, of increasing sensitiveness, and of determining intensities of lines (logarithmic sector and microphotometer); causes of discrepancies between chemical and spectrochemical analysis; percentage to which quantitative spectrochemical analysis is applicable; and detection of nonmetallic substances. British Institute of Metals paper.

Another article describes spectrographic equipment. *Engineer*, March 24, 1939, pages 387–388 and 380–381, 4 illus. Paper by Twyman and discussion. *Engineering*, March 31, 1939, pages 384–386, 362–363.

Technical Notes. New German procedure for revealing blowholes in castings uses a coating of varnish which changes its color according to temperature to which it is subjected. Casting which has been previously subjected to X-ray examination to prove its freedom from blowholes, is used as a standard and is coated with the varnish. On heating of the casting, the varnish changes color according to thermal conductivity and thickness of the casting on different sides. Final color obtained is used as a standard. Other castings of the same dimensions are varnished and heated and their final color is compared with that of the standard casting. Any difference in color denotes the presence of blowholes. Same process is used to verify thermal distribution and efficiency in cooling of aircraft-engine cylinders. Brief note. *Les Ailes*, March 9, 1939, page 7.

The Examination of Metal Surfaces. Finch electron-diffraction camera primarily developed for examination of metal surfaces. Standard camera and oil diffusion pump are described with diagram. *Metal Industry*, March 3, 1939, pages 267–268, 2 illus.

Spectrographic Analysis. F. Twyman. Industrial application of spectrography in the non-ferrous metallurgical industry. Accepted principles of procedure; homologous line pairs; means of producing radiation, of increasing sensitiveness, and of determining intensities of lines by means of the logarithmic sector and microphotometer; causes of discrepancies between chemical and spectrochemical analysis; avoidance of effect of heterogeneity; preparation of electrodes; applicability of quantitative analysis; and detection of nonmetallic substances. *Metal Industry*, March 10, 1939, pages 299–302.

The Use of Metallic Shot in X-Raying Steel. C. D. Moriarty. New technique utilizes a fine metallic shot as a medium for improving the quality of certain types of radiographs, and is applied chiefly in X-raying of irregular steel objects. Problems relating to theory and application are discussed. Packing characteristics, mass characteristics, linear absorption of steel shot, copper shots, and other materials are considered. *General Electric Rev.*, March, 1939, pages 109–113, 8 illus., 5 equations.

WELDING

Advantages of Titanium in Low-Alloy Structural Steels for Welding. G. F. Comstock. Possibilities of titanium additions for controlling the hardenability of high-carbon high-tensile steel. Preliminary tests of 0.25-percent carbon steels (induction-furnace melts) showed that a titanium to carbon ratio between 2 and 3.5 is best for strength, yield ratio, ductility, and toughness. Welding tests of steel made in an open-hearth furnace with and without titanium additions indicated an improvement in lessened hardenability for the titanium steels. Influence of titanium in reducing degree of weld hardening produced by a single fillet weld in high-tensile steel is illustrated by two examples. Special test for determining cracking tendency of high-tensile steel during welding is described and quench-aging effects are discussed. *Metals & Alloys*, February, 1939, pages 48–51, 2 illus., 2 tables.

Spot Welding Aluminum. F. C. Pyne. Advantages of spot welding; machine settings for spot and seam welding aluminum alloys of various thickness; materials welded; cleaning sheet before spot welding; relation between shear strength of spot welds and time of current application, current density, and electrode pressure, as determined by G. O. Hoglund and G. S. Bernard, Jr.; and types of electrodes. *Western Flying*, January, 1939, pages 10–13, 7 illus., 3 tables.

Notes on Welding Practice. J. G. Waterworth and A. R. Mowbray. Specification, material, strength values, and chemical composition for weldable low-carbon and non-corrosive steels and aluminum alloys. Tables for three articles previously published. *Aircraft Engineering*, March, 1939, page 138, 2 tables.

Welding Chromium and Chromium-Nickel Corrosion and Heat-Resisting Steels—Review of Literature to July 1, 1937. W. Spraragen and G. E. Claussen. Oxyacetylene, metal-arc, atomic-hydrogen, and carbon-arc welding of 18-8 stainless steel; recovery; mechanical properties; heat treatment; resistance welding; 18-8 welding rods; welding 18-8 to plain steel and to non-ferrous metals; welding 18-8 with additions of columbium, manganese, molybdenum, molybdenum-columbium, nitrogen, silicon, tantalum, titanium, tungsten and vanadium; welding other high-alloy corrosion- and heat-resisting steels; welding stainless irons and martensitic stainless steels; soft soldering; silver soldering; brazing; forge welding; pickling and polishing; flame cutting; and suggested research problems. Correlated abstracts. *Welding Jour., Welding Res. Sup.*, March, 1939, pages 66–107, 7 illus., 56 tables.

MISCELLANEOUS

British Standard Specifications. Tensile testing of metals (Specification 18), cast iron surface plates and tables (Specification 817, 1938), rubber-insulated cables and flexible cords (Specification 7, 1939), steel storage bins and racks (Specification 826), mild steel drums for lubricating oils (Specification 814), and paint materials (Specifications 282, 388 and 390 covering lead chromes, aluminum powder and paste and oil pastes, respectively). Brief references to these British standard specifications. *Aircraft Engineering*, March, 1939, pages 110, 126.

Plastics

More About the B.I.F. Aircraft plastics exhibited in the London section of the British Industries Fair. *Flight*, March 2, 1939, pages 225–226.

Double Refraction and Change in Length of Certain Plastics. H. W. Farwell. Plasticized Vinylite XYSG is very sensitive photoelastically. Change in length under constant load was measured as well as that for succeeding recovery. Change in color of light transmitted through crossed Polaroid plates shows large change in birefringence. Further study was made with uniform length increments at constant temperature using Mach's method to measure birefringence, both for stretching and recovery. Data are sufficient to give a measure of dispersion in birefringence and of a Poisson's ratio of 0.50. *Jour. Applied Physics*, February, 1939, pages 109–113, 6 illus.

Rubber

The Physics of Rubber. E. Guth. Elastic and thermal behavior of rubber from the theoretical point of view. Actual application of thermodynamics is carried through further than in any earlier discussion, and experimental technique employed in the stress-strain work at the University of Notre Dame is described. Poisson's ratio, heat development of rubber with adiabatic stress, thermal expansion coefficient, and equations of state are considered. *Jour. Applied Physics*, March, 1939, pages 161–171, 15 illus., 3 tables, equations.

Meterology

Formation of Ice on Aircraft. G. Severi. Meteorological conditions leading to ice formation are described with charts from the Bulletin of Meteorological Studies of the Italian Air Ministry, and from German sources. Three types of ice and the mechanism of the formation of deposits which can take place on an aircraft are explained and the dangers in alteration of the characteristics of the aircraft due to the additional weight and to change in form of the wing profile are considered. A previous article from *L'Aeronautique* is discussed. To be continued. *Rivista Aeronautica*, December, 1938, pages 489–506, 5 illus.

Distribution of Air-Mass Types and Frequency of Change in the Western United States during 1937–38. A. C. Gerlach. Study of air masses and their movements. Data were taken from manuscript maps at Seattle Airport Weather Bureau. Frequency of air mass types at Seattle, Spokane, Williston, San Francisco, Los Angeles, and Salt Lake City in January, April, July, and October are shown. *Monthly Weather Rev.*, November, 1938, pages 376–377, 1 illus., 2 tables.

Fuels and Lubricants

The Viscosity of Pennsylvania Oils at High Pressure. R. M. Dibert, R. B. Dow, and C. E. Fink. Viscosity-pressure-temperature data for six Pennsylvania oils differing in chemical and physical properties at atmospheric pressure. Continuation of study previously reported. While pressure coefficient of viscosity increases in general with molecular weight, relationship seems to be significant only for fractions of a narrow boiling range from a single oil. Mean temperature coefficient of viscosity, between 100° and 210°F. Increases with molecular weight at all pressures for all the oil samples. *Jour. Applied Physics*, February, 1939, pages 113–115, 6 illus., 3 tables.

New Petrol-From-Coal Process. Experimental plant has been erected at Bedlay, near Glasgow, for production of synthetic gasoline from coal by a new British process discovered by Professor Fischer, a German chemist. Plant is producing 200 gal./day and it is claimed that the gasoline is of such high quality that it is suitable for aircraft engine use. New process is a catalytic one and involves the production of water gas by passing steam over coke. Output consists of 50 percent engine gasoline, 30 to 40 percent fuel oil and a fraction of lubricating oil. Plant has proved that 1 ton of coal yields 40 gallons of oil. *Flight*, March 2, 1939, page 211.

Action of Inhibitors on Polymer Gasoline. W. B. Ross and L. M. Henderson. Data presented show that the addition of small amounts of commercially available antioxidants to Gray treated poly distillates inhibits gum formation. Experimental data relative to the use of U.O.P. inhibitors in gasoline produced by the U.O.P. catalytic polymerization process was furnished by G. Egloff, or from work of the Pure Oil Company on their polymerized gasoline. *Oil & Gas Jour.*, March 23, 1939, pages 107–108, 4 illus., 6 tables.

Bearings

Investigation of Light-Metal Bearing Materials in the D.V.L. Bearing Testing Machine. G. Fischer. Running properties of seven aluminum and four magnesium alloys for bearings were determined on the D.V.L. bearing testing machine in combination with tempered and hardened journals. Bearing-capacity limit, behavior under repeated stress and at breakdown of oil supply were also investigated.

Bearing capacity limits for the hardened aluminum alloy were throughout above $p = 700$ kg./cm.^{2}. With an eutectic aluminum-silicon alloy an average bearing pressure of 925 kg./cm.^{2} can be attained for continuous operation. Remaining bearing materials failed at pressures from 470 to 65 kg./cm. on account of heavier working (rolling-down) or prevailing dry friction. D.V.L. report. *Luftfahrtforschung*, January 10, 1939, pages 1–13, 32 illus., 8 tables.

The Manufacture of Aircraft Engine Bearings. New equipment and various refinements in processing technique which have been adopted in the laboratory of the Michigan Smelting and Refining Division of the Bohn Aluminum and Brass Corporation, applying to the ingot as well as to fabricated units. Use of the Hilger microphotometer greatly increases speed and accuracy of spectrographic analyses and places them on a routine control basis. By use of this instrument, relative intensities of spectral lines corresponding to various impurities such as iron, antimony, aluminum, silicon, nickel, manganese, arsenic, occurring in the spectra of the samples taken from the molten charge may be read as galvanometer deflections. Another addition is a General Electric 200,000-volt oil-immersed industrial X-ray unit including a completely equipped dark room, the unit being used to detect defects. A number of the more important castings such as aircraft are checked individually. *Automotive Industries*, March 18, 1939, pages 364–367, 7 illus.

Lead Segregation in Nickel Bronzes. J. Marechal. Occurrence of lead segregation in nickel bronzes with varying tin contents. Amount of lead which can be incorporated in such a bearing bronze is determined by nickel and tin contents. Bearing bronzes best responding to conditions of good lubrication are those containing 5 to 6 percent tin, 4 to 5 percent nickel and 32 to 35 percent lead. Nickel has the effect of dispersing lead particles and of postponing appearance of lead segregation toward the high lead contents, both effects increasing lubricating qualities of the bronze. *Metal Industry*, March 24, 1939, pages 339–340, 3 illus., 2 tables.

Engine Design and Research

New method of securing heads of aircooled aircraft-engine cylinders. Top end of cylinder is externally threaded and a ring nut is provided which has an internal offset or shoulder. A turned flange on the cylinder head is clamped between end of cylinder and offset in bore of the ring nut. Brief reference to British patent of Skoda Works. *Automotive Industries*, March 25, 1939, page 407.

Abstracts. New method of providing an engine cylinder of light alloy with a liner of hard metal by casting it in has been patented by the German firm of Fichtel and Sachs. Hard metal is poured into an annular space formed

between interior of cylinder proper and a core set into it through a central hole through the core. During pouring cylinder is revolved around its axis at high speed and resulting high pressure of molten metal against the cylinder wall is said to cause it to alloy with the light alloy at the junction surface, thus providing a bond that assures excellent heat flow to the cooling fins. Very brief abstract and drawing from *Revue de L'Aluminium*, December. *Automotive Industries*, March 25, 1939, page 390, 1 illus.

Aircraft-Engine Valve Mechanisms. V. C. Young. Effect of cam design on the lift diagram is illustrated. Lift actually was measured at each cam angle by a specially developed micrometer operating in conjunction with stroboscopes at valve and camshaft. Effect of seating velocity with respect to valve and cylinder-seat life is discussed and formula for the cam ramp is given. Factors influencing the relation of the valve to its seat are pointed out, such as distortion in the port shape proper and out-of-square condition between seat and valve guide, and high velocity. The hydraulic valve lifter is described and way in which it accomplishes its compensation is illustrated.

Valve-material requirements, effect of temperature on ultimate strength and hot hardness, and importance of fatigue value under alternating stress are considered and illustrated. The benefit of carrying the guide-boss cooling as close to the valve seat as possible is illustrated. Value of the hollow-head over the straight-hole type of internally-cooled valve in a reduction of operating temperature is shown. Development of suitable seat inserts is discussed. *S.A.E. Jour. (Trans.)*, March, 1939, pages 109–116, 15 illus.

Cylinder Bore Wear. A. Taub. Bore wear in the United States; factors affecting bore wear; effect of carburation; effect of cylinder-wall and piston temperatures; spark timing; effect of fuel; effect of mixture ratios; blowby in engines; piston-ring design; oil control; materials for cylinder blocks and pistons; oil consumption; laboratory testing of piston rings; use of thermostats; and piston-ring practice. Long paper presented before the Institution of Mechanical Engineers. *Automobile Engineer*, March, 1939, pages 82–90, 19 illus., 2 tables.

Low-Compression Diesels. V. V. Smirnoff. Possibility of improving the performance of four-stroke compression-ignition engines for aircraft. Disparity between the four-stroke Diesel and gasoline engine will probably never be sufficiently narrowed by the increase of boosting, unless this is accompanied by a decrease in compression ratio. Means are suggested for making possible the operation of four-stroke compression-ignition engines at low compression ratios.

On the basis of calculated performance of the compression-ignition aero engine with low compression ratio it is shown that this engine, even without any cooling of air supply, could develop considerably more power than a comparable gasoline engine of the same swept volume. Ratios of frontal area and of weight to power are less in the case of the compression-ignition engine and fuel consumption at normal maximum output is about 0.425 lb./b.hp. *Flight, Aircraft Engr. Sup.*, January 26, 1939, pages 1–4, 8 illus., 1 table.

The Technique of the Radiator. L. Breguet and R. Devillers. If power cannot be wasted, the radiator must be streamlined or, better, placed in the interior of the fuselage. Under the assumption of a radiator of high quality and a special cooling liquid, for a speed of 560 km./hr., the cooling obtained will absorb 30 percent of the engine power and 40 percent at 650 km./hr. This proportion will be about doubled with water cooling.

First solution consists in streamlining the radiator, but the power absorbed by friction on the external surface of the fairing is of the same order as that necessary to support the internal circulation of air. In taking account of radiator weight, total power for cooling the engine can be reduced to around 7 percent of the power developed at a speed of 600 km./hr., or around 18 percent with water. Arrangement permitting evacuation of heat with maximum economy will consist evidently in placing the radiator in the fuselage or engine nacelle. Abstract from *La Science Aérienne*. *Les Ailes*, March 2, 1939, page 8, 1 illus.

Torsional Vibration of Diesel-Engine Crankshafts. O. Malychevitch. Series of calculations for crankshafts for four- and six-cylinder high-speed automotive Diesel engines of the same bore and stroke, compression ratio, i.m.e.p., and weights of reciprocating and rotating parts. Crankshafts of both engines are identical in every respect except that of length but flywheel of the four is heavier.

First issue—Forced vibration; magnification factor; damping elastic hysteresis; normal elastic curve for finding maximum stress at node of crankshaft and stress at any other section of the shaft during free vibration; amplitude of torsional vibration; shearing stresses; and equivalent length and moment of inertia of each crank unit. Table gives frequency calculation of one-node vibration and one-node frequency with maximum vibration stresses at resonance speed with hysteresis damping.

Second issue—Formulas are derived for approximate values of frequencies for first and second modes of vibration for a six-cylinder-engine crankshaft, and vibration stresses at resonance in one-node vibration are calculated. Calculations for the 4-cylinder engine are compared with those for the six-cylinder. It is shown that the higher the frequency of the crankshaft assembly the better, as it gives assurance against shaft breakage and tends toward smoother engine performance. Ten means by which the frequency of the assembly can be increased are discussed. *Automotive Industries*, March 18 and 25, 1939, pages 372–378 and 402–406, 409, 20 illus., 6 tables, 26 equations.

A Year of Nickel. "From France come reports of an outstanding achievement in aircraft-engine cast iron in which high-strength cast iron rich in nickel and manganese is cast in a toughened condition so that air-cooling fins are not brittle. After machining, an aging or tempering treatment is applied to provide sufficient hardness and wear resistance." Use of Inconel for aircraft exhaust manifolds or collector rings, and use of nickel in aircraft, aircraft-engine and automotive parts are also referred to in a general review. *Automotive Industries*, March 18, 1939, pages 370–371, 379, 2 illus.

The Development of Liquid Cooling. W. N. Twelvetrees. Pressure cooling presents very large possibilities and use of higher operational temperatures will permit corresponding reductions in radiator size. Theoretical problem is useful diversion of enormous amount of heat. Coolant is a mixture of water with 30 percent glycol and the positive pressure relief is adjusted to 30 lb./sq.in. Precautions necessary in the installation of the system and in test plant are pointed out.

Thermostatic control is discussed with its effects on actual flight conditions and actual construction of the modern instrument is illustrated (by courtesy of Rolls Royce and British Thermostat Company). Retractable radiator installation widely used in Service airplanes until recently is also illustrated. Glycol cooling is considered, and a typical glycol-cooled installation for a 12-cylinder vee engine incorporating thermostatic control and dual radiators and a layout of a composite cooling system (both by courtesy of Rolls Royce) are illustrated. Early liquid-cooling systems, early experiments in temperature control and boiling difficulties are described. *Aircraft Engineering*, March, 1939, pages 107–110, 7 illus.

Recent Aero-Engine Research Work. H. C. Mansell. Ideally, the engine should be assembled at the manufacturer's plant complete in its casing, giving minimum drag, and remain undisturbed for its economic period of life, and research is directed toward this end. Stages and accomplishments leading to the present position of aircraft engines are reviewed, and development and needs of the near future are pointed out.

Engine design characteristics, limitations in fuels, superchargers, fuel economy, reliability, durability and reduction in servicing demands are considered. Next major achievements will be engines for consistent flight at high altitude, the compression-ignition engine, direct gasoline injection, and advance in instrumentation. Author is engaged on research work in the Bristol Aeroplane Company. *Aircraft Engineering*, March, 1939, pages 92–94.

Some Factors Controlling the Development of Electrical Ignition of Aero Engines. G. E. Bairsto. Difficulties encountered in designing ignition equipment for use on aero engines. Conditions in which ignition has to operate; effect of electrical leakage on performance of a magneto; effect of reduced available space for installation of magnetos; effect of air temperature and reduced density in which system has to operate; standard density test for R.A.F. magnetos; coil ignition systems; development of specialized coil systems; self-regulating generator; interference suppressors; other types of ignition systems; spark plugs; erosion of spark plug electrodes; effect of electrode material; effect of variation of initial plug size; effect of capacity of cables and nature of spark discharge; effect of distributed nature of capacity; use of series resistance; comparative tests of erosion with magnetos and coil systems; effect of electrode shape and material on erosion; bonding and screening; braided and harness high-tension cables for high temperature conditions (effects of heat, oil, gasoline, ozone and alternative materials to rubber); molded insulation for high-temperature use. Test data quoted were obtained on the Rolls Royce Kestrel X engine. *Royal Aeronautical Soc., Preprint for Meeting*, February 16, 1939, 46 pages, 40 illus., 6 tables.

Engine, Fuel and Lubricant Testing

A Wear and Lubricant Testing Machine Developed by the Timken Roller Bearing Co. Lubricant tester provides accurate information on load-carrying capacity of lubricants, on measurement of friction, and, in a simple accurate manner, on wear characteristics of any kind of material packings (metal products, wood products, and textiles). Description of machine and its operation, and procedure for testing greases. *Metal Industry*, March 24, 1939, pages 347–348, 1 illus.

Duration of Combustion in a Commercial Diesel Engine. A. F. Robertson, R. A. Rose, and G. C. Wilson. Photoelectric combustion indicator developed at the University of Wisconsin and previously described was used in the present experiments with several improvements. Film drum was connected to a 1200 r.p.m. synchronous motor providing a fixed time base for all diagrams and furnishing an accurate method of determining engine speed. New TDC indicator with unique features and test engine are also described.

Not only does a high-centane Diesel fuel start to burn earlier in the cycle due to its shorter ignition-lag period, but it continues to burn longer during the expansion stroke than does a low-cetane fuel. Results of investigation of effect of fuel quality and injection advance angle on ignition lag and combustion duration in a 4-cycle high-turbulence Diesel engine in which combustion characteristics of 27 different fuels were determined. Test data obtained from an open-head engine compared with those obtained from the separate-chamber type show that high turbulence in the latter had no direct effect on ignition lag. *S.A.E. Jour. (Trans.)*, March, 1939, pages 117–124, 140, 15 illus., 1 table.

Proof of Power. Methods used in assaying Bristol engines before delivery, and modern test equipment used. Detailed description. *Flight*, March 9, 1939, pages 244a–244d, 11 illus.

Testing of High Antiknock Fuels in the Single-Cylinder Aircraft Engine. F. Seeber. In contrast to octane-number determination of fuels, the method described permits a test of fuel under most diverse conditions of temperature and fuel-air ratio. From suggestion of C. D. Boerlage the fuel testing method was developed at the D.V.L. which applied the overloadability as the evaluation scale. This engine test will contribute toward a better distinction of knock resistance of fuels for high-powered aircraft engines. Possibility of testing temperature dependence, as well as behavior of fuels of different mixture compositions, is a valuable supplement for engine testing of fuels. *Luftfahrtforschung*, January 10, 1939, pages 18–20, 2 illus.

Engines

Bristol Perseus X 9-cylinder air-cooled radial aircraft engine going into production is the first highly supercharged sleeve-valve aircraft engine. It is quite similar to the Perseus XII but supercharger has an impeller of larger diameter and turns at higher speed. In a special 50-hr. weak-mixture test fuel consumption was 0.448 lb./hp.-hr. at 520 hp. Bore $5^3/_4$ in. Stroke $6^1/_2$ in. Displacement 1520 cu. in. Maximum output 880 hp. at 15,500 ft. altitude. Brief reference only. *Automotive Industries*, March 25, 1939, page 407.

Aircraft Engines Manufactured under Approved Type Certificates. Data on 55 basic types of American aircraft engines, including specifications, construction, accessories, and photograph.

Second article gives similar information on six basic types of American aircraft engines which had not been awarded approved type certificates at time the magazine went to press. *Aero Digest*, March, 1939, pages 148–178 (alternate pages), 61 illus.

An Aircraft Engine Which Operates on Gasoil. R. Rabion. New system of fuel feed, invented by A. Brandenburg, consists in admitting an ultra-rich mixture to the interior of a grooved valve seat. Liquid fuel is mixed with a very small quantity of air to form an ultra-rich mixture. Displacement of piston creates suction of pure air in the inlet manifold, this inflow of air by its passage at high speed around the valve leading to induction of the ultra-rich mixture. Hollow valve of bronze or beryllium consists of two pieces turned and screwed one in the other in such a way as to constitute an interior chamber joined to the combustion chamber by annular tube. Air and fuel are drawn in at the same time, but remain separated up to their arrival in the cylinder. Description. *Les Ailes*, February 23, 1939, page 7, 1 illus.

"Bristol Fashion"—Rise of the Radial. Historical review of engine development in the Bristol Aeroplane Company in the last twenty years, including: first Bristol Jupiter; high-compression research; forged cylinder heads, automatic boost control and automatic timing controls to magnetos; development of the Mercury and Pegasus engines; new features making possible the higher power obtainable from these engines; latest types of engines; sleeve-valve development; and Perseus and Aquila engines. *Flight*, March 9, 1939, pages 236–244, 22 illus.

Bristolian in Derby. A. H. R. Fedden. Answers to questions raised by Rolls Royce engineers regarding the Bristol sleeve valve engines following

the presentation of Mr. Fedden's Royal Aeronautical Society paper before the Derby Branch of the Institution of Automobile Engineers. Both the Scylla type and a twin-engined military airplane have been found to be quieter with sleeve-valve engines. Theory that wreckage in case of a sleeve-valve engine would be greater has been shown in practice to be wrong. Sleeve drive failures were localized. Advantages a user obtained from the sleeve valve engine; difficulties in adopting the sleeve valve on inline liquid-cooled engines; and references to cylinder arrangement, sleeve drive, oil film in large-bore cylinders, smoothness of power acceleration and low-speed effect on ignition, cold starting, heat losses, and increase in oil circulation. *Flight*, March 2, 1939, page 224.

New Engine for Aircraft Use Shown in Los Angeles. Designed primarily for aircraft the new engine demonstrated by Lt. S. W. Neighbors is said to weigh only 412 lb., to develop 500 hp. at 4500 r.p.m., to consume 8 gal./hr. fuel, and to have attained 10,000 r.p.m. in tests without vibration. Engine contains only 30 moving parts, is full rotary in principle and measures 26 in. in diameter and 18 in. in overall length. It runs on five ball bearings and eliminates entirely the use of pistons, connecting rods and cylinders. Brief reference only. *Automotive Industries*, March 25, 1939, page 392.

Design of Aero-Engines for Production. F. Nixon. Development of Bristol engines has in the main been carried out by continuous overload testing, which has served to indicate directions in which modifications to components have been necessary. Modifications have been effected with least possible change in design, so that production has not been hampered and one engine series has been merged quite gradually into the next.

Factors which have enabled present results in Bristol Mercury and Pegasus engines to be achieved are dealt with to show the way in which production and design have collaborated. Cylinders and cylinder heads, exhaust valves, crankshafts, and connecting rods are considered in detail. Photographs of a specially designed connecting-rod testing machine and parts of engines are included. *Aircraft Engineering*, March, 1939, pages 127–131, 13 illus.

A Civil Hercules. New Bristol Hercules IV engine for civil aircraft has an international power rating of 1010–1030 hp. developed at 2400 r.p.m. at 4500 ft. Maximum output for all-out level flight is 1220 hp. at 2800 r.p.m. at 5500 ft. but 1380 hp. for take-off at same crankshaft speed is available. Hercules have been chosen for the new class of Short flying boat for Imperial Airways and for the experimental 31-ton transport landplanes. Brief note referring to successful 250-hours' endurance test. *Flight*, March 16, 1939, page 273. *Aeroplane*, March 15, 1939, page 328.

An "M" and "S" Hercules. Version of the Bristol Hercules two-row sleeve-valve engine fitted with a two-speed supercharger, referred to in *Les Ailes*, is said to be the Hercules IV which, operating on 100-octane fuel, develops 1570 hp. for take-off, 1420 hp. at 4920 ft. and 1290 hp. at 14,760 ft. Hercules I (moderately supercharged) has been homologated at Chalais Meudon. Presumably alterations will be made to bring it into line with the Hercules II. Two Hercules are to be fitted in production type Lioré et Olivier 45 bomber which normally has Hispano-Suiza or Gnôme-Rhône two-ow radials of about 1000 hp. each. Brief ref. *Flight*, March 23, 1939, page 289.

Parts and Accessories

Keeping the Dust Out. Principle of the Vokes filters is to present a maximum of effective filter surface to flow by corrugation of the filtering material so that ratio of area of filter surface to that of intake is high. Air or oil passes through the filter at $^1/_{200}$th or $^1/_{600}$th of normal velocity in a circulating system.

Vokes air filter used on the Westland Lysander weighs 12½ lb. and is of the oil-wetted three-ply pattern designed for use on airplanes where no provision was made in the original design for an air cleaner. Few details of this filter and its maintenance, and illustration of the Vokes air cleaners built into the cowling of liquid-cooled aircraft engines. *Aeroplane*, March 15, 1939, page 354, 2 illus.

Aircraft Accessories. Engine parts made available in the past year are briefly reviewed including Chandler Evans non-icing carburetor, Lunkenheimer fuel strainer, Cuon self-cleaning oil filter, Ryan exhaust manifold joints, and BG aviation spark plugs. *Aero Digest*, March, 1939, pages 191, 192, 4 illus.

A New Torsional Vibration Damper. New type of torsional vibration damper invented by E. Thege and built by Aktiebolaget Atlas Diesel in Sweden. Hub is bolted to the shaft. Rim or damping mass is free to move angularly on the hub and in regular operation has an oscillating motion which is limited by an oil cushion formed in the spaces between inwardly projecting parts of damping mass and outwardly projecting parts of hub. Oil introduced into the damper from the nearest engine bearing is conducted to the damping chambers. Conducting grooves are so designed that in certain extreme positions they cut off communication with the chambers. Between these positions damping mass moves freely, only retarding force being friction of sliding surfaces. Long description. *Automotive Industries*, March 11, 1939, pages 344, 349, 2 illus.

Steel Piston Rings. Cord steel piston ring; "Steelcraft" piston ring with normal and oval cylinder; "Ondulex" oil-control ring; Champion and Ondulex multiple piston rings; and Dran-Brac oil control ring. Description. *Automobile Engineer*, March, 1939, page 90, 7 illus.

Aircraft Radio

Aircraft Accessories. American aircraft radio equipment made available in the past year is reviewed including aircraft transmitters, receivers, direction finders, and radio accessories. *Aero Digest*, March, 1939, pages 184, 187–188, 5 illus.

Aircraft Transmitter. "Waller Communicator" 150-watt 65-lb. aircraft transmitter, developed by Spartan School of Aeronautics, is remote controlled, covers three frequencies, using separate crystals for each, and incorporates side tone, interphone, and transmission on both long and short antennas, with automatic loading on the short. Brief reference. *Electronics*, February, 1939, page 69, 1 illus.

Imperial Airways' Wireless. Hermes portable trans-receiver now being tested for use as auxiliary equipment on board Imperial Airways flying boats for North Atlantic mail service. Apparatus comprises transmitter, receiver, and rotary converter. It has a wave range of from 5 to 1000 meters, is crystal controlled on any required frequency, can be used for CW, MCW or telephony, and feeds 15 to 20 watts to the aerial. Optional AVC is included in the superhet receiver, and there is a BFO for CW reception. Communication on short waves was maintained with London up to a distance of 3300 miles in tests. Short note. *Wireless World*, March 16, 1939, page 259, 1 illus.

M.I.T. Metcalf Blind Landing Passes First Flight Tests. "It is the first blind landing system whose principles—the straight glide path—meets the requirements of hardboiled Army fliers." Details and advantages of the new radio-beam method. *Science News Letter*, March 18, 1939, page 167.

All-Purpose Radio. Hermes lightweight Transreceiver, Type 1050/51 was originally designed for Imperial Airways to their own specification for use on their Empire routes and first set maintained contact with Transreceivers' own short-wave station in London over a range of more than 3000 miles. Case is divided into three separate compartments, each housing a self-contained unit independent of the other, the transmitter unit being on top, receiver unit in the center and power unit in the bottom. Transmitter is designed to work on long, medium, or short waves, actual wave range being from 5 to 1000 meters. A limited number of crystals are supplied with the set. Public address or intercommunication unit is incorporated so that pilot can talk directly to his passengers. Total weight 43 lb. Description. *Flight*, March 23, 1939, pages 292c–292d, 2 illus.

An American Approach System. Bendix transmitting and receiving equipment for its instrument landing system. Two beams are used, interlocking in plan form, while each is directed by ground radiation into the customary lozenge shape, when viewed horizontally. Aerial system consists of two horizontally polarized arrays excited in phase. Axes of arrays are in the same horizontal plane forming an angle of 30° relative to one another. Single receiving set is used unless marker beacon reception is required and transmission is received on a special nondirectional loop aerial. Short description. *Flight*, March 23, 1939, page 292b.

Blind Approach Equipment. Large order has been placed by the British Air Ministry with the American company which manufactures the Air-Track radio blind-approach equipment, according to report. From this it is to be presumed that difficulty has been experienced in obtaining delivery of the Lorenz transmitters and receivers ordered for both service and civil use. Few details of Air-Track scheme. *Flight*, March 23, 1939, page 293.

Book Review

Conquering the Air, by Archibald Williams (revised and enlarged by Marion Barton Crowell); Thomas Nelson and Sons, New York, 1930; 360 pages, $2.00.

First published in 1926, this book has been revised several times to keep it up-to-date with the fast moving field of aviation. While it does not give accounts of the more recent flights or of late developments in air transport it is an excellent summary of the background of aeronautics. It is particularly valuable for reference regarding the great flights that were made from the time Dr. Jeffries financed and made the first flight across the English Channel with Blanchard, up through 1930. The concluding chapters on parachutes, airways, and the future of flying, round out the historical portions of the book so that the reader receives a comprehensive idea of the scope of the art, as of 1930. The essential details of the flights are given in a readable style.

It gives the necessary information for the general reader and, particularly, for young people who wish to acquire a general knowledge of the development of aviation since the early beginnings.